DESIGN AND SYNTHESIS OF POTENTIAL CHROMONE-BASED ANTI-TUBERCULOSIS AGENTS

by

MOGOLLA SHIBE NCINA

18013414

Dissertation submitted in fulfilment of the requirements for the Master of Science Degree in Chemistry

Faculty of Science, Engineering and Agriculture

Department of Chemistry

University of Venda

Thohoyandou, Limpopo, South Africa

Supervisor : Prof IDI Ramaite

Co-supervisor: Prof T Van Ree

© University of Venda

DECLARATION

I**, Mogolla Shibe Ncina**, hereby declare that this dissertation for the Master's degree in Chemistry at the University of Venda has not been submitted previously for a degree at this or any other institution, that it is my own work in design and execution, and that all the references contained therein have been duly acknowledged.

Student signature: …… Date: 28 May 2025

© University of Venda

PLAGIARISM DECLARATION

I, Mogolla Shibe Ncina, hereby declare the following:

- I am aware of and acknowledge that plagiarism is wrong. Plagiarism is the use of another person's ideas or published work as if it is one's own and it is a serious academic offence for which the university may impose severe penalties.
- I declare that this dissertation is my own work and that I have correctly acknowledged the work of others. The work has not been previously submitted to the University of Venda or elsewhere for this degree.
- I have not allowed and will not allow anyone to copy my work with the intention of passing it off as their own work.



Signature: …… Date: 28 May 2025

© University of Venda

ABSTRACT

This dissertation describes the design and synthesis of 4-(4-oxochromen-3-yl)-3,4-dihydropyrimidin-2-one derivatives and the assessment of their biological activity against a strain of the causative agent of TB.

In this investigation, two classes of chromone-based compounds were synthesised. Different reactions were exploited to synthesise target compounds. In the first route, a Vilsmeier-Haack reaction was applied to convert the 3,5-disubstituted/unsubstituted 2-hydroxyacetophenones to corresponding 6,8-disubstituted/unsubstituted chromone-3-carbaldehydes. The 6,8-disubstituted/unsubstituted chromone-3-carbaldehydes were oxidized to afford 6,8-disubstituted/unsubstituted chromone-3-carboxylic acids with poor percentage yield 15-28%. Additionally, a second series of compounds were obtained by employing the Biginelli reaction to afford ethyl 6-hydroxy-4-(6-substituted/unsubstituted chromon-3-yl)-2-oxo-6-trifluoromethyl-1,2,3,4-tetrahydropyrimidine-5-carboxylate derivatives with moderate to good percentage yield of 53 – 74%. Ethyl 6-hydroxy-4-(6-substituted/unsubstituted chromon-3-yl)-2-oxo-6-trifluoromethyl-1,2,3,4-tetrahydropyrimidine-5-carboxylates were successfully dehydrated to ethyl 4-(6-substituted/unsubstituted chromon-3-yl)-2-oxo-6-trifluoromethyl-1,2,3,4-tetrahydropyrimidine-5-carboxylate derivatives using a Dean-Stark method at 140 °C, purified by recrystallization.

All target compounds were purified by recrystallization and flash chromatography, and then characterized using NMR and FTIR, LC-MS and HRMS. After fully characterizing target compounds, they were screened for activity against the *Mtb* H37Rv clinical strain. Three media were used for screening and MABA was used for quantitative analysis. Unfortunately, all compounds tested were inactive with an MIC value >62.5 µM. Ethyl 2-oxo-4-(4-oxo-6-phenyl-4*H*-chromen-3-yl)-6-(trifluoromethyl)-1,2,3,4-tetrahydropyrimidine-5-carboxylate with reported MIC of 3.39 µM also did not show any activity. The discrepancies in the results could be due to differences in media used, incubation conditions, bacteria or contamination. Derivatives with 4-substututed phenyl substituents, were insoluble with solubility <5 µM. The OH group was critical for solubility as removing it resulted in poor solubility. Ethyl 4-(6-substituted/unsubstituted chromon-3-yl)-2-oxo-6-trifluoromethyl-1,2,3,4-tetrahydropyrimidine-5-carboxylate derivatives did not show any cytotoxicity against HepG2 cell line, with all compounds showing >50 µM toxicity.

Keywords: Chromones**,** Vilsmeier-Haack formylation, *Mycobacterium tuberculosis*, Hofmann rearrangement, Drug resistance.

© University of Venda

ACKNOWLEDGEMENTS

First and foremost, I would like to thank God for strength, knowledge, wisdom, and courage to undertake this research project. I express deepest gratitude to my supervisor, Professor I.D.I. Ramaite, for his constant encouragement, expert guidance, and enthusiasm that has been my greatest provision and source of inspiration throughout the entire project. It is indeed an honour and privilege to have been under his supervision. I would also like to thank my co-supervisor Prof. T. van Ree for his contribution throughout this project.

I would also like to thank Ms N. Maseko and Mr F.B. Mutshaeni, laboratory technicians, NMR operator Mr P. Pandelani, and the Chemistry department for their assistance and resources towards the completion of this project.

Special thanks to my family, relatives, and friends, whose continuous support and love have been significant to a much greater degree than they suspect or understand.

I would like to offer thanks to the H3D Drug Discovery and Development Centre-University of Cape Town for offering access to their laboratories for purification and biological screening of the target compounds and attending medicinal chemistry workshops.

Finally, the National Research Foundation (NRF) and South African Medical Research Council (SAMRC) for munificent financial support.

© University of Venda

LIST OF SCHEMES

Scheme 1: Kostanecki acylation reaction 7

Scheme 2: Baker-Venkataraman rearrangement 8

Scheme 3: Gammill's Protocol reaction 8

Scheme 4: Vilsmeier-Haack formylation reaction 9

Scheme 5: Proposed Synthetic Scheme 20

Scheme 6: Synthesis of 5-bromo-2-hydroxyacetophenone derivative **42B** 21

Scheme 7: Synthesis of 5-nitro-2-hydroxyacetophenone derivative **42C** 24

Scheme 8: Synthesis of 5-(4-subsituted phenyl)-2-hydroxyacetophenone derivatives **42D-F** 27

Scheme 9: Synthesis of 3,5-disubstituted/unsubstituted 2-hydroxyacetophenone derivatives **43A-E** 30

Scheme 10: Synthesis of chromone-3-carbaldehyde derivatives **44A-D** 33

Scheme 11: Proposed mechanism for the formation of chromone-3-carbaldehydes 35

Scheme 12: Synthesis 6-substituted/unsubstituted chromone-3-carbaldehyde derivatives **48A-E** 36

Scheme 13: Synthesis of 6-substituted chromone-3-carbaldehyde derivatives **48A-E** 39

Scheme 14: Synthesis of 6-nitrochromone-3-carbaldehyde **44E** 43

Scheme 15: Synthesis of substituted/unsubstituted chromone-3-carboxylic acid derivatives **45A-B** 45

Scheme 16: Attempted synthesis of 6-nitrochromone-3-carboxamide **46A** 49

Scheme 17: Synthesis of ethyl 6-hydroxy-4-(chromon-3-yl)-2-oxo-6-trifluoromethyl-1,2,3,4-tetrahydropyrimidine-5-carboxylate derivatives **51A-E** 52

Scheme 18: Synthesis of ethyl 4-(chromon-3-yl)-2-oxo-6-trifluoromethyl-1,2,3,4-tetrahydropyrimidine-5-carboxylate derivatives **52A-D** 58

Scheme 19: Mechanism for the synthesis of ethyl 4-(chromon-3-yl)-2-oxo-6-trifluoromethyl-1,2,3,4-tetrahydropyrimidine-5-carboxylate derivatives **52A-D** 60

© University of Venda

LIST OF TABLES

Table 1: Synthesized 5-[4-substituted/unsubstituted-phenyl]-2-hydroxyacetophenone derivatives **42D-F** 27

Table 2: ^{13}C NMR chemical shift values (ppm) of 5-substituted/unsubstituted-2-hydroxyacetophenones **42D-F** in $CDCl_3$ (at 100 MHz) 28

Table 3: Synthesized 3,5-disubstituted/unsubstituted 2-hydroxyacetophenones **43A-E** 30

Table 4: ^{13}C NMR chemical shift values (ppm) of 3,5-disubstituted/unsubstituted 2-hydroxyacetophenones **43A-D** in $CDCl_3$ (at 100 MHz) 32

Table 5: Synthesized 6,8-disubstituted/unsubstituted chromone-3-carbaldehyde derivatives **44A-D** 35

Table 6: ^{13}C NMR chemical shift values (ppm) of 6,8-disubstituted/unsubstituted-chromone-3-carbaldehyde derivatives **44A-C** in $CDCl_3$ (at 100 MHz) 37

Table 7: Synthesized 6-substituted chromone-3-carbaldehyde derivatives **48A-E** 38

Table 8: ^{13}C NMR chemical shift values (ppm) of 6-substituted-chromone-3-carbaldehydes **48A-E** in $CDCl_3$ (at 400 MHz) 41

Table 9: Synthesized substituted/unsubstituted chromone-3-carboxylic acid derivatives **45A-B** 44

Table 10: ^{13}C NMR chemical shift values (ppm) of substituted/unsubstituted chromone-3-carboxylic acid derivatives **45A-B** in $CDCl_3$ (at 100 MHz) 47

Table 11: Synthesized ethyl 6-hydroxy-4-(chromon-3-yl)-2-oxo-6-trifluoromethyl-1,2,3,4-tetrahydropyrimidine-5-carboxylate derivatives **51A-E** 51

Table 12: ^{13}C NMR chemical shift values (ppm) of ethyl 6-hydroxy-4-(chromon-3-yl)-2-oxo-6-trifluoromethyl-1,2,3,4-tetrahydropyrimidine-5-carboxylate derivatives **51A-E** (at 400 MHz) 56

Table 13: Synthesis of ethyl 4-(chromon-3-yl)-2-oxo-6-trifluoromethyl-1,2,3,4-tetrahydropyrimidine-5-carboxylate derivatives **52A-D** 57

Table 14: ^{13}C NMR chemical shift values (ppm) of ethyl 4-(chromon-3-yl)-2-oxo-6-trifluoromethyl-1,2,3,4-tetrahydropyrimidine-5-carboxylate derivatives **52A-E** (at 400 MHz) 64

© University of Venda

Table 15: *In vitro* biological assays for synthesized ethyl 6-hydroxy-4-(chromon-3-yl)-2-oxo-6-trifluoromethyl-1,2,3,4-tetrahydropyrimidine-5-carboxylate derivatives 51A-E against *Mtb* H37Rv strain 66

Table 16: *In vitro* biological assays for synthesized Ethyl 4-(6-substituted/unsubstituted chromone-3-)-2-oxo-6-trifluoromethyl-1,2,3,4-tetrahydropyrimidine-5-carboxylate derivatives **52A-D** against *Mtb* H37Rv strain and cytotoxicity 68

© University of Venda

LIST OF FIGURES

Figure 1: *Mycobacterium tuberculosis* 10

Figure 2: Transmission of TB 12

Figure 3: ^{1}H NMR spectrum of compound **42B** in $CDCl_3$ (at 400 MHz) 22

Figure 4: Expanded ^{1}H NMR spectrum of compound **42B** in $CDCl_3$ (at 400 MHz) 22

Figure 5: ^{13}C NMR spectrum of compound **42B** in $CDCl_3$ (at 100 MHz) 23

Figure 6: DEPT 135 spectrum of compound **42B** in $CDCl_3$ 23

Figure 7: ^{1}H NMR spectrum of compound **42C** in $CDCl_3$ (at 400 MHz) 25

Figure 8: Expanded ^{1}H NMR spectrum of compound **42C** in $CDCl_3$ (at 400 MHz) 25

Figure 9: ^{13}C NMR spectrum of compound **42C** in $CDCl_3$ (at 100 MHz) 26

Figure 10: ^{1}H NMR spectrum of 2-hydroxy-5-phenylacetophenone **42F** 28

Figure 11: ^{13}C NMR spectrum of 2-hydroxy-5-phenylacetophenone **42F** 29

Figure 12: DEPT 135 spectrum of 2-hydroxy-5-phenylacetophenone **42F** 29

Figure 13: ^{1}H NMR spectrum of compound **43A** in $CDCl_3$ (at 400 MHz) 31

Figure 14: ^{13}C NMR spectrum of compound **43A** in $CDCl_3$ (at 100 MHz) 32

Figure 15: ^{1}H NMR spectrum of compound **44A** in $CDCl_3$ (at 400 MHz) 34

Figure 16: ^{13}C NMR spectrum of compound **44A** in $CDCl_3$ (at 100 MHz) 34

Figure 17: ^{1}H NMR spectrum of compound **44B** in $CDCl_3$ (at 400 MHz) 37

Figure 18: ^{13}C NMR spectrum of compound **44B** in $CDCl_3$ (at 100 MHz) 37

Figure 19: ^{1}H NMR spectrum of 6-phenylchromone-3-carbaldehyde **48C** 40

Figure 20: Expanded ^{1}H NMR spectrum of 6-phenylchromone-3-carbaldehyde **48C** 40

Figure 21: ^{13}C NMR spectrum of 6-phenylchromone-3-carbaldehyde **48C** 41

Figure 22: DEPT 135 spectrum of 6-substituted-chromone-3-carbaldehyde **48C** 41

Figure 23: ^{1}H NMR spectrum of 6-nitrochromone-3-carbaldehyde **48F** at 400MHz 43

Figure 24: ^{13}C NMR spectrum of 6-nitrochromone-3-carbaldehyde **48F** at 100 MHz 44

© University of Venda

Figure 25: DEPT 135 spectrum of 6-nitrochromone-3-carbaldehyde **48F** 44

Figure 26: ^{1}H NMR spectrum of compound **45B** in $CDCl_3$ (at 400 MHz) 46

Figure 27: ^{13}C NMR spectrum of compound **45B** in $CDCl_3$ (at 100 MHz) 46

Figure 28: DEPT 135 spectrum of compound **45B** in $CDCl_3$ 47

Figure 29: FTIR spectrum of compound **45B** 47

Figure 30: ^{1}H NMR spectrum of compound **52** in C_5D_5N (at 400 MHz) 50

Figure 31: ^{13}C NMR spectrum of compound **52** in C_5D_5N (at 100 MHz) 50

Figure 32: DEPT 135 spectrum of compound **52** in C_5D_5N 51

Figure 33: ^{1}H NMR spectrum of ethyl 6-hydroxy-4-(chromon-3-yl)-2-oxo-6-trifluoromethyl-1,2,3,4-tetrahydropyrimidine-5-carboxylate derivatives **51D** 53

Figure 34: ^{13}C NMR spectrum of ethyl 6-hydroxy-4-(4-ochromon-3-yl)-2-oxo-6-trifluoromethyl-1,2,3,4-tetrahydropyrimidine-5-carboxylate derivative **51D** 54

Figure 35: DEPT 135 spectrum of ethyl 6-hydroxy-4-(chromon-3-yl)-2-oxo-6-trifluoromethyl-1,2,3,4-tetrahydropyrimidine-5-carboxylate derivative **51D** 54

Figure 36: FT-IR spectrum of compound **51D** 55

Figure 37: LC-MS of compound **51D** 56

Figure 38: ^{1}H NMR spectrum of ethyl 2-oxo-4-(4-oxo-4*H*-chromen-3-yl)-6-(trifluoromethyl)-1,2,3,4-tetrahydropyrimidine-5-carboxylate **52C** 61

Figure 39: Expanded ^{1}H NMR spectrum of ethyl 2-oxo-4-(4-oxo-4*H*-chromen-3-yl)-6-(trifluoromethyl)-1,2,3,4-tetrahydropyrimidine-5-carboxylate **52C** in DMSO-DMF 61

Figure 40: ^{13}C NMR spectrum of ethyl 2-oxo-4-(4-oxo-4*H*-chromen-3-yl)-6-(trifluoromethyl)-1,2,3,4-tetrahydropyrimidine-5-carboxylate **52C** 62

Figure 41: DEPT 135 NMR spectrum of ethyl 2-oxo-4-(4-oxo-4*H*-chromen-3-yl)-6-(trifluoromethyl)-1,2,3,4-tetrahydropyrimidine-5-carboxylate **52C** 63

Figure 42: FT-IR spectrum of compound **52C** 63

Figure 43: HRMS spectrum of compound **52C** 64

FIGURE 44: FT-IR spectrum of **44B** 92

FIGURE 45: ^{1}H NMR spectrum of **42D** in $CDCl_3$ (at 100 MHz). 92

FIGUR 46: Expanded ^{1}H NMR spectrum of **4D** in $CDCl_3$ (at 100 MHz) 93

© University of Venda

FIGURE 47: ^{13}C NMR spectrum of **4D** in $CDCl_3$ (at 100 MHz).....93

FIGURE 48: ^{1}H NMR spectrum of **43B** in $CDCl_3$ (at 100 MHz).....94

FIGURE 49: ^{13}C NMR spectrum of **43B** in $CDCl_3$ (at 100 MHz).....94

FIGURE 50: ^{1}H NMR spectrum of **43C** in $CDCl_3$ (at 100 MHz).....95

FIGURE 51: ^{13}C NMR spectrum of **43C** in $CDCl_3$ (at 100 MHz).....95

FIGURE 52: FT-IR spectrum of **44A**.....96

FIGURE 53: ^{1}H NMR spectrum of **44F** in $CDCl_3$ (at 100 MHz).....96

FIGURE 54: ^{1}H NMR spectrum of **44D** in $CDCl_3$ (at 100 MHz).....97

FIGURE 55: ^{13}C NMR spectrum of **44D** in $CDCl_3$ (at 100 MHz).....97

FIGURE 56: ^{1}H NMR spectrum of **44C** in $CDCl_3$ (at 100 MHz).....98

FIGURE 57: ^{13}C NMR spectrum of **44C** in $CDCl_3$ (at 100 MHz).....98

FIGURE 58: ^{1}H NMR spectrum of **44B** in $CDCl_3$ (at 100 MHz).....99

FIGURE 59: ^{13}C NMR spectrum of **44B** in $CDCl_3$ (at 100 MHz).....99

FIGURE 60: FT-IR spectrum of **44E**.....100

FIGURE 61: ^{1}H NMR spectrum of **45A** in DMSO (at 100 MHz).....100

FIGURE 62: ^{13}C NMR spectrum of **45A** in DMSO (at 100 MHz).....101

FIGURE 63: ^{1}H NMR spectrum of **51E** in DMSO (at 100 MHz).....101

FIGURE 64: ^{13}C NMR spectrum of **51E** in DMSO (at 100 MHz).....102

FIGURE 65: LC-MS spectrum of **51E**.....102

FIGURE 66: HR-MS spectrum of **51E**.....103

FIGURE 67: ^{1}H NMR spectrum of **51A** in $CDCl_3$ (at 100 MHz).....103

FIGURE 68: Expanded ^{1}H NMR spectrum of **51A** in $CDCl_3$ (at 100 MHz).....104

FIGURE 69: ^{13}C NMR spectrum of **51A** in $CDCl_3$ (at 100 MHz).....104

FIGURE 70: LC-MS spectrum of **51A**.....105

FIGURE 71: LC-MS spectrum of **51A**.....105

FIGURE 72: ^{1}H NMR spectrum of **51C** in $CDCl_3$ (at 100 MHz).....106

© University of Venda

FIGURE 73: Expanded ^{1}H NMR spectrum of **51C** in $CDCl_3$ (at 100 MHz) 106

FIGURE 74: ^{13}C NMR spectrum of **51C** in $CDCl_3$ (at 100 MHz) 107

FIGURE 75: LC-MS spectrum of **51C** 107

FIGURE 76: HR-MS spectrum of **51C** 108

FIGURE 77: LC-MS spectrum of **51B** 108

FIGURE 78: HR-MS spectrum of **51B** 109

FIGURE 79: ^{1}H NMR spectrum of **52D** in $CDCl_3$ (at 100 MHz) 109

FIGURE 80: Expanded ^{1}H NMR spectrum of **52D** in $CDCl_3$ (at 100 MHz) 110

FIGURE 81: ^{13}C NMR spectrum of **52D** in $CDCl_3$ (at 100 MHz) 110

FIGURE 82: LC-MS spectrum of **52D** 111

FIGURE 83: HR-MS spectrum of **52D** 111

FIGURE 84: ^{1}H NMR spectrum of **52B** in $CDCl_3$ (at 100 MHz) 112

FIGURE 85: ^{13}C NMR spectrum of **52B** in $CDCl_3$ (at 100 MHz) 112

FIGURE 86: C-MS spectrum of **52D** 113

FIGURE 87: ^{1}H NMR spectrum of **52A** in $CDCl_3$ (at 100 MHz) 113

FIGURE 88: ^{13}C NMR spectrum of **52A** in $CDCl_3$ (at 100 MHz) 114

FIGURE 89: LC-MS spectrum of **52A** 114

© University of Venda

LIST OF ABBREVIATIONS

Ac_2O	Acetic anhydride
AcONa	Sodium acetate
AIDS	Acquired immunodeficiency syndrome
$CDCl_3$	Deuterochloroform
Covid 19	Coronavirus
DCM	Dichloromethane
DEPT	Distortionless enhancement by polarization transfer
DMF	*N,N*-dimethylformamide
DMSO	Dimethyl sulfoxide
FTIR	Fourier Transform Infrared Spectroscopy
HIV	Human immunodeficiency virus
Hz	Hertz, s^{-1}
h	Hour(s)
INH	Isoniazid
LHS	Left Hand Side
MABA	Microplate Alamar Blue Assay
mL	Millilitres
m.p.	Melting point
NBS	*N*-bromosuccinimide
NIS	*N*-iodosuccinimide
NMR	Nuclear Magnetic Resonance
^{1}H NMR	Proton Nuclear Magnetic Resonance
^{13}C NMR	Carbon-13 Nuclear Magnetic Resonance
OADC	Oleic Albumin Dextrose Catalase
Ph	Phenyl
ppm	Parts per million

© University of Venda

rt	Room temperature
RHS	Right Hand Side
RIF	Rifampicin
TB	Tuberculosis
TEA	Triethylamine
WHO	World Health Organization

© University of Venda

TABLE OF CONTENTS

DECLARATION i
PLAGIARISM DECLARATION ii
ABSTRACT i
ACKNOWLEDGEMENTS ii
LIST OF SCHEMES iii
LIST OF TABLES iv
LIST OF FIGURES vi
LIST OF ABBREVIATIONS x
CHAPTER 1: INTRODUCTION 1
1.1 Chromones 1
1.1.1 Sources of chromones 1
1.1.2 Naturally occurring chromones and their anti-tuberculosis activities 2
1.1.3 Synthetic anti-TB chromone derivatives 3
1.1.4 Synthesis of chromones 6
1.2 Tuberculosis 10
1.2.1 TB in South Africa 10
1.2.2 Symptoms and transmission of TB 10
1.2.3 Types of TB 11
1.2.4 Pathogenesis of TB 11
1.2.5 Drug Resistance 12
1.2.6 Treatment of TB 13
CHAPTER 2: PROBLEM STATEMENT AND MOTIVATION OF STUDY 15
CHAPTER 3: AIM AND OBJECTIVES 17
3.1 Aim of the study 17
3.2 Objectives of the study 17
CHAPTER 4: RESULTS AND DISCUSSION 18
4.1 RESEARCH METHODOLOGY 19
4.1.1 Synthesis of 5-bromo-2-hydroxyacetophenone 42B 21
4.1.2 Synthesis of 5-nitro-2-hydroxyacetophenone 42C 24
4.1.3 Synthesis of 5-[4-substituted/unsubstituted-phenyl]-2-hydroxyacetophenone derivatives 42D-F 26
4.1.4 Synthesis of 3,5-disubstituted/unsubstituted 2-hydroxyacetophenones 43A-E 30
4.1.5 Synthesis of chromone-3-carbaldehydes 44A 34
4.1.6 Synthesis of 6.8-disubstituted chromone-3-carbaldehydes 44B-D 36
4.1.7 Synthesis of 6-substituted chromone-3-carbaldehydes 48A-E 39

© University of Venda

4.1.8 Synthesis of 6-nitrochromone-3-carbaldehyde 44F 43

4.1.9 Synthesis of substituted/unsubstituted-chromone-3-carboxylic acids 45A-B 45

4.1.10 Synthesis of 6-nitrochromone-3-carboxamide 46A 49

4.1.11 Synthesis of ethyl 6-hydroxy-4-(chromon-3-yl)-2-oxo-6-trifluoromethyl-1,2,3,4-tetrahydropyrimidine-5-carboxylate derivatives 51A-E 52

4.1.12 Ethyl 4-(6-substituted chromone-3-)-2-oxo-6-trifluoromethyl-1,2,3,4-tetrahydropyrimidine-5-carboxylate derivatives 52A-D 58

4.1.12 Mechanism for synthesis of Ethyl 4-(6-substituted chromone-3-)-2-oxo-6-trifluoromethyl-1,2,3,4-tetrahydropyrimidine-5-carboxylate derivatives 52A-D 60

4.2 Biological Results 67

CHAPTER 5: CONCLUSION AND PERSPECTIVE 71

5.1 Conclusions 71

5.2 Future work 72

CHAPTER 6: EXPERIMENTAL 73

6.1 General methods 73

6.2 Syntheses 73

6.2.1 General synthesis of 5-bromo-2-hydroxyacetophenone 42B 73

6.2.2 Synthesis of 5-nitro-2-hydroxyacetophenone 42C (56%) 73

6.2.3 General synthesis of 3,5-disubstituted/unsubstituted 2-hydroxyacetophenones 43A-D 74

6.2.4 General synthesis of 6,8-disubstituted/unsubstituted chromone-3-carbaldehyde derivatives 44A-C 76

6.2.5 General synthesis of 6,8-disubstituted/unsubstituted chromone-3-carboxylic acid derivatives 45A-B 77

6.2.6 General synthesis of 5-(4-substituted/unsubstituted phenyl)-2-hydroxyacetophenones (42D-F) 78

6.2.7 General synthesis of 6-substituted/unsubstituted chromone-3-carbaldehydes (48A-E) 79

6.2.9 General synthesis of ethyl 6-hydroxy-4-(6-substituted/unsubstituted chromone-3-)-2-oxo-6-trifluoromethyl-1,2,3,4-tetrahydropyrimidine-5-carboxylate derivatives 51A-E 81

6.2.10. General synthesis of ethyl 4-(chromon-3-yl)-2-oxo-6-trifluoromethyl-1,2,3,4-tetrahydropyrimidine-5-carboxylate derivatives 52A-E 84

6.3. *In vitro* antimycobacterial assay 87

6.4. Solubility assay 88

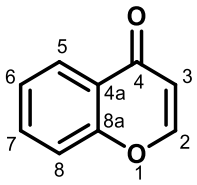
REFERENCES 89

© University of Venda

CHAPTER 1: INTRODUCTION

1.1 Chromones

Chromone **1** is a naturally occurring heterocyclic molecule with a benzopyrone skeleton and oxygen as a heteroatom. The majority of chromones are found in plants, and most of them have unique chemical interactions or/ and a variety of medicinal uses.[1, 3]

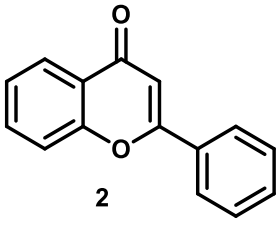


1

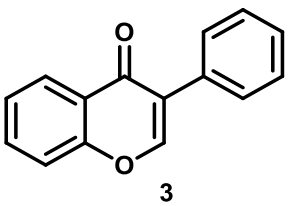
Chromone chemistry has been investigated extensively and reviewed in current history. The rigid bicyclic chromone fragment has been designated as a preferential structure in pharmaceutical research due to its employment in a broad variety of pharmacologically active compounds, including several therapeutic medicines. Chromones are utilized as scaffolds in the production of bioactive compounds as well as in medicinal chemistry applications such as fluorescence probe preparation.[3-6] Naturally occurring and synthetic chromones have intriguing biological activities.

1.1.1 Sources of chromones

Thousands of natural and synthetic chromone derivatives have been identified, leading to the creation of novel medications, some of which are now on the market.[7] Most plants and a few fungi contain high quantities of chromones.[8] The bulk of chromones found in nature are flavones **2** and isoflavones **3**, 3-methylchromone **4**, 2-styrylchromone **5**, and other naturally occurring chromone.[9-11]

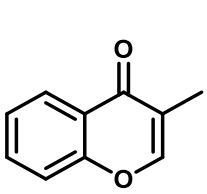


2

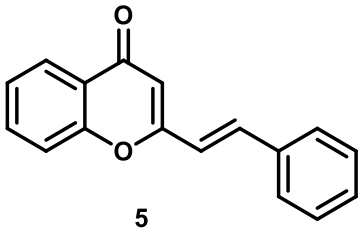


3

© University of Venda



4

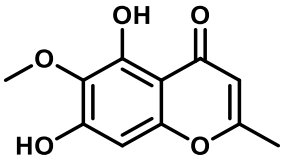


5

1.1.2 Naturally occurring chromones and their anti-tuberculosis activities.

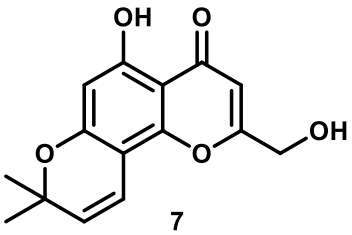
About half of all drugs in current use incorporate naturally occurring compounds and their derivatives. Naturally occurring pharmaceutical and chemical significance of chromones offer interesting possibilities in exploring their more pharmacological and biocidal potentials despite the large investment by the pharmaceutical industry in modern drug discovery technology, such as combinatorial chemistry and robotic based high-throughput screening.[12]

Wu *et al*. found pisonip B **6** and an abundance of additional compounds in a methanol extract of various parts of the shrub *Pisonia aculeate*. Using *Mtb* strain H37Rv, the antitubercular activity of each compound was tested *in vitro* and **6** was found to be in one of the most potent isolates having a MIC of 25 µg/mL.[23]



6

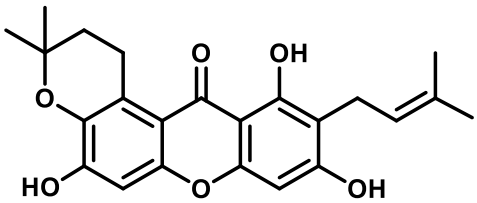
Tuntiwachwuttikul *et al.*, using the Microplate Alamar Blue Assay (MABA), evaluated the antitubercular activity of the extracts against *Mtb* H37Ra, with the most active isolate containing perforamone D **7** with MIC 25 µg/mL.[24]



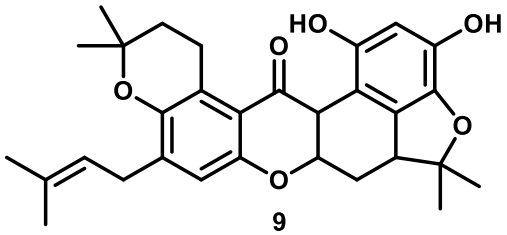
7

Namdaung *et al.* isolated compound **9** with the most potent antitubercular action (MIC 6.25 µg/mL) of all the compounds tested. Additionally, prenylated bioactive natural compounds have been extracted from *Garcinia mangostana* fruit hulls. Garcinone B **8** was found to the most effective of these compounds against *Mtb* H37Ra.[25]

© University of Venda



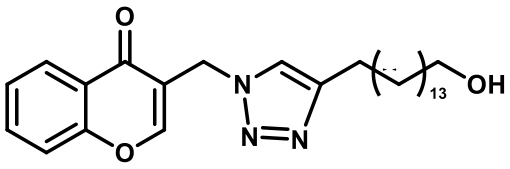
8



9

1.1.3 Synthetic anti-TB chromone derivatives

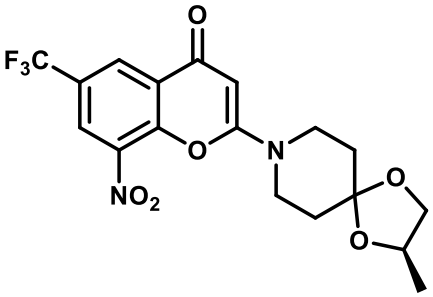
Chromone-embedded [1,2,3]-triazoles were synthesized and screened by Nalla *et al.* for *in vitro* antitubercular efficacy versus *Mtb* H37Rv. Compound **10** was found to be the most effective substance *in vitro*, with a MIC of 1.56 µg/mL, which was 4.8 times more potent than the reference medication ethambutol with MIC 7.64 µg/mL. Replacing the aromatic substituents on the triazole core with cyclic or acyclic aliphatic groups increased the antitubercular activity. With the exception of the 4-*t*-butyl group, replacing the substituents on the phenyl ring with linear alkyl groups did not improve activity. Enoyl acyl carrier protein reductase (InhA) was discovered as a possible target by molecular docking investigations conducted by the same group. This enzyme is involved in the production of mycolic acid.[26]



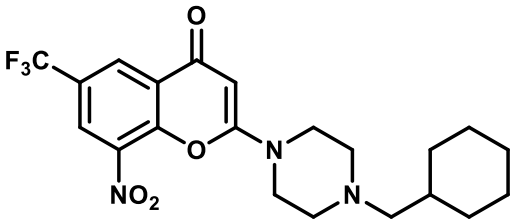
10

Li *et al*. synthesized the 2-azacyclo-5-trifluoromethyl-8-nitrobenzopyran-4-one derivatives **15-17** and evaluated their MABA MIC against *Mtb* H37Rv. The antitubercular activities of these derivatives were comparable to those of conventional drugs, but were inferior to their benzothiopyran-4-one equivalents. However, both benzothiopyranones and benzopyranones were created by scaffold morphing from benzothiazinones, and targeted DprE1 together with benzoxazinones.[30]

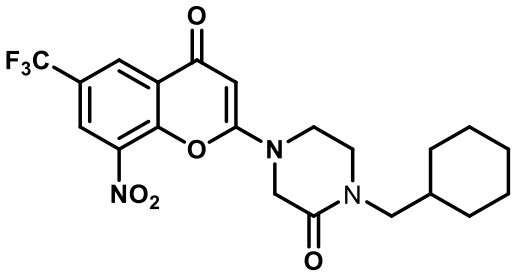
© University of Venda



15

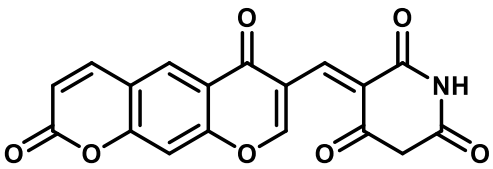


16



17

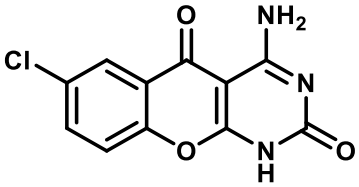
The synthesis and activity against *Mtb* H37Rv of 6-methyl-4,8-dioxo-4,8-dihydropyrano[3,2-g]chromone **11** in BACTEC 12B medium was reported by Laxmi *et al*. Analog **11** was determined to be the most active *Mtb* inhibitor, with the MABA MIC (IC_{90}) value = 5.90 µg/mL. It had higher antitubercular activity than the antitubercular medication pyrazinamide (IC_{90} > 20 µg/mL). With a selectivity index (SI) of 2.41, however, the chemical proved toxic to Vero cell lines. Compound **11** might therefore be regarded a candidate for further optimisation in the hunt for a novel anti-tuberculosis agent.[27]



11

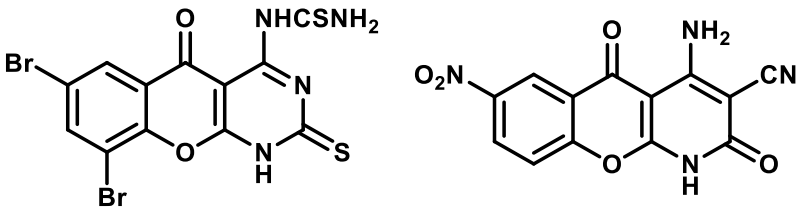
Haveliwa *et al*. synthesized several chromone-fused analogues of cytosine, which were tested against *Mtb* H37Rv by means of the Lowenstein-Jensen (L-J) technique. The most active compound against *Mtb* H37Rv strain, compound **12,** showed 99.9% inhibition at a concentration of 40 µg/mL. The electron-withdrawing 7-chloro substitution showed improved activity, but electron-donating groups were detrimental.[28]

© University of Venda



12

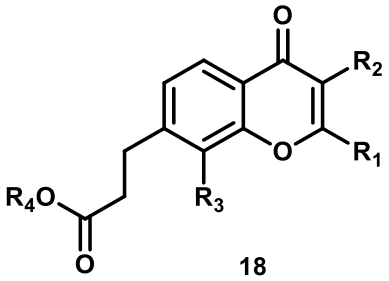
The activity of the chromone derivative was increased by attaching two bromo substituents to the phenyl ring in compound **13**, as determined by Haveliwa *et al*. As expected, the electron-withdrawing halogen substituents enhanced the inhibitory action. The same research group also described the production of functionalized H-[1]benzopyrano[2,3-b]pyridine derivatives using the Friedlander reaction of 2-amino-4-oxo-4*H*-chromene-3-carbonitriles with ethyl cyanoacetate. The L-J technique was used to study the antitubercular activity of these compounds against *Mtb* H37Rv at 62.5 □g/mL. Compound **14** was the most effective against the *Mtb* H37Rv strain in this experiment, inhibiting it by 99.9%.[29]



13 **14**

Ananthan *et al.* reported a series of multisubstituted benzopyran-4-ones that were among the active compounds found by high-throughput screening of entire cells. Of the 68 compounds tested against the *Mtb* H37Rv strain, 51% exhibited greater than 90% bacterial suppression in the first single dose testing. Compounds **18A–E** exhibited significant antitubercular action with MICs between 0.43 and 1.8 μg/mL. Commonly, C-3 and C-7 substituted compounds were the most powerful, regardless of the aromatic substituents at R_2 (directly connected to C-3 through carbon) resulted in higher activity than aromatic substituents attached via oxygen. Esters such as methyl, ethyl, cyclohexyl, and benzyl esters were discovered to be active. When R_1 was swapped with a methyl group, no change in efficacy was detected. Likewise, substituting the hydrogen at R_3 with a methyl had no effect on the compound's activity.[31]

© University of Venda



18

(**A**) R_1 = H, R_2 = 2-methylphenyl, R_3 = H, R_4 = Et, MIC_{90} (*Mtb* H37Rv) = 0.43 µg/mL

(**B**) R_1 = H, R_2 = 2-ethylphenyl, R_3 = H, R_4 = C_6H_{11}, MIC_{90} (*Mtb* H37Rv) = 0.47 µg/mL

(**C**) R_1 = CH_3, R_2 = 2-chlorophenyl, R_3 = H, R_4 = CH_3, MIC_{90} (*Mtb* H37Rv) = 0.82 µg/mL

(**D**) R_1 = H, R_2 = 2-chlorophenyl, R_3 = H, R_4 = CH_3, MIC_{90} (*Mtb* H37Rv) = 0.86 µg/mL

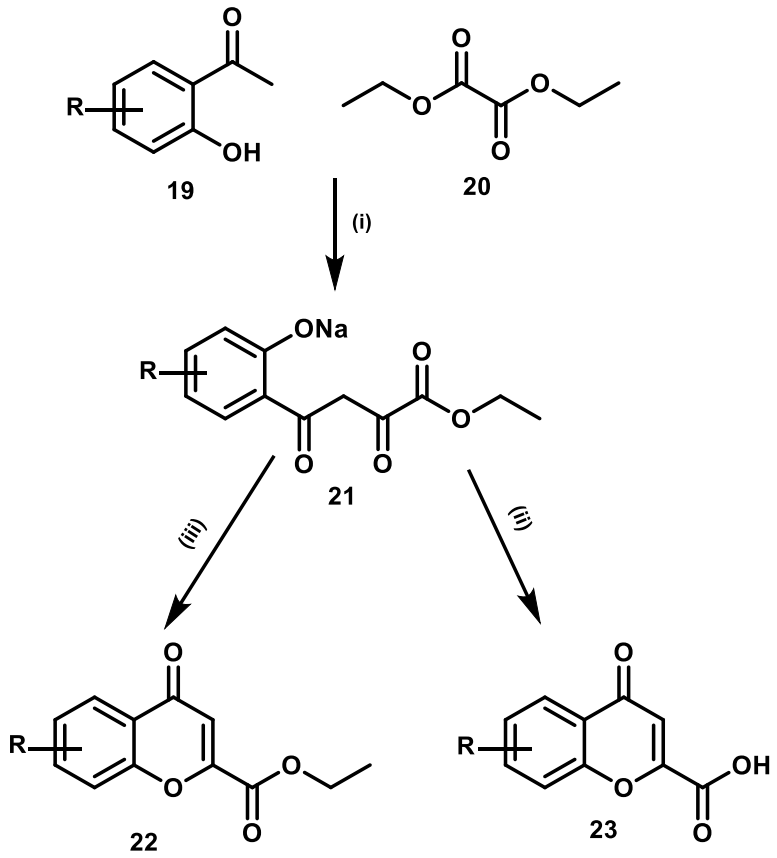
(**E**) R_1 = CH_3, R_2 = 2-chlorophenyl, R_3 = CH_3, R_4 = Et, MIC_{90} (*Mtb* H37Rv) = 1.8 µg/mL

1.1.4 Synthesis of chromones

1.1.4.1 Kostanecki's acylation reaction

The Kostanecki acylation is an organic synthetic method that involves acylating *o*-hydroxyaryl ketones **19** with aliphatic acid anhydrides **20**, followed by cyclization of the resultant compound **21** to afford chromones **22** and **23,** scheme 1.[36-37]

© University of Venda



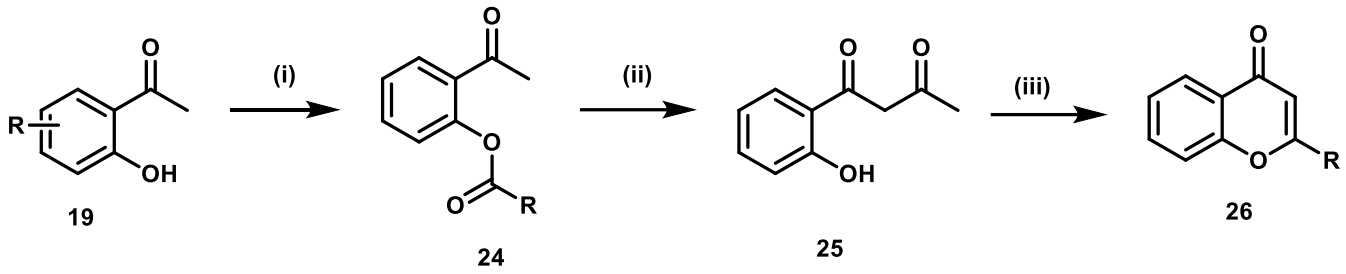
Reagents and conditions: (i) Base (ii) conc. HCl (iii) conc. HCl and AcOH

Scheme 1: Kostanecki's acylation reaction.

1.1.4.2 Baker-Venkataraman reaction

The Baker-Venkataraman rearrangement is the chemical reaction between 2-acetoxyacetophenones and bases resulting in 1,3-diketones. This rearrangement process commences with the synthesis of an enolate, which is subsequently followed by acyl transfer. The Baker-Venkataraman rearrangement is widely employed in the synthesis of chromones and flavonoids. Following the base-catalysed rearrangement, acid treatment often yields the chromone or flavone core. Esters **24** were prepared using $POCl_3$ with various aromatic carboxylic acids from substituted-2-hydroxyacetophonone **19**. Compounds **24** were treated with powdered KOH in dry pyridine to yield the corresponding 1,3-diones **25**. The resulting 1,3-diones thus obtained were cyclized to form 2-substituted chromone **26** using ethanoic acid as a solvent under reflux (Scheme 2).[38-39]

© University of Venda



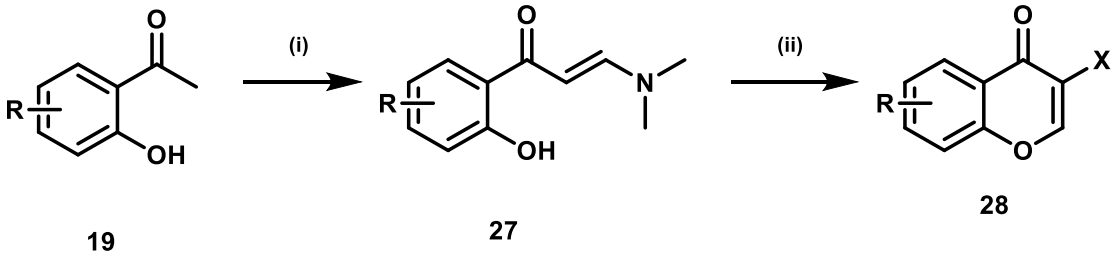
R = Aryl

Reagents: (i) RCOOH, $POCl_3$ (ii) KOH, piperidine (iii) CH_3COOH, reflux.

Scheme 2 Baker-Venkataraman reaction.

1.1.4.3 Gammill's Protocol

Gammill's protocol comprises condensation of substituted 2-hydroxyacetophenones **19** with DMF-DMA to form intermediates **27** as depicted by scheme 3. Ring closure of compounds **27** yields 3-halochromones **28**. Compound **28** is a precursor for the synthesis of isoflavones.[40-41]



R= halogen, aryl, alkyl

X= halogen

Reagents: (i) DMF-DMA, (ii) X_2, $CHCl_3$.

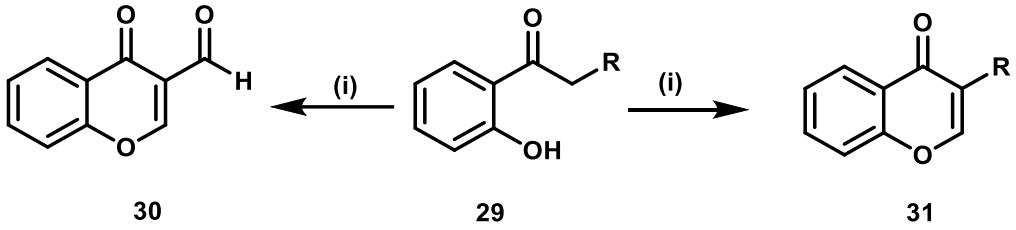
Scheme 3: Gammill's Protocol.

1.1.4.4 Vilsmeier−Haack reaction

The Vilsmeier-Haack reaction involves the reaction of 2-hydroxyarylalkylketone **29** and a formylating reagent, Vilsmeier-Haack reagent, is used to synthesize chromones. The chloroiminium ion formed *in situ* from the reaction with DMF and $POCl_3$ reacts with the ketone enolate formed from the 2-hydroxyalkylarylketone in this reaction. The reaction mechanism includes the formation of an unsubstituted chromone as an intermediate, which then

© University of Venda

undergoes a second attack of chloronium ion to yield chromone-3-carbaldehyde **30**, while a single attack results in the formation of 3-substituted chromones **31,** scheme 4.[42-43]



30 **29** **31**

R = H, allyl, benzyl, alkyl

Reagents: (i) DMF, $POCl_3$.

Scheme 4: Vilsmeier-Haack reaction.

© University of Venda

1.2 Tuberculosis

Tuberculosis (TB) is an illness caused by the microorganism *Mycobacterium tuberculosis* (*Mtb*) (Figure 1) and most commonly affects the lungs.[44-45] Every year, 10 million people contract TB.[44-45] Despite being a preventable and curable disease, about 1.5 million people die of tuberculosis each year, making it the world's leading infectious killer.[44-46] TB is the main cause of death of HIV positive patients and a key contributor to antimicrobial resistance. Approximately half of all TB cases are found in eight countries: Bangladesh, China, India, Indonesia, Nigeria, Pakistan, the Philippines, and South Africa.[44-47]



Figure 1: *Mycobacterium tuberculosis*.[48]

1.2.1 TB in South Africa

Tuberculosis has been the leading cause of death in South Africa for over 20 years. South Africa reports over 400 000 cases of tuberculosis (TB) each year, with over 300 people dying from the disease every day.[44] In 2020, deaths due to TB ranked second with 1.5 million deaths due to TB and HIV-TB after COVID-19. About 5.6 million males, 3.3 million females, and 1.1 million children were infected with TB worldwide in the year 2020.[44,47]

1.2.2 Symptoms and transmission of TB

Airborne bacteria invade and infect a person's airways and lungs, resulting in tuberculosis. When a tuberculosis patient coughs, spits, or sneezes, the TB organisms in their sputum are spread to other people.[44,55]

Cell-degrading enzymes are also used by these bacteria to destroy the tissue they infect. The infected patient will feel chest pain and cough up blood and sputum as a result. The lack of oxygen caused by lung damage can also cause hormonal imbalances, appetite loss, fatigue,

© University of Venda

and other symptoms. Infectious microbes have a proclivity to infect the kidneys, intestines, and brain, to name a few organs.[44-47]

1.2.3 Types of TB

1.2.3.1 Latent tuberculosis

When a person possesses TB bacteria in their body, they have latent TB, however, the bacteria are present at extremely low levels. People with latent tuberculosis are not contagious and do not feel ill. [44,49] They are unable to spread the tuberculosis bacterium to others. Latent TB has the potential to become active despite not being contagious. Latent infections are the root cause of most adult cases of active tuberculosis.[44,49]

1.2.3.2 Active tuberculosis

Tuberculosis is caused when a person has latent tuberculosis and becomes ill when tuberculosis bacteria multiply in the body and the immune system is unable to prevent them from spreading illness, resulting in tuberculosis symptoms. This is sometimes referred to as having active tuberculosis.[44,49] If active tuberculosis affects the lungs, the disease can spread quickly to other people when a person with tuberculosis coughs, speaks, or sings, TB bacteria are transferred via the air from one person to another. When TB bacteria are inhaled, they can settle in the lungs and begin to develop.[49-53]

1.2.4 Pathogenesis of TB

Airborne particles with 1–5 micron-diameter, known as droplet nuclei, carry mycobacterium tuberculosis. People with pulmonary or laryngeal tuberculosis produce infectious droplet nuclei when they cough, sneeze, yell, or sing.[44,44] Depending on the surrounding conditions, these minute particles can float in the air for several hours.[55] The transmission of mycobacterium tuberculosis is through the air, not through surface contact. Transmission happens when a person inhales *Mtb* containing droplet nuclei.[56] The droplet nuclei of TB go through the mouth or nasal passages, upper respiratory tract, and bronchi to the alveoli of the lungs (Figure 2).[57-58]

© University of Venda

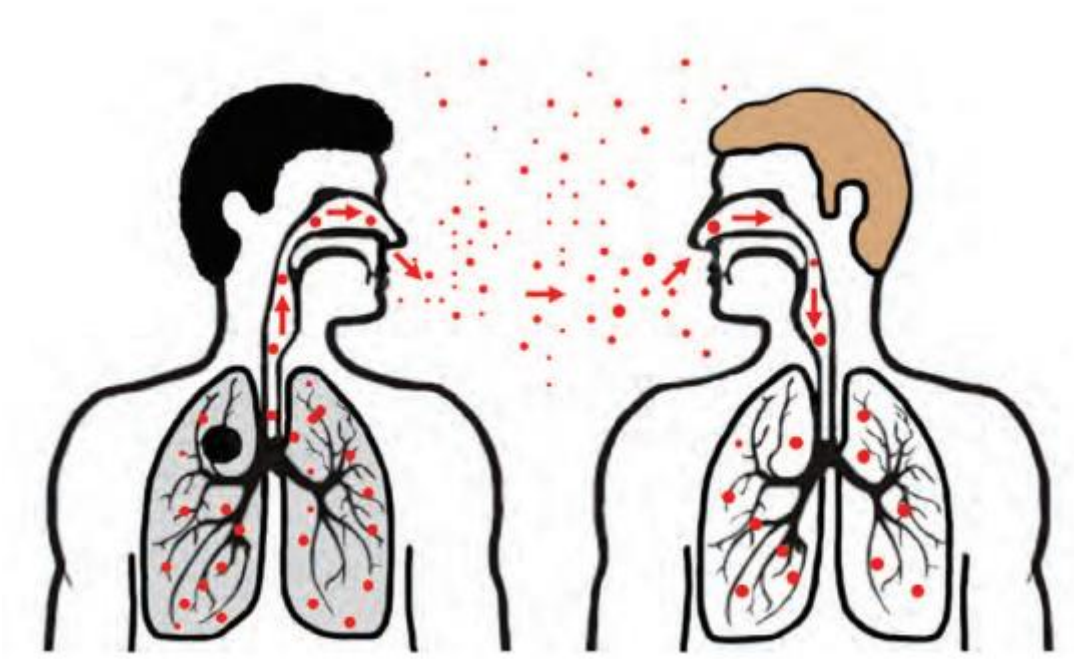


Figure 2: Transmission of TB.[6]

Within the first week following inhalation of the TB bacillus, the first stage takes place. Once the bacillus reaches the lung's alveoli, macrophages absorb it. The macrophages ingest the TB bacillus. The quantity of TB bacilli present, and the macrophage's potency largely dictate. After a week, if the macrophage is unable to suppress the TB bacillus, the infection advances to the second stage.[60] There are two new TB bacilli for every original one when the bacilli start to grow rapidly. As a result, the original TB bacillus multiplies quickly, and the macrophages are powerless to stop the spread. This phase lasts for three weeks after the first infection.[58-60] Following the third week, the infection moves into its third stage, during which the proliferation of bacilli and their destruction by macrophages seem to be in balance. The TB bacilli can survive for years inside macrophages while being shielded from lung tissue. Patients at this stage are not contagious. Roughly 5% of individuals do not heal from the original complex, and 12 to 24 months after the first infection, the TB bacilli reactivate, this is stage 4 of the disease. At this point, the patient is very contagious because active TB bacteria are present in their sputum.[64]

1.2.5 Drug Resistance

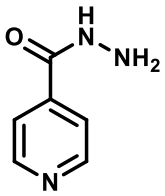
One of the most serious dangers to global health and economic security is antimicrobial resistance. Drug-resistant tuberculosis (DR-TB), for example, accounts for around one-third of all antimicrobial resistance deaths globally.[44-47] Drug-resistant tuberculosis is a type of antimicrobial resistance that is difficult to treat and expensive. It is caused by tuberculosis bacteria that are resistant to at least one of the first-line TB drugs now available, resulting in

© University of Venda

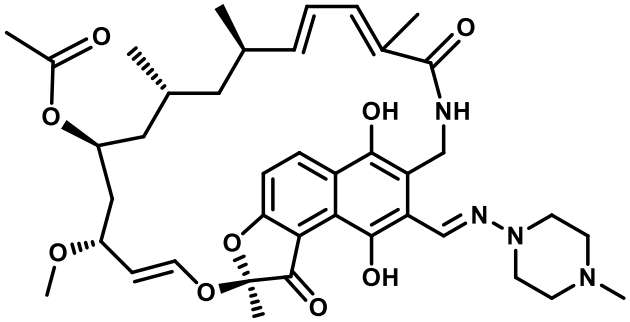
fewer treatment options and higher fatality rates.[44,59] Multi-drug resistant TB (MDR-TB) refers to TB bacteria that are resistant to two of the most significant TB medications, isoniazid (INH) and rifampicin (RIF). Extensively drug-resistant tuberculosis (XDR-TB) occurs when an individual develops MDR-TB that is resistant to additional medications such as fluoroquinolones and injectables. Because XDR-TB disease is resistant to first-line and second-line drugs, patients are left with treatment options that are more toxic, more expensive, and much less effective.[54-61]

1.2.6 Treatment of TB

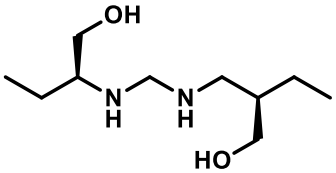
Most TB patients can be cured with treatment.[44] The current gold standard of care for patients with drug-susceptible TB illness is a 6-months regimen of four first-line medications: isoniazid **32**, rifampicin **33**, ethambutol **34**, and pyrazinamide **35**. This is despite the fact that the components of TB treatment regimens have changed over time.[44,64]



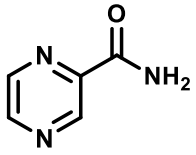
32



33



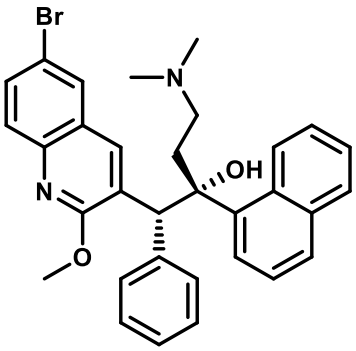
34



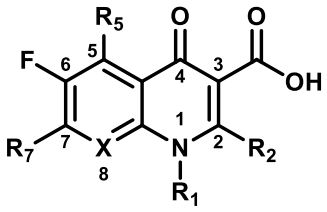
35

Rifampicin-resistant TB (RR-TB), isoniazid-resistant TB (IR-TB), and multidrug-resistant TB (MDR-TB, defined as resistance to both isoniazid **32** and rifampicin **33**) require second-line drugs like bedaquiline **36** and fluoroquinolones **37**, which are more expensive and have more side effects than first-line treatments for drug-susceptible TB.[44] Pre-XDR-TB (TB resistant to rifampicin **33** and any fluoroquinolone **37**) and XDR-TB (TB resistant to rifampicin **33**, any fluoroquinolone **37**, and at least one of bedaquiline **36** or linezolid **38**) are even more difficult to treat.[44-47,69] The new medication delamanid **39** was authorised in 2012 to treat MDR-TB. Delamanid plus a background regimen led to a higher rate of study patients becoming non-infectious than placebo plus a background regimen, according to a phase 2B experiment.[44,69]

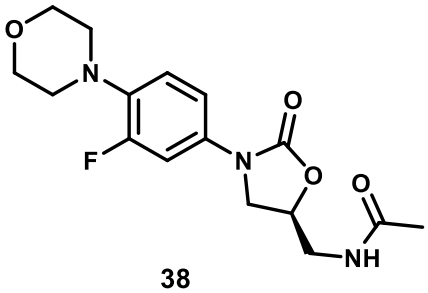
© University of Venda



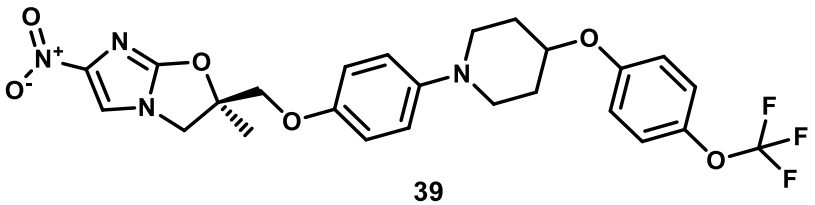
36



37



38



39

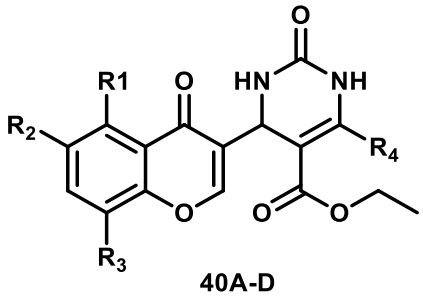
© University of Venda

CHAPTER 2: PROBLEM STATEMENT AND MOTIVATION OF STUDY

Tuberculosis is a deadly illness that can easily spread through the air when someone coughs or sneezes. TB is still a serious and enduring danger to world health. TB remains one of the top infectious agents that cause death. Over 1.6 million people died from active TB in 2021, which is estimated to have infected 10,6 million individuals.[44] Although various treatment protocols of TB are available, the epidemic is also being fuelled by the recent pandemic and the rise of anti-TB treatment resistance. Furthermore, limited approved medications are available to treat extensively and multi-drug-resistant tuberculosis. Additionally, therapy is too costly, ineffective, and has negative side effects.[44-47]

Heterocyclic systems are extremely essential in the field of medicinal chemistry due to their wide range of established applicability. More than 85% of all chemical entities that provoke a biological reaction are believed to consist of at least one heterocycle.[8-10] Flavones, isoflavones, and chromones are heterocyclic compounds that play a crucial role in the development of novel pharmacological entities for therapeutic applications. In response to the constraints of conventional TB therapies, scientists have already designed and developed novel chemical entities (NCEs) containing potential antitubercular chemicals.[12-14]

Raju and co-workers[70] developed a range of chromon-3-yl-1,2,3,4-tetrahydropyrimidine-5-carboxylates and evaluated their antimycobacterial efficacy against *Mtb* H37Rv *in vitro* with the agar dilution technique. Six compounds, **40A–D**, and **41A-B**, exhibited outstanding action with MIC values between 3.4 and 7.4 μM and were more effective than the conventional medications ethambutol (MIC - 7.6 μM) and ciprofloxacin (MIC - 9.5 μM). The electron-withdrawing trifluoromethyl group in position 6 (R_4) of the 1,2,3,4-tetrahydropyrimidine-5-carboxylate derivatives promotes antimycobacterial action more effectively than the methyl and phenyl substituents. In addition to halides, nitro substitution on the phenyl ring plays a significant role in increasing activity.[70]



40A-D

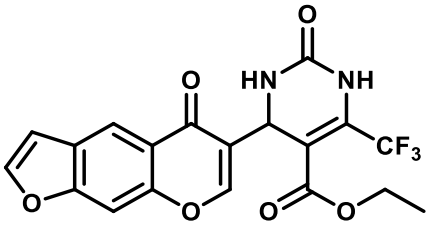
(**A**) R1 = H, R_2 = Ph, R_3 = H, R_4 = CF_3, MIC (*Mtb* H37Rv) = 3.4 μM

(**B**) R1 = CH_3, R_2 = H, R_3 = H, R_4 = CF_3, MIC (*Mtb* H37Rv) = 3.9 μM

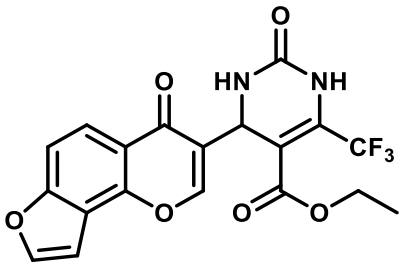
© University of Venda

(**C**) R1 = H, R_2 = NO_2, R_3 = H, R_4 = CH_3, MIC (*Mtb* H37Rv) = 4.2 µM

(**D**) R1 = H, R_2 = H, R_3 = NO_2, R_4 = CH_3, MIC (*Mtb* H37Rv) = 4.2 µM



41A



41B

The potency of these derivatives was also maintained when a furan ring was attached to the phenyl moiety of chromones **41A-B**.[70] These findings by Raju and colleagues[31] drove our interest into further investigating these compounds in this study.

© University of Venda

CHAPTER 3: AIM AND OBJECTIVES

3.1 Aim of the study

The aim of the study is to design, synthesize chromone-based carbaldehyde derivatives and their evaluation as potential antituberculosis agents.

3.2 Objectives of the study

I. To synthesize 5-substituted/unsubstituted-3-iodo-2-hydroxyacetophenones and convert them to 6-substituted/unsubstituted-8-iodochromone-3-carbaldehydes.

II. Conversion of 6-substituted/unsubstituted-8-iodochromone-3-carbaldehydes to 6-substituted/unsubstituted 8-iodochromone-3-carboxylic acids and 6-substituted/unsubstituted 8-iodochromone-3-carboxamides.

III. Conversion of these compounds to carbamates and other derivatives.

IV. Conversion of chromone-3-carbaldehydes to chromone-1,2,3,4-tetrahydropyrimidine-5-carboxylate derivatives.

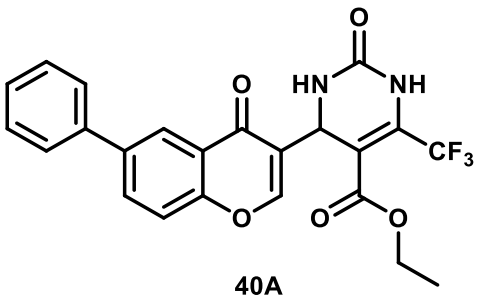
V. To characterize the synthesized compounds using various spectroscopic techniques.

VI. Biological screening of the synthesized compounds as potential anti-tuberculosis agents.

© University of Venda

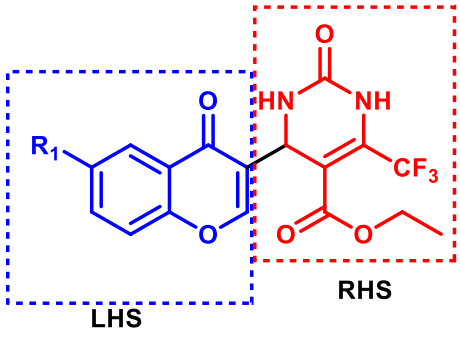
CHAPTER 4: RESULTS AND DISCUSSION

Pyrimidines and chromones are privileged scaffolds with proven desirable antimycobacterial properties. A study conducted by Raju *et al.* incorporated pyrimidine and chromone derivatives and evaluated them for anti-tuberculosis activity against the clinical *Mtb* strain H37Rv.[31] Of the synthesized derivatives, ethyl 4-(6-phenylchromone-3-)-2-oxo-6-trifluoromethyl-1,2,3,4-tetrahydropyrimidine-5-carboxylate **40A** was identified as the most effective compound with a MIC value of 3.4 μM, more effective than the conventional medications ethambutol (MIC - 7.6 μM) and ciprofloxacin (MIC - 9.5 μM). Most of the compounds from this series exhibited cytotoxicity against a human cell line. This provides an opportunity to improve cytotoxicity, activity and other physiochemical properties of these compounds in an effort to find novel compounds to combat TB and drug-resistant TB.[70]



40A

This lead compound **40A** can be considered as consisting of two structurally distinct parts: the left-hand side (LHS) chromone moiety and the right-hand side (RHS) pyrimidine system. The presence of the pyrimidine ring is crucial for antitubercular activity. The electron-withdrawing trifluoromethyl group in position-6 on the RHS improves the activity. In addition to halides, nitro substitution on the phenyl ring of the chromone plays a significant role in increasing activity. [70] In the present study, the main focus will be the functionalization on the LHS chromone core of the molecule **52**, and here we report the synthesis and characterization of the desired target compounds.



52

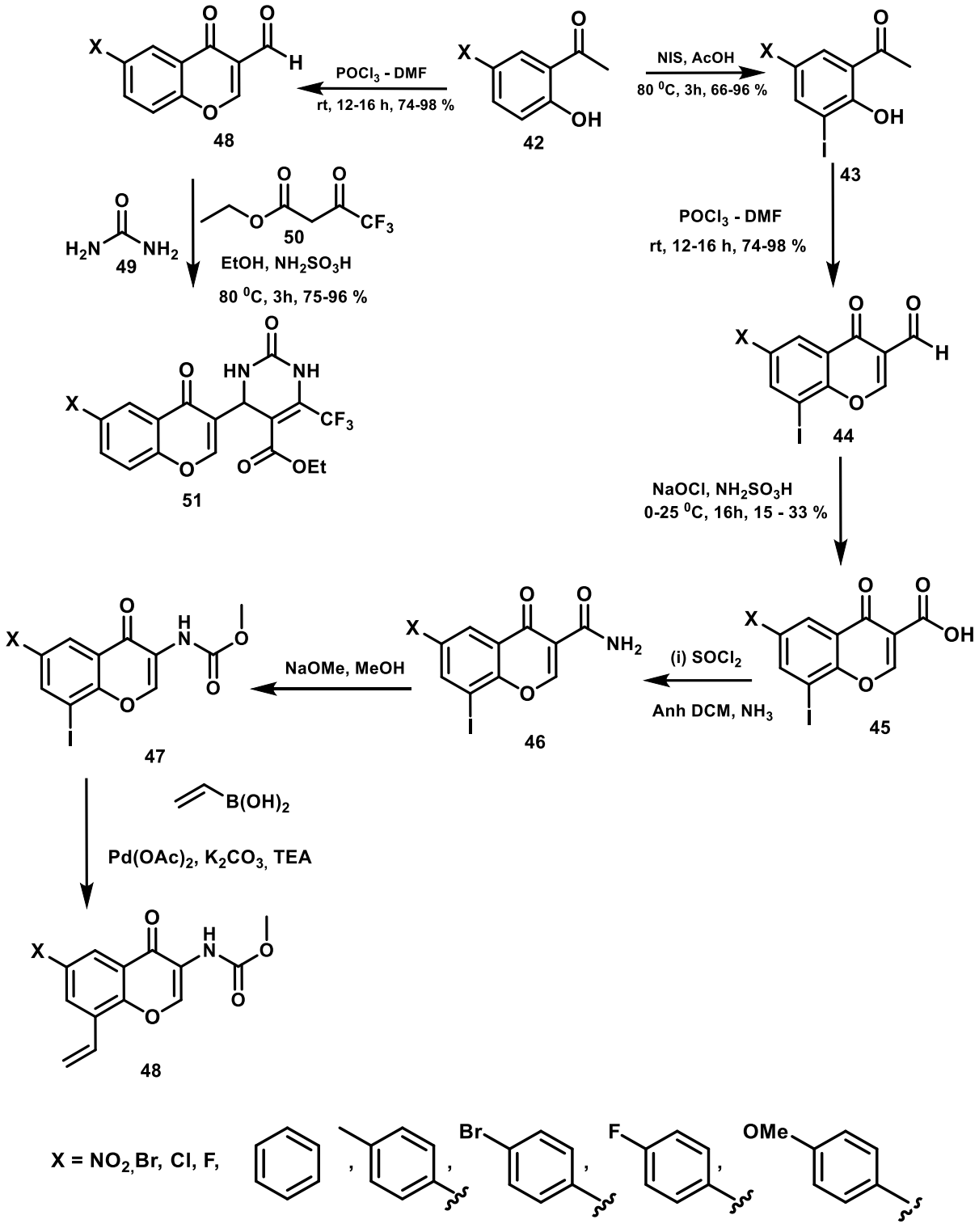
© University of Venda

4.1 RESEARCH METHODOLOGY

Scheme 5 summarizes the generic proposed synthetic scheme of two types of target compounds, namely 6,8-disustituted-chromone-3-carbamates **48A-I** and 4-(6-substituted/unsubstituted-chromon-3-yl)-1,2,3,4-tetrahydropyrimidine-5-carboxylates investigated in this study. The precursors, 2-hydroxyacetophenones **42A-B** were used to synthesize the first series of compounds (Scheme 5). The Vilsmeier-Haack reaction was used to synthesize the 6,8-disubstituted/unsubstituted chromone-3-carbaldehydes **44A-B** from the corresponding 3,5-disubstituted/unsubstituted 2-hydroxyacetophenone analogues **43A-E**.[68-69] The 6,8-disubstituted/unsubstituted chromone-3-carbaldehydes were oxidized to obtain 8-iodo-6-substituted/unsubstituted chromone-3-carboxylic acid derivatives **45A-B** to be converted into corresponding carbamates **47A-E**.

The second series of compounds **51A-E** was synthesized by applying the Biginelli reaction of chromone-3-carbaldehydes **48A-F** with urea and ethyl 4,4,4-trifluoromethyl acetoacetate as outlined in Scheme 5. The chromone-3-carbaldehydes **48A-E** were synthesized utilizing the Vilsmeier–Haack reaction of the corresponding 2-hydroxyacetophenones **42A-E** as outlined in **Scheme 5**. All synthesized products were characterized using ^{1}H, ^{13}C, and DEPT NMR, FT-IR spectroscopic techniques and LC-MS for target compounds.

© University of Venda

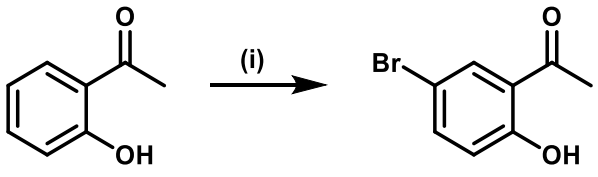


Scheme 5: Proposed synthetic scheme.

© University of Venda

4.1.1 Synthesis of 5-bromo-2-hydroxyacetophenone 42B

Scheme 5 in section 4.1 clearly shows the need for an array of 5-substituted/unsubstituted 2-hydroxyacetophenone derivatives **42**. While 5-flouro and 5-chloro-2-hydroxyacetophenone derivatives were bought from commercially suppliers, 5-bromo and 5-nitro-2-hydroxyacetophenone derivatives were prepare from 2-hydroxyacetophenone. The results of the preparations of these reagents are presented below. The synthesis of 5-bromo-2-hydroxyacetophenone **42B** was carried out using commercially available 2-hydroxyacetophenone **42A** which was then halogenated using NBS in acetic acid and heating under reflux for two hours (Scheme 6). After the reaction solution was allowed to cool, the resulting reaction mixture was filtered, evaporated to dryness, and recrystallized from ethanol to yield pure 5-bromo-2-hydroxyacetophenone **42B** in 54% yield.[71]



42A **42B**

Reagents and conditions: (i) NBS, AcOH, reflux, 2 h.

Scheme 6: Synthesis of 5-bromo-2-hydroxyacetophenone **42B**.

Proton, carbon, DEPT NMR and Fourier transform infrared (FT-IR) spectroscopy were used to characterize the synthesized 5-bromo-2-hydroxyacetophenone **42B**. The ^{1}H NMR spectrum (Figure 3 and 4) revealed 3 proton signals or resonances in the aromatic region and one signal in the aliphatic region, as expected. The first signal confirming the structure of the synthesized compound **42B** was the aromatic 6-H, resonating as a doublet at 7.75 – 7.74 ppm. The second proton signal, 4-H, was observed as a doublet of doublets in the aromatic region, resonating at 7.47 - 7.44 ppm, the third signal in the aromatic region was 3-H, a doublet at 6.82 ppm – 6.79 ppm. Thus, all aromatic protons were accounted for. Additionally, a 3-proton singlet resonating at 2.55 ppm confirmed the presence of CH_3. Finally, a characteristic downfield singlet at 12.98 ppm confirmed the presence of a chelated OH proton.

The ^{13}C NMR spectrum (Figure 5) revealed 8 carbon signals or resonances, C-5 resonating at 110.4 ppm and C-3 resonating at 120.4 ppm. The FT-IR spectrum (figure 44 in the appendix) revealed the presence of aromatic C-H bonds at 3063.8 cm^{-1}, and the C=O group at 1641.3

© University of Venda

cm^{-1}. The attachment of Br at the *meta* position or C-5 was confirmed by DEPT 135 (Figure 6) as only three aromatic CH signals can be observed. Figures 3 – 6 show spectra for **42B**.

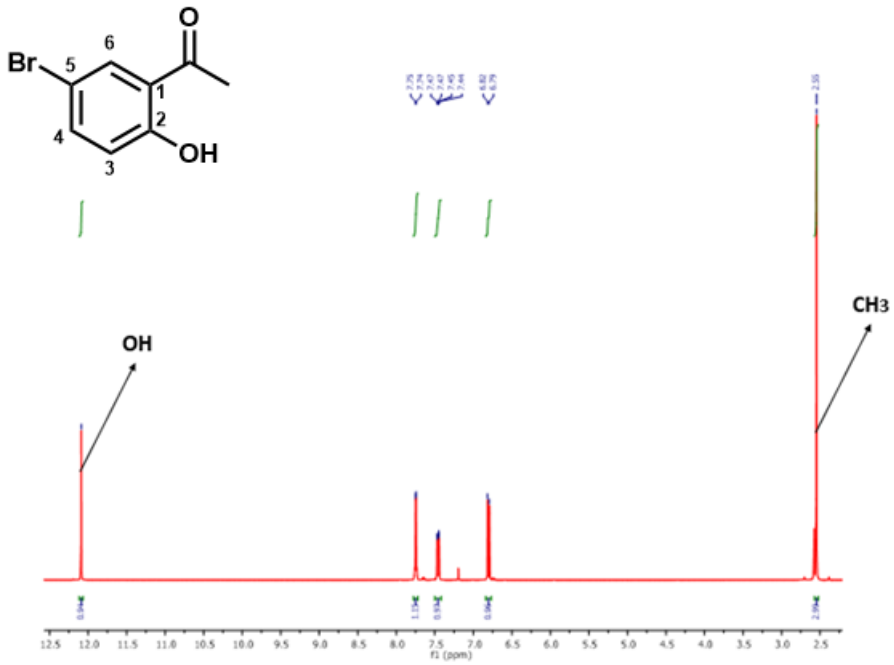


Figure 3: ^{1}H NMR spectrum of compound **42B** in $CDCl_3$ (at 400 MHz).

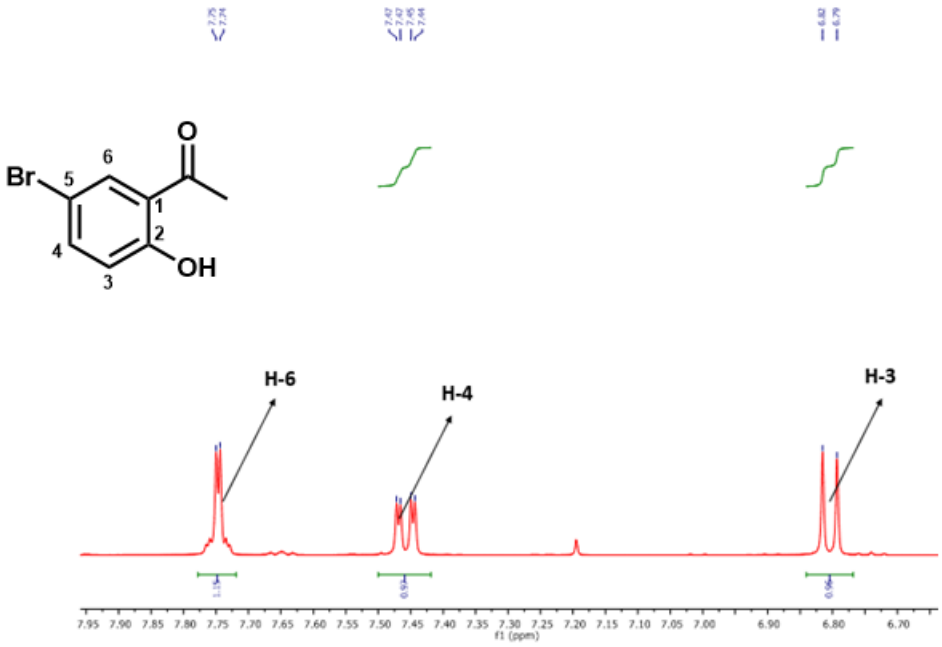


Figure 4: Expanded ^{1}H NMR spectrum of compound **42B** in $CDCl_3$ (at 400 MHz).

© University of Venda

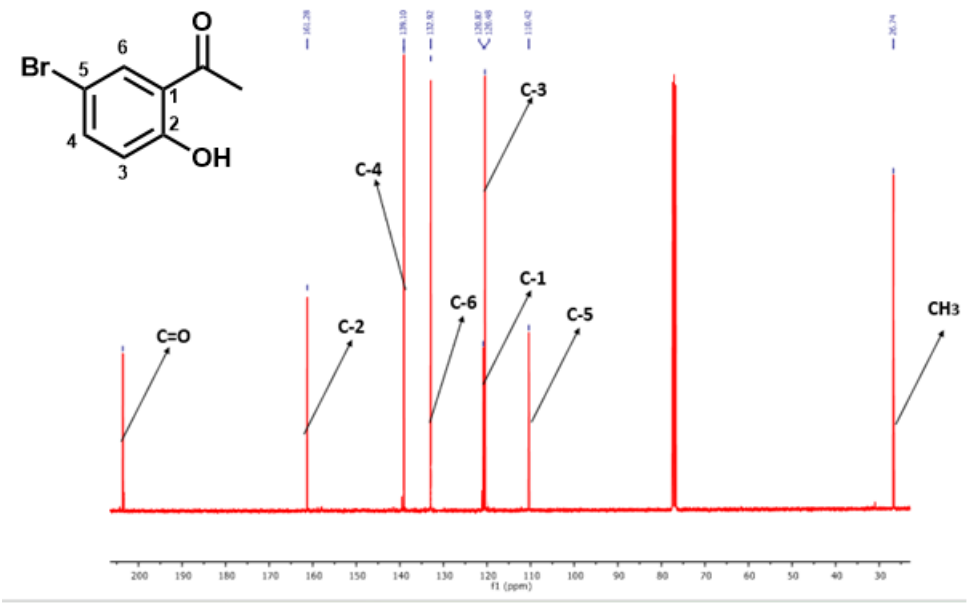


Figure 5: ^{13}C NMR spectrum of compound **42B** in $CDCl_3$ (at 100 MHz).

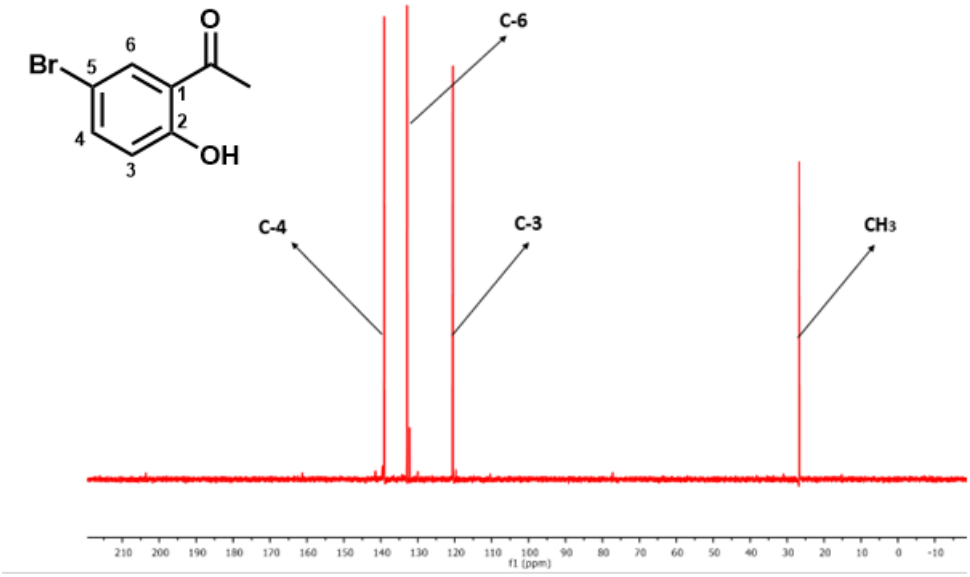
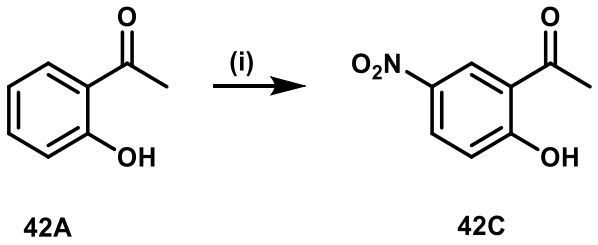


Figure 6: DEPT 135 spectrum of compound **42B** in $CDCl_3$.

© University of Venda

4.1.2 Synthesis of 5-nitro-2-hydroxyacetophenone 42C

Next in this investigation, commercially available 2-hydroxyacetophenone **42A** was nitrated by reacting it with nitric and sulfuric acids at 0 - 25 ℃ for 3 hours (Scheme 7). The mixture was quenched with water, and a yellow precipitate was formed. The product was filtered, dried, and recrystallized from ethanol to yield 5-nitro-2-hydroxyacetophenone **42C** in a reasonable yield of 56%.



42A **42C**

Conditions: (i) Nitric acid, sulfuric acid, stir, 0 – 25 °C, 3 h.

Scheme 7: Synthesis of 5-nitro-2-hydroxyacetophenone **42C**.

Utilising NMR (^{1}H, ^{13}C, DEPT) and FT-IR spectroscopy, the synthesized 5-nitro-2-hydroxyacetophenone **42C** was characterized. Melting point was also determined. The ^{1}H NMR spectrum (Figure 7 and 8) revealed 3 proton signals in the aromatic region and one signal in the aliphatic region as expected. The aromatic 6-H signal of compound **42C** resonated at 8.72 ppm as a doublet. Aromatic proton 4-H was observed as a doublet of doublets resonating at 8.36 – 8.33 ppm, and the third aromatic proton was observed as a doublet at 7.10 – 7.03 ppm. Thus, all aromatic protons were accounted for. Additionally, a signal was observed in the aliphatic region as a 3-proton singlet resonating at 2.77 ppm for CH_3. Lastly, the characteristic downfield singlet at 12.98 ppm confirmed the presence of an OH proton.

The ^{13}C NMR spectrum (Figure 9) revealed 8 carbon signals, with C-5 resonating at 139.5 ppm and C-3 resonating at 1195 ppm. The FTIR spectrum revealed the presence of aromatic C-H bonds at 3063.8 cm^{-1}, and the C=O group at 1641.3 cm^{-1}. Figures 7 – 9 show spectra for **42C**.

© University of Venda

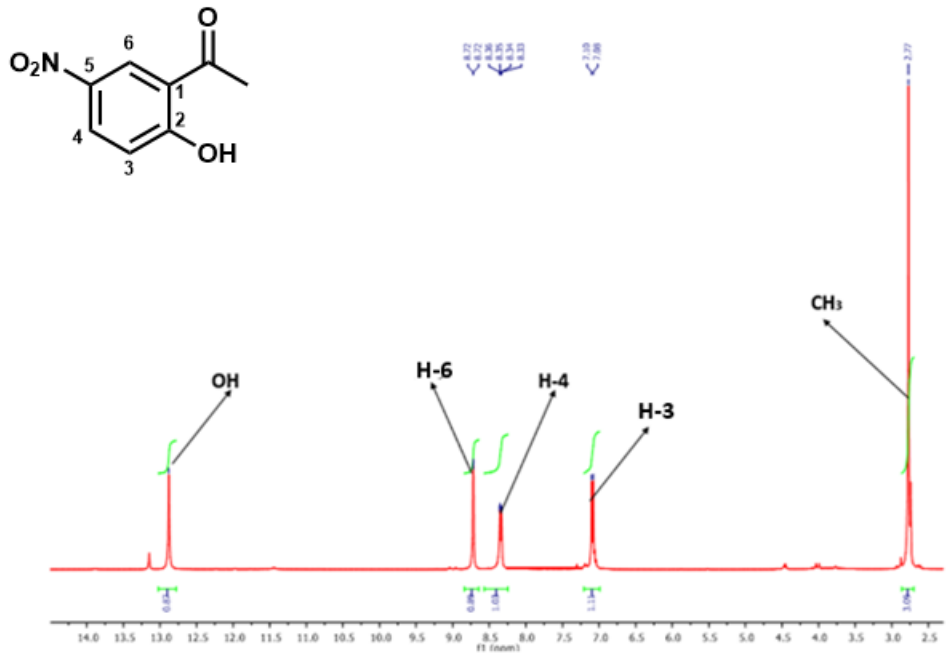


Figure 7: ^{1}H NMR spectrum of compound **42C** in $CDCl_3$ (at 400 MHz).

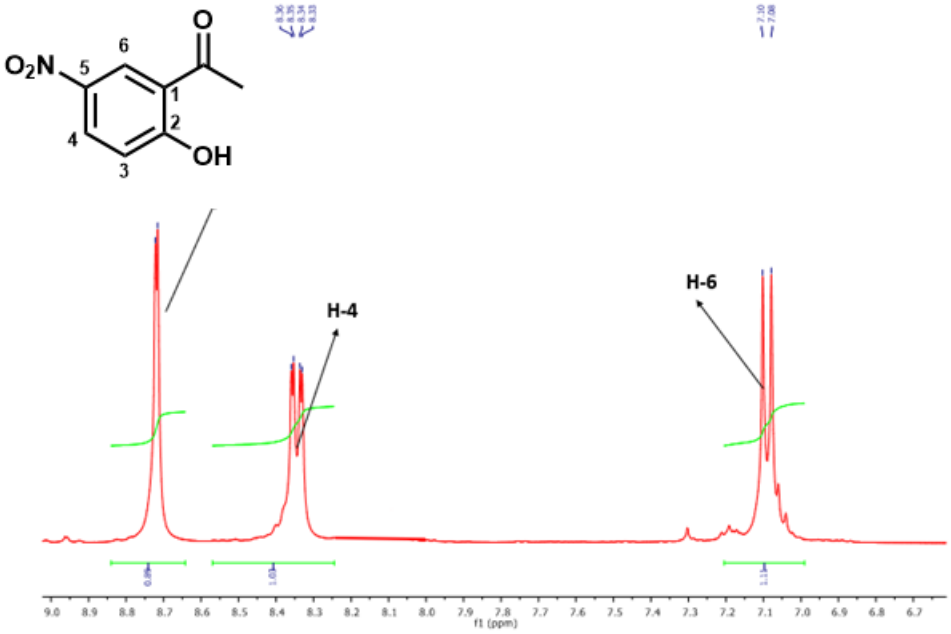


Figure 8: Expanded ^{1}H NMR spectrum of compound **42C** in $CDCl_3$ (at 400 MHz).

© University of Venda

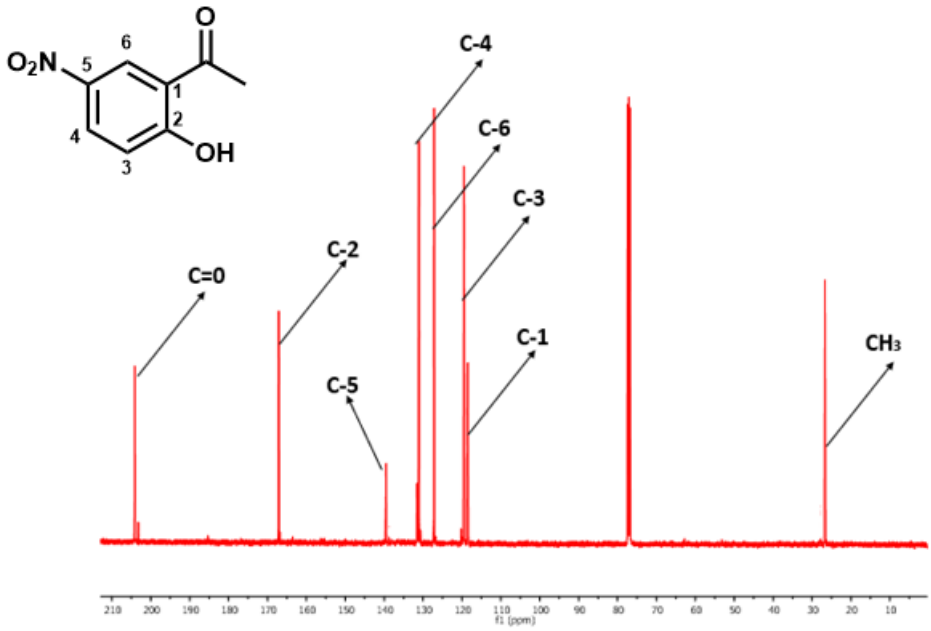
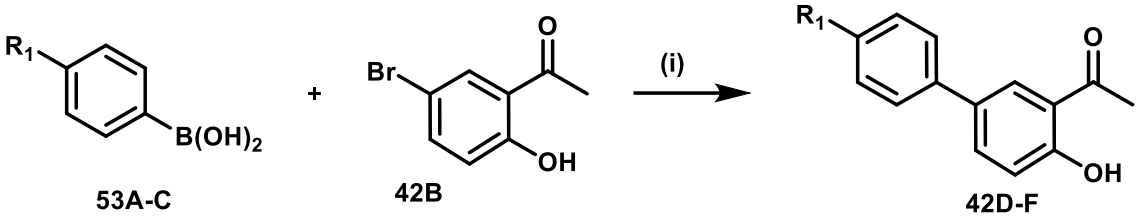


Figure 9: ^{13}C NMR spectrum of compound **42C** in $CDCl_3$ (at 100 MHz).

4.1.3 Synthesis of 5-[4-substituted/unsubstituted-phenyl]-2-hydroxyacetophenone derivatives 42D-F

Building on the synthesis of 5-bromo-2-hydroxyacetophenone **42B**, we next investigated its application in Suzuki cross coupling reactions to access a range of 5-[4-substituted/unsubstituted-phenyl]-2-hydroxyacetophenone derivatives **42D-F**.[73] 5-Bromo-2-hydroxyacetophenone **42B** was subjected to Suzuki cross-coupling reaction, by treatment with 4-substituted/unsubstituted phenylboronic acids and a catalytic amount of palladium acetate in triethylamine and stirring for 16-24 hours under reflux conditions (Scheme 8). To obtain corresponding 5-[4-substituted/unsubstituted-phenyl]-2-hydroxyacetophenone derivatives **42D-F**, the reaction mixture was quenched with ice water, and the solid was filtered, dried, and recrystallized from ethanol. Table 1 below shows mass yield and melting point values for 5-[4-substituted/unsubstituted phenyl]-2-hydroxyacetophenone derivatives **42D-F**.

© University of Venda



Reagents and conditions: (i) $Pd(OAc)_2$, TEA, Na_2CO_3, H_2O, 120 °C, 16 - 24 h.

Scheme 8: Synthesis of 5-[4-substituted/unsubstituted phenyl]-2-hydroxyacetophenone derivatives **42D-F**.

Table 1: Synthesized 5-[4-substituted/unsubstituted-phenyl]-2-hydroxyacetophenone derivatives **42D-F**.

Compound 42	R_1	Mass yield (g)	% Yield	Lit. melting point (℃)	Melting point (℃)
D	F	3.7	93	-	58
E	Br	0.52	47	-	61
F	H	2.3	80	57 - 59	56 - 59

^{1}H NMR spectra revealed 7 proton signals for **42D-E** and 8 for proton signals **42F** at the aromatic region and one signal at the aliphatic region as expected. The first signal observed to verify synthesized compound **42D-F** was aromatic H-2' resonating around 7.50 ppm with a multiplicity of a multiplet and integration of 2 protons. The second signal H-3' was observed as a multiplet around the aromatic region, resonating around 7.42 ppm with an integration of 2 protons, the third signal, around the aliphatic region is a singlet resonating around 2.63, corresponds to protons of the acetyl group. Finally, the presence of a singlet further downfield at 12,98 ppm showed a characteristic OH proton. ^{13}C NMR spectra (Table 2) revealed 14 carbon signals, C-5 resonating at 111.1 ppm - 156.7 ppm and C-3 resonating at 86.2 ppm - 87.7 ppm. ^{13}C NMR spectrum for **42D** revealed some carbon signals doubled, this is influenced by the interaction between the carbons and fluorine. All carbons signals on the corresponding structure were accounted for. Figures 10 – 12 shows spectra for **42F**. Figures 45, 46 and 47 in the appendix present ^{1}H NMR, expanded ^{1}H NMR and ^{13}C NMR spectra for **42D**, respectively.

© University of Venda

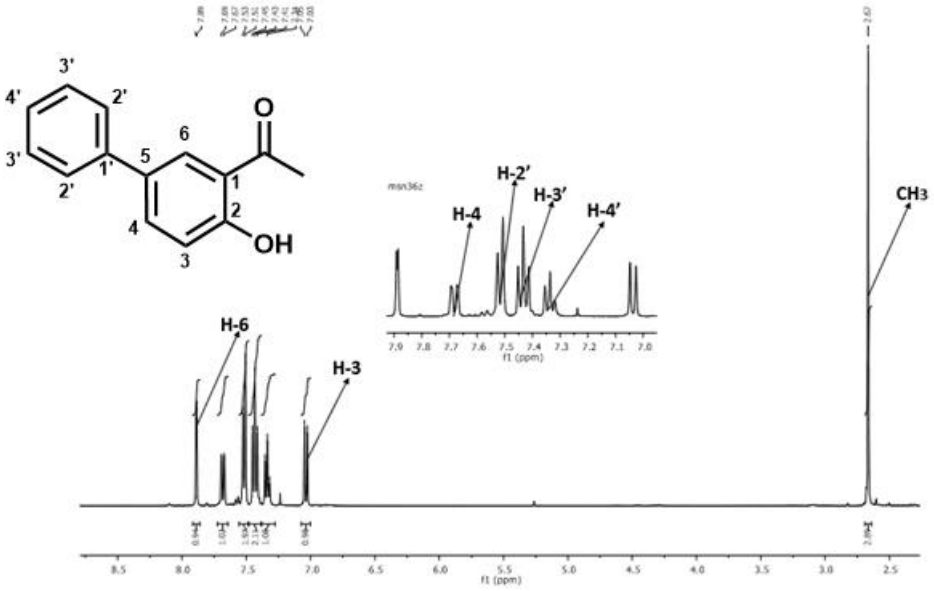


Figure 10: ^{1}H NMR spectrum of 2-hydroxy-5-phenylacetophenone **42F**.

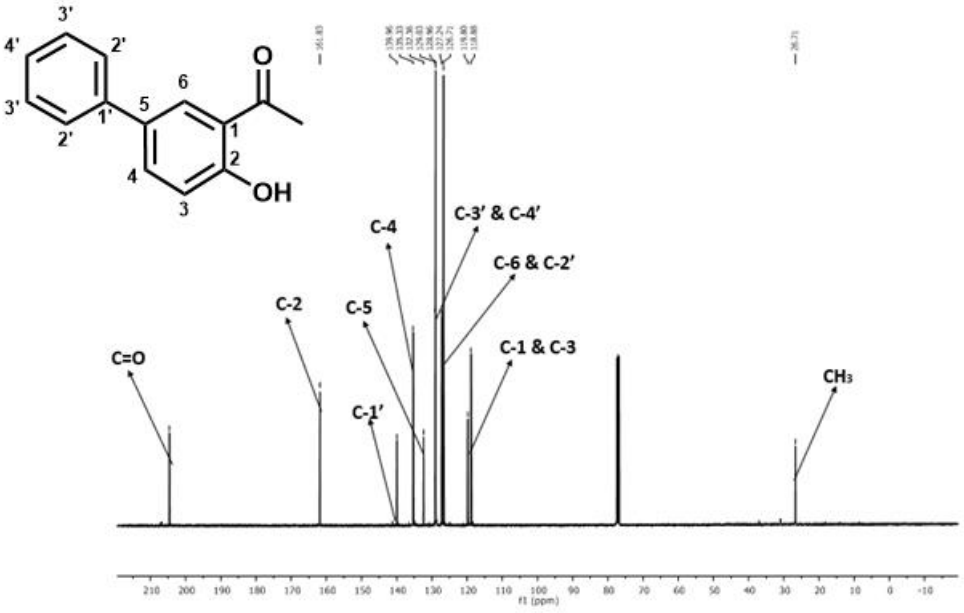


Figure 11: ^{13}C NMR spectrum of 2-hydroxy-5-phenylacetophenone **42F**.

© University of Venda

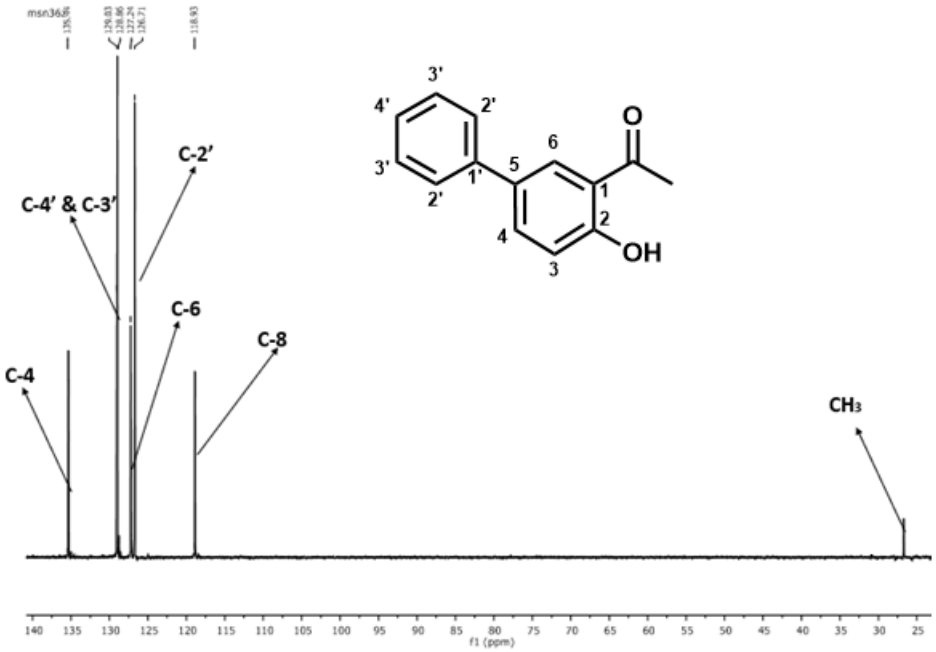


Figure 12: DEPT 135 spectrum of 2-hydroxy-5-phenylacetophenone **42F**.

.

© University of Venda

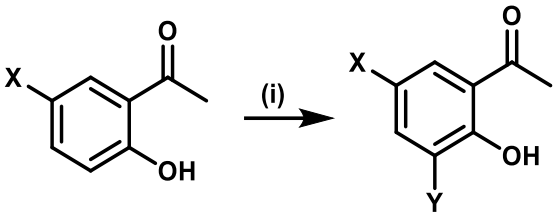
Table 2: ^{13}C NMR chemical shift values (ppm) of 5-substituted/unsubstituted-2-hydroxyacetophenones **42D-F** in $CDCl_3$ (at 100 MHz).

NUCLEUS	42D	42E	42F
C-1	119.9	121.1	119.8
C-2	161.9	158.0	161.8
C-3	119.2	119.7	118.8
C-4	135.4	134..2	135.3
C-5	131.6	132.9	132.4
C-6	129.1	129.9	127.7
C=0	204.8	203.3	204.2
CH_3	26.9	26.8	26.71
C-1'	136.3	139.1	139.9
C-2'	128.5	141.5	126.7
C-3'	116.0	132.3	128.9
C-4'	163.5	113.2	129.0

4.1.4 Synthesis of 3,5-disubstituted/unsubstituted 2-hydroxyacetophenones 43A-E

With 5-susbstituted 2-hydroxyacetophenone derivatives in hand, iodination and bromination of these derivatives were investigated. Both synthesised and commercially available 5-substituted/unsubstituted 2-hydroxyacetophenones **42A-E** were halogenated in acetic acid under reflux for 2 hours using NIS/NBS (Scheme 9).[71] The resultant solids were isolated by filtration, dried, and then recrystallized from ethanol to produce the resultant 3,5-disubstituted/unsubstituted 2-hydroxyacetophenones **43A-E**.

© University of Venda



42A-E 43A-E

Conditions: (i) NIS/NBS, AcOH, reflux, 2 h.

Scheme 9: Synthesis of 3,5-disubstituted/unsubstituted 2-hydroxyacetophenones **43A-E**.

The 3,5-disubstituted/unsubstituted 2-hydroxyacetophenones **43A–E** that were synthesised were all characterised using FTIR and NMR (^{1}H, ^{13}C, DEPT) spectroscopy. Melting points were also determined. Some physical data of the synthesised 3,5-disubstituted/unsubstituted 2-hydroxyacetophenones **43A-E** are summarised in Table 3.

Table 3: Synthesized 3,5-disubstituted/unsubstituted 2-hydroxyacetophenones **43A-E**.

Compound 43	**X**	**Y**	**% Yield**	**Melting point (°C)**	**Lit. melting point (°C)**[71]
A	F	I	98	90 – 98	-
B	Br	I	78	90 – 93	89
C	Cl	I	80	108 - 111	105
D	NO_2	I	65	132 - 136	-
E	Cl	Br	92	99 - 104	100 - 103

After taking into consideration the chemical shifts and coupling constants observed in the proton NMR spectra, the protons of compounds **43A-E** could all be accounted for. Both the ^{1}H and ^{13}C NMR spectra of compounds **43A-43E** are comparable in appearance, therefore only the NMR spectra of **43A** will be discussed.

The ^{1}H NMR spectrum of **43A** (Figure 13) revealed 2 proton signals in the aromatic region and one signal in the aliphatic region as expected. The 2 proton signals H-6 and H-4 in the aromatic region appeared as a doublet of doublets due to H-F coupling because of the presence of fluorine at position 6. The three-proton singlet in the aliphatic region resonating at 2.71 ppm

© University of Venda

was assigned to the CH_3 group of the ketone group. Finally, the characteristic downfield singlet at 12.98 ppm confirmed the presence of an OH proton.

The ^{13}C NMR spectrum for **43A** (Figure 14) revealed 8 carbon signals with carbonyl signal of the ketone resonating at 203.6 – 203.2 ppm and CH_3 resonating at 26.5 ppm. All other remaining carbon signals were for the aromatic region with C-1 resonated at 118.3 -118.2 ppm and C-6 at 166.2 – 115.9 ppm. The spectrum revealed all the carbon signals doubled, this is influenced by the coupling between the carbon and fluorine. Extra peaks can be observed on some of the spectra at 2.0 ppm on ^{1}H NMR and 30 ppm and 210 ppm on the ^{13}C NMR, due to the acetone used when rinsing the NMR tubes. FT-IR spectroscopy was used to confirm the presence of functional groups in the chemical structures of 5-substituted/unsubstituted 3-iodo-2-hydroxyacetophenones, such as the C=O band at around 1686,4 cm^{-1} and aromatic C-H at around 3062.5 cm^{-1}. The ^{13}C chemical shifts for **43A-E** are summarized in table 4. Figures 48 – 51 represent NMR spectra for **44B-C**.

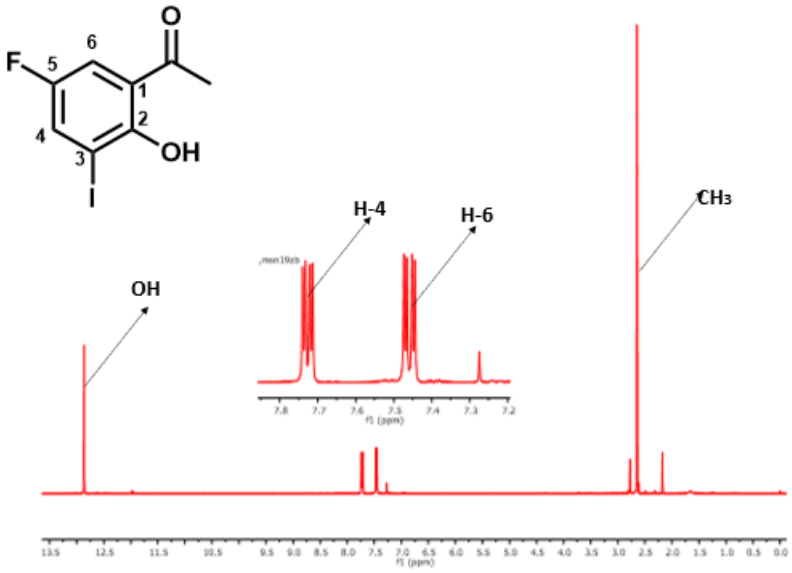


Figure 13: ^{1}H NMR spectrum of compound **43A** in $CDCl_3$ (at 400 MHz)

© University of Venda

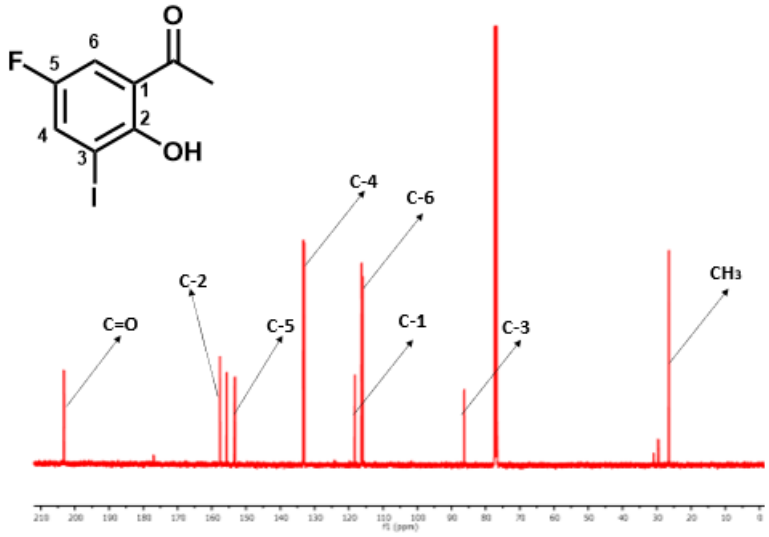


Figure 14: ^{13}C NMR spectrum of compound **43A** in $CDCl_3$ (at 100 MHz).

Table 4 below shows ^{13}C NMR chemical shift values (ppm) of 3,5-disubstituted/unsubstituted 2-hydroxyacetophenones **43A-D** in $CDCl_3$ (at 100 MHz). Chemical shifts for C-5 are different due to different substituents at the position. C-1 to C-8 signals for **43A** appeared as doublets due to the splitting caused by fluorine.

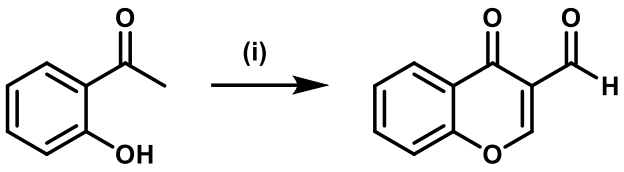
Table 4: ^{13}C NMR chemical shift values (ppm) of 3,5-disubstituted/unsubstituted 2-hydroxyacetophenones **43A-D** in $CDCl_3$ (at 100 MHz).

NUCLEUS	**43A**	**43B**	**43C**	**43D**
C-1	118.3 - 118.2	120.2	124.4	118.5
C-2	157.7 –157.7	166.2	159.8	167.2
C-3	86.3 - 86.2	87.7	87.2	86.7
C-4	133.3 - 133.1	147.3	144.8	140.2
C-5	156.7 - 153.3	111.1	119.5	144.7
C-6	116.2 - 115.9	133.1	130.1	131.1
C=O	203.6 - 203.2	203.2	203.5	203.9
CH_3	26.5	26.5	26.5	26.7

© University of Venda

4.1.5 Synthesis of chromone-3-carbaldehydes 44A

The Vilsmeier-Haack reaction is a versatile tool for formylating aromatic and heteroaromatic compounds. Here, we report the synthesis of chromone-3-carbaldehyde **44A** *via* Vilsmeier-Haack reaction using commercially available 2-hydroxyacetophenone **42A** as the starting material (Scheme 10). The reaction involved the treatment of 2-hydroxyacetophenone **42A** with Vilsmeier-Haack reagent (DMF/$POCl_3$) to afford the chromone-3-carbaldehyde **44A** in good yield, 95%, and melting point of 154 – 160 °C.[70] The product was characterised using spectroscopic techniques, confirming the structure, Figures 12 – 13.



42A **44A**

Conditions: (i) $POCl_3$, DMF, 0-25 °C, 12 h.

Scheme 10: Synthesis of chromone-3-carbaldehyde derivatives **44A-D**.

The ^{1}H NMR spectrum of chromone-3-carbaldehyde is expected to exhibit characteristics signals corresponding to the aldehyde proton and aromatic protons. The ^{1}H NMR spectrum of compound **44A,** Figure 15, depicted a sharp and distinct singlet signal around 10.4 ppm, corresponding to the aldehyde proton. Five aromatic signals, a singlet around 8.56 ppm for H-2, a doublet of doublets for proton signal H-5 at 8.30 – 8.28 ppm and H-6, H-7, H,8 appear as multiplets at 7.79 – 7.49 ppm, due to the coupling between adjacent protons.

The ^{13}C NMR spectrum is expected to show signal corresponding to the different carbon atoms in the molecule. ^{13}C NMR of compound **44A**, Figure 16, reveals 10 signals. A signal at 188.5 ppm corresponds to the aldehyde carbon, another signal for carbonyl carbon at 175.9 ppm for C-4. Further confirmation of the presence of a formyl group was supported by the infrared spectrum (Figure 52 in the appendix) at 1649.9 cm^{-1}. In addition, the methyl protons as well as the hydroxyl signals have disappeared indicating ring closure to form the chromone-3-carbaldehyde.[68-69]

© University of Venda

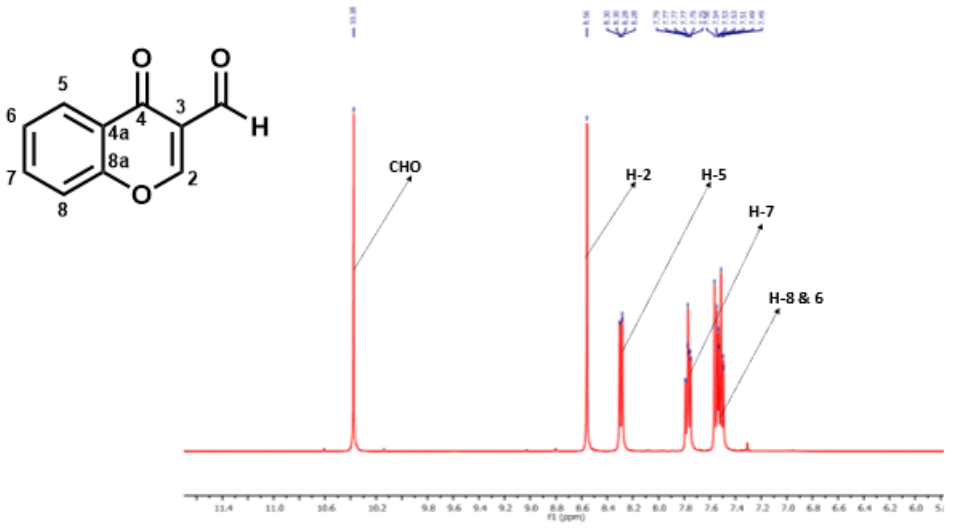


Figure 15: ^{1}H NMR spectrum of compound **44A** in $CDCl_3$ (at 400 MHz).

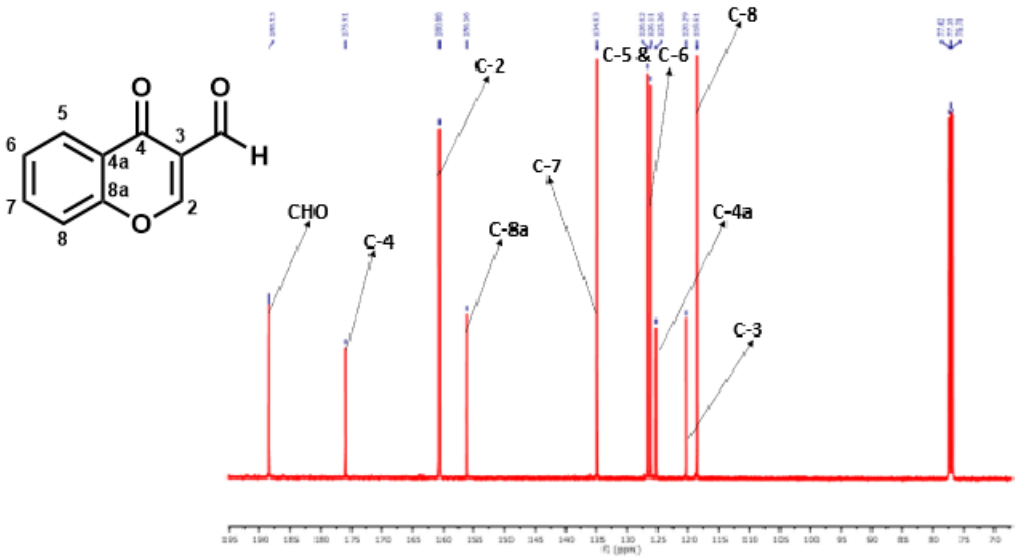
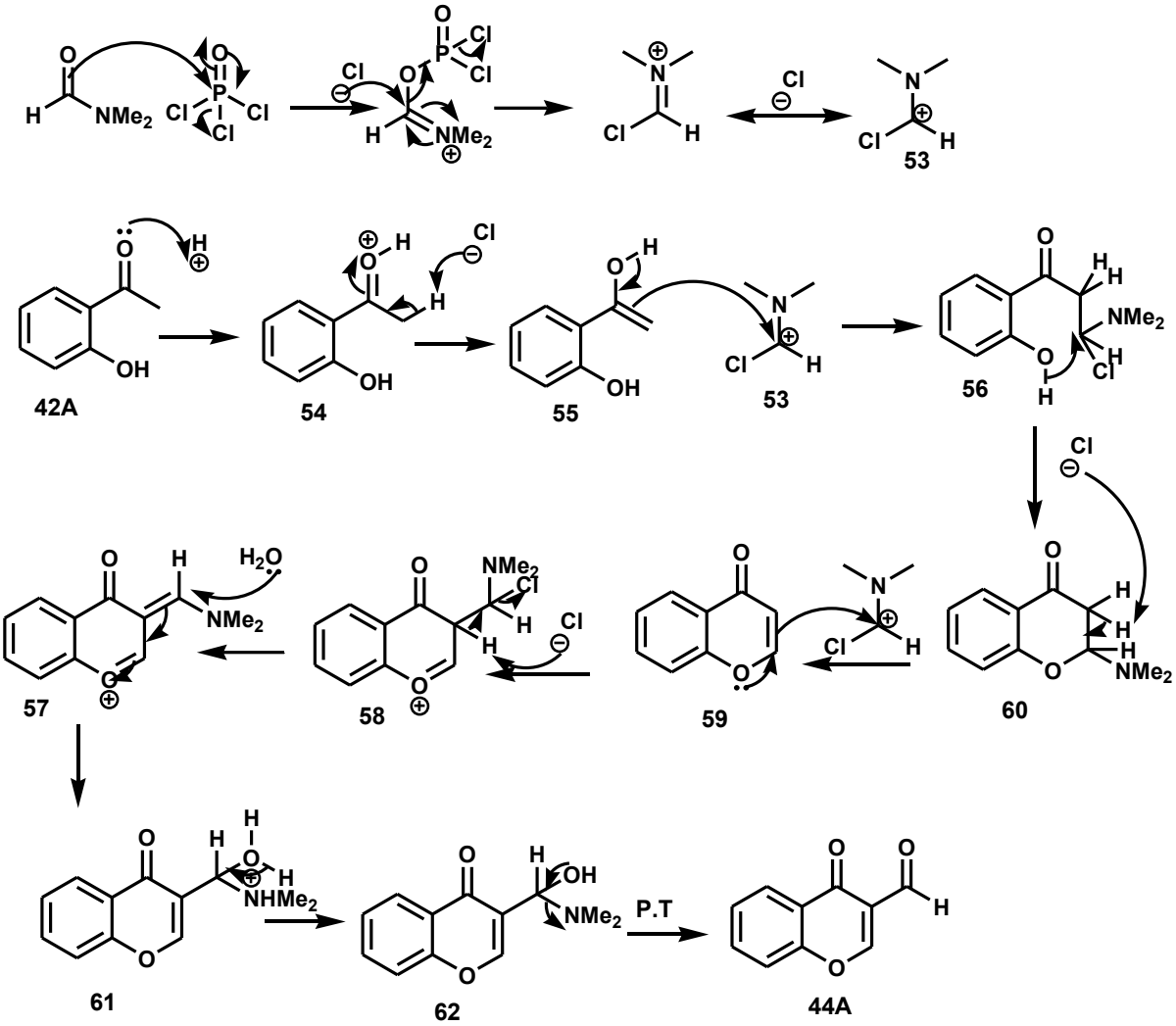


Figure 16: ^{13}C NMR spectrum of compound **44A** in $CDCl_3$ (at 100 MHz).

N,N-dimethylformamide and phosphorus oxychloride are combined in a Vilsmeier-Haack reaction to produce a chloroiminium ion, a carbon electrophile **53**. The acetophenone enolate that is created when the carbonyl oxygen is protonated subsequently interacts with the iminium cation. To create a cationic intermediate, this generates a chromen-4-one, which then targets another iminium cation. Chromone-3-carbaldehydes are produced by adding a formyl group at position 3 of the chromone ring after hydrolysis and proton transfer (P.T.).[21]

© University of Venda

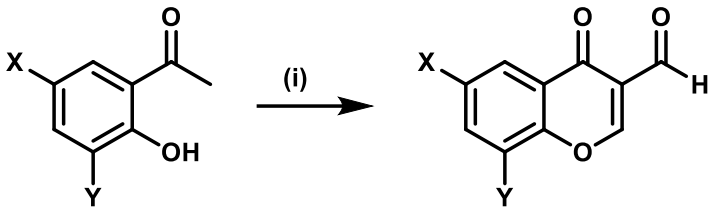


Scheme 11: Proposed mechanism for the formation of chromone-3-carbaldehydes.

4.1.6 Synthesis of 6.8-disubstituted chromone-3-carbaldehydes 44B-D

Subsequently, for 6,8-disubstituted chromone-3-carbaldehydes **44A** derivatives, a similar synthetic approach employed in the synthesis of chromone-3-carbaldehyde in the previous section above (Scheme 10) was used, Vilsmeier-Haack reaction involving the treatment of 3,5-substituted 2-hydroxyacetophenone with DMF/$POCl_3$ afforded corresponding 6.8-disubstituted chromone-3-carbaldehydrate derivatives. The substituents at the 6^{th} and 8^{th} position may influence the reactivity and regioselectivity of the reaction. However, the general mechanism of the Vilsmeier-Haack reaction remains the same.

© University of Venda



43A-D 44A-D

Conditions: (i) $POCl_3$, DMF, 0-25 °C, 12 h.

Scheme 12: Synthesis of 6,8-disubstituted chromone-3-carbaldehyde derivatives **44A-E**.

Table 5: Synthesized 6,8-disubstituted chromone-3-carbaldehyde derivatives **44B-E**.

Compound 44	**X**	**Y**	**% Yield**	**Lit. melting point (℃)**	**Melting point (℃)**
B	F	I	98	-	158 – 159
C	Cl	I	86	-	194 – 146
D	Br	I	94	-	164-166
E	Cl	Br	96	-	109 – 112

.

^{1}H NMR spectra (Figures 17, 53, 54 and 58) revealed 2 new proton signals, one resonating around 8.62 - 8.53 ppm integrating for one proton and was assigned to the newly formed chromone proton adjacent to the oxygen in the chromone ring H-2, this shift is due to the heteroatom and neighboring double bond. The second signal around 10.36 - 10.26 ppm confirmed the presence of the characteristic aldehyde proton. All the aromatic protons were accounted for.

^{13}C NMR spectra (Figures 18, 55 and 57) revealed 10 carbon signals, C-2 resonating at 160.7 – 160.6 ppm and a characteristic CHO signal resonating at 187.2 ppm - 188.5 ppm.

© University of Venda

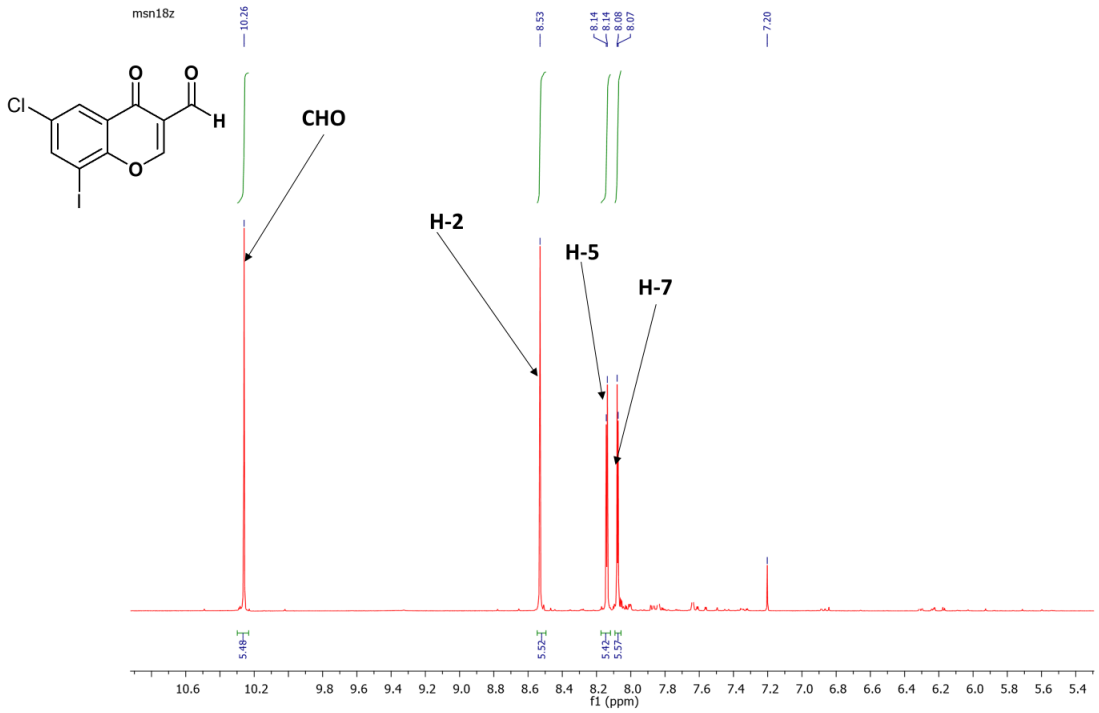


FIGURE 17: ^{1}H NMR spectrum of **44C** in $CDCl_3$ (at 100 MHz).

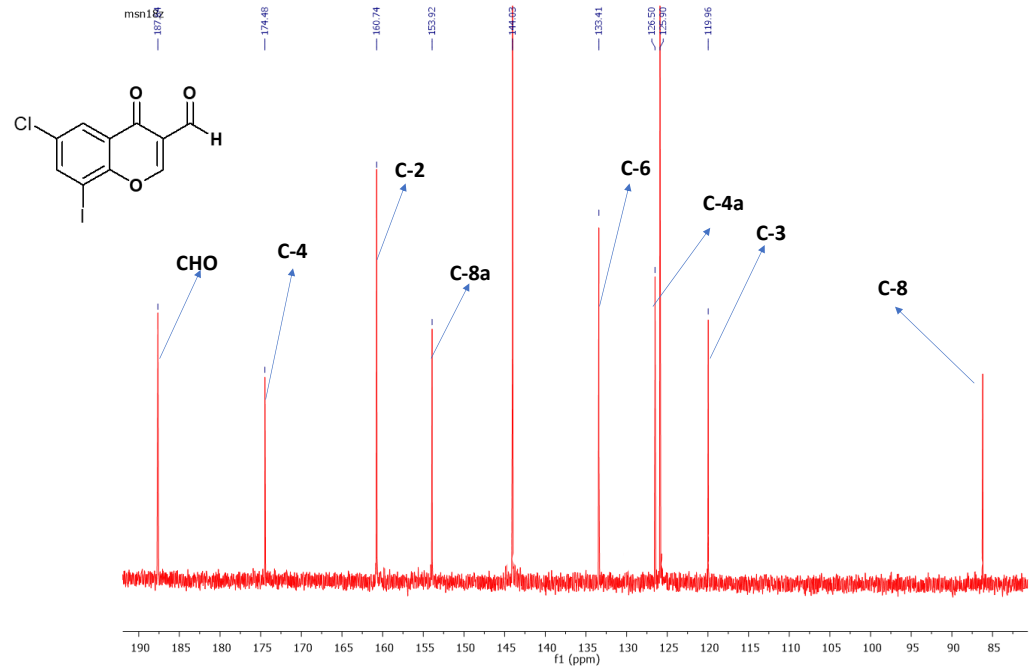


FIGURE 18: ^{1}H NMR spectrum of **44C** in $CDCl_3$ (at 100 MHz).

Table 6 presents ^{13}C NMR chemical shift values (ppm) of 6,8-disubstituted/unsubstituted chromone-3-carbaldehyde derivatives **44B-E** in $CDCl_3$ (at 100 MHz). Chemical shifts at C-6 are different for **44B-D** due to different substituents, and **44E** has the same chemical shift as

© University of Venda

44B since they possess the same substituent, Chlorine. Compounds **44B-D** have similar chemical shifts for C-8 due to iodine, and **44C** has a different shift due to bromine.

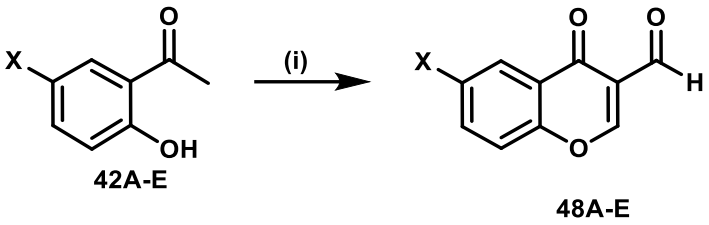
Table 6: ^{13}C NMR chemical shift values (ppm) of 6,8-disubstituted chromone-3-carbaldehyde derivatives **44B-E** in $CDCl_3$ (at 100 MHz).

NUCLEUS	44B	44C	44D	44E
C-2	160.8	160.7	160.7	106.7
C-3	119.3	119.9	120.9	120.1
C-4	174.9	174.5	174.4	174.3
C-4a	126.8	126.5	126.5	127.2
C-5	111.8	125.9	129.1	125.0
C-6	159.8	133.1	120.1	133.0
C-7	132.7	144.0	146.6	138.0
C-8	86.0	86.2	86.5	113,3
C-8a	151.9	153.9	154.3	151.6
CHO	187.8	187.2	187.7	187.7

4.1.7 Synthesis of 6-substituted chromone-3-carbaldehydes 48A-E

With both synthesized and commercially available 5-substituted 2-hydroxyacetophenones **42A-E** in hand, the synthesis of 6-substituted chromone-3-carbaldehyde derivatives **48A-E** proceeded according to the procedure described in Scheme 12. The synthesized 5-substituted 2-hydroxyacetophenones **42A-E** were subjected to Vilsmeier-Haack reaction by treating them with DMF and $POCl_3$ and stirring for 12 hours at room temperature. To obtain the corresponding 6-substituted chromone-3-carbaldehydes **48A-E**, the solid was filtered, dried, and recrystallized from ethanol.[70]

© University of Venda

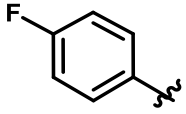
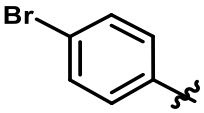
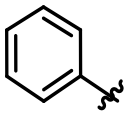


42A-E 48A-E

Reagents and conditions: (i) $POCl_3$-DMF, rt, 12 – 16 h.

Scheme 13: Synthesis of 6-substituted chromone-3-carbaldehyde derivatives **48A-E**.

Table 7: Synthesized 6-substituted chromone-3-carbaldehyde derivatives **48A-E**.

Compound 48	**X**	**Mass yield (g)**	**% Yield**	**Lit. melting point (℃)**	**Melting point (℃)**
A		3.7	98	-	119
B		0.52	57	-	120
C		0.82	96	-	115
D	**Br**	1.78	63	190 - 193	191 – 196

^{1}H NMR spectra revealed 2 new proton signals, one resonance around 8.56 ppm integrating to one proton was assigned to the newly formed chromone proton adjacent to the oxygen in the chromone ring H-2, this shift is due to the heteroatom and neighbouring double bond and one signal above 10 ppm which confirms the presence of the aldehyde. ^{13}C NMR spectra (Table 8) revealed 10 carbon signals, C-2 resonating at 160.7 ppm – 163.2 ppm and CHO resonating at 187.2 ppm - 188.5 ppm. Further confirmation of the presence of formyl group was observed on the infrared spectrum. In addition, the methyl protons and hydroxyl proton disappeared. Figures 17 – 20 show spectra for **48C**.

© University of Venda

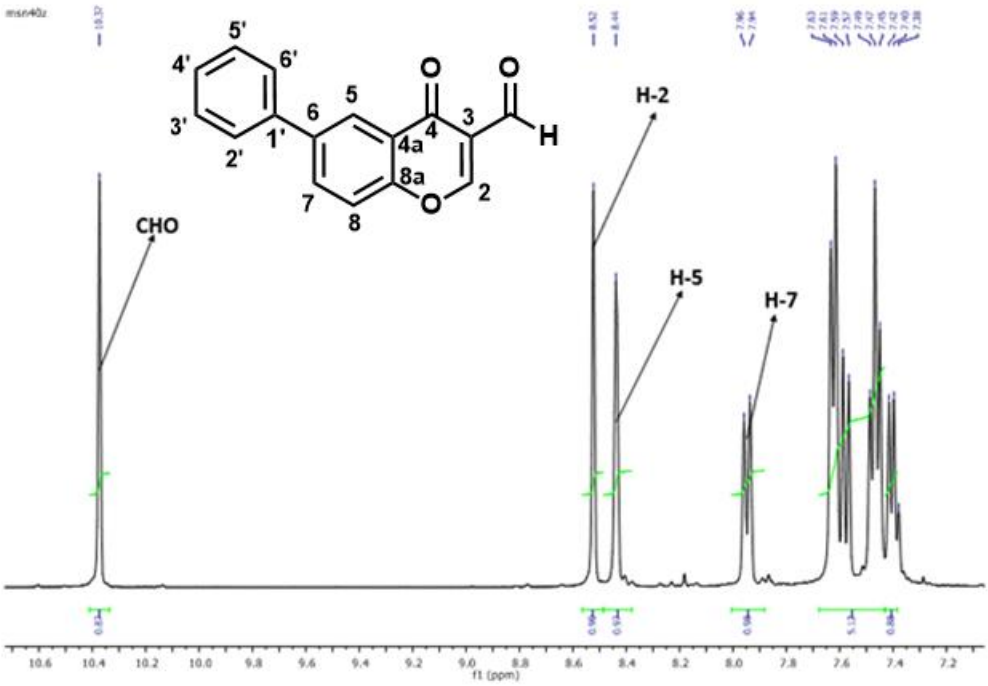


Figure 19: ^{1}H NMR spectrum of 6-phenylchromone-3-carbaldehyde **48C**.

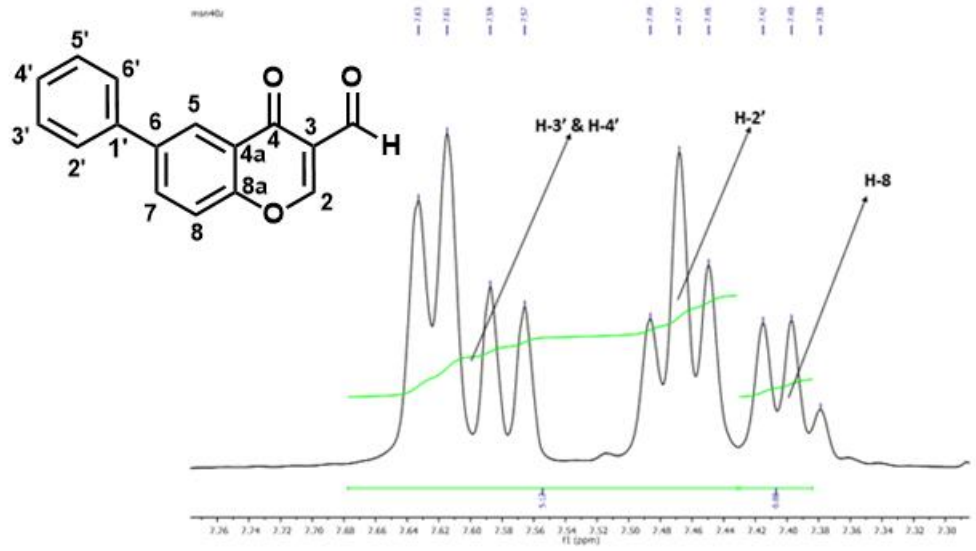


Figure 20: Expanded ^{1}H NMR spectrum of 6-phenylchromone-3-carbaldehyde **48C**.

© University of Venda

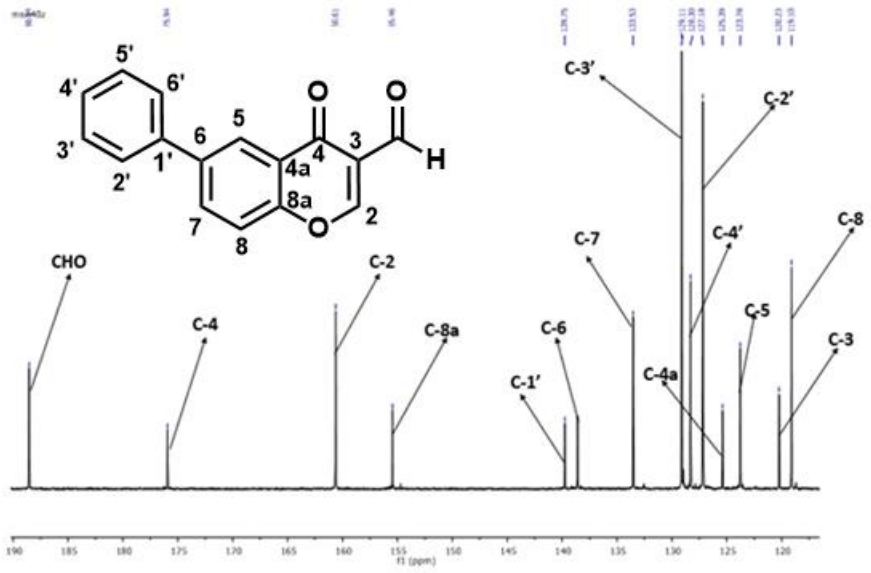


Figure 21: ^{13}C NMR spectrum of 6-phenylchromone-3-carbaldehyde **48C**.

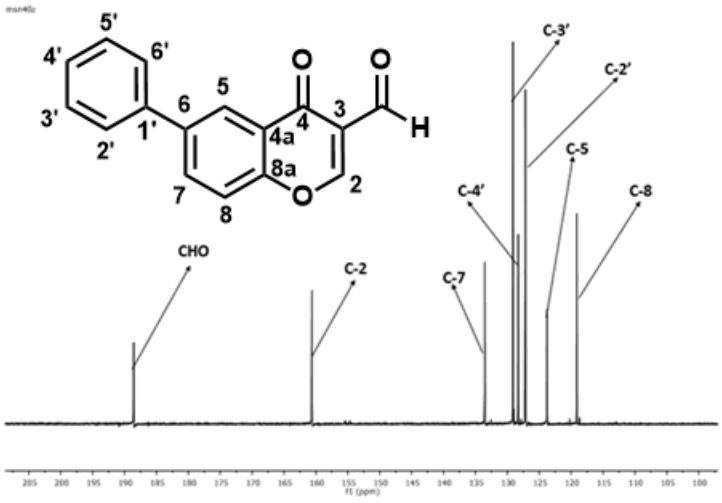


Figure 22: DEPT 135 spectrum of 6-substituted chromone-3-carbaldehyde **48C**.

© University of Venda

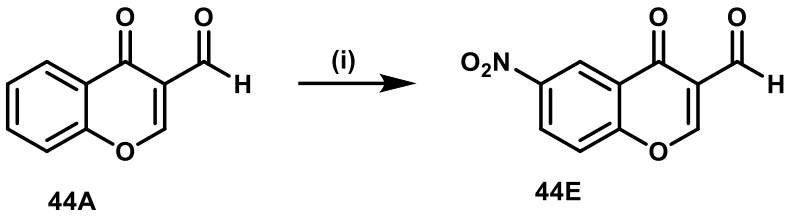
Table 8: ^{13}C NMR chemical shift values (ppm) of 6-substituted chromone-3-carbaldehydes **48A-E** in $CDCl_3$ (at 400 MHz).

NUCLEUS	48A	48B	48C	48E
C-2	160.2	169.2	160.6	162.2
C-3	120.1	120.1	120.2	120.1
C-4	175.3	168.7	174.9	174.1
C-4a	125.4	125.3	125.4	119.2
C-5	127.1	127.1	123.4	127.5
C-6	130.4	136.6	138.6	126.3
C-7	135.5	135.5	133.5	137.8
C-8	119.8	119.6	119.1	121.1
C-8a	156.7	155.0	155.5	155.1
CHO	188.1	188.2	188.5	187.1
C-1'	139..8	140.3	139.6	-
C-2'	129.0	129.5	127.2	-
C-3'	116.5	125.3	129.1	-
C-4'	163.5	125.3	128.3	-

4.1.8 Synthesis of 6-nitrochromone-3-carbaldehyde 44F

To introduce a nitro substituent on position 6 of the chromone skeleton, in addition to 6,8-disubstituted chromone-3-carbaldehydes **44A-D** synthesized in 4.1.5 above. Chromone-3-carbaldehyde **44A** was nitrated by treating it with nitric and sulfuric acid for 3 hours at 0 - 25 ℃ (Scheme 13). The reaction was quenched with water, and the resulting solid was filtered, dried, and recrystallized from ethanol to produce 6-nitrochromone-3-carbaldehyde **44F** with a percentage yield of 53%.[72]

© University of Venda



44A **44E**

Reagents and conditions: (i) nitric acid, sulfuric acid, stir, 0 – 25 °C, 3 h.

Scheme 14: Synthesis of 6-nitrochromone-3-carbaldehyde **44F**.

^{1}H NMR spectrum (Figure 21) revealed 3 proton signals around the aromatic region, first resonance around 9.15 ppm integrating for one proton was assigned 5-H with the multiplicity of a double due to the *meta*-positioned proton and 7-H which appears as a doublet of doublets between 8.62-8.59 ppm due to the *meta*-positioned proton 5-H and 8-H, which appears as a doublet *ortho* to 7-H, this was confirmed by the *J* values. The ^{13}C NMR spectrum (Figure 22) revealed 10 carbon signals, with C-2 resonating at 160.9 ppm, C-6 at 145.7 ppm and CHO resonating at 187.5 ppm. Further confirmation of substitution of the nitro group was observed on the DEPT 135 spectrum (Figure 23), with only three aromatic CH peaks. Figures 21 – 23 shows spectra for **44F**. Figure 60 in the appendix shows FT-IR spectrum of **44F**.

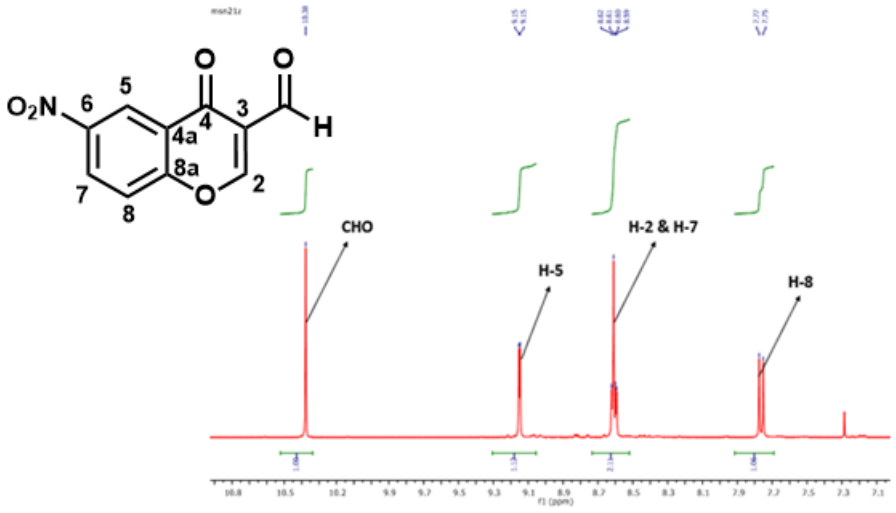


Figure 23: ^{1}H NMR spectrum of 6-nitrochromone-3-carbaldehyde **44F** at 400MHz.

© University of Venda

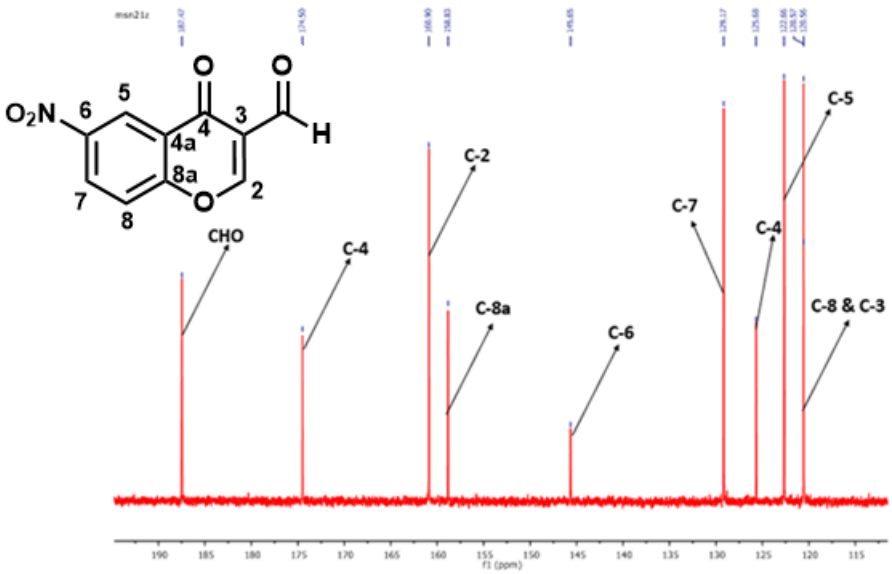


Figure 24: ^{13}C NMR spectrum of 6-nitrochromone-3-carbaldehyde **44E** at 100 MHz.

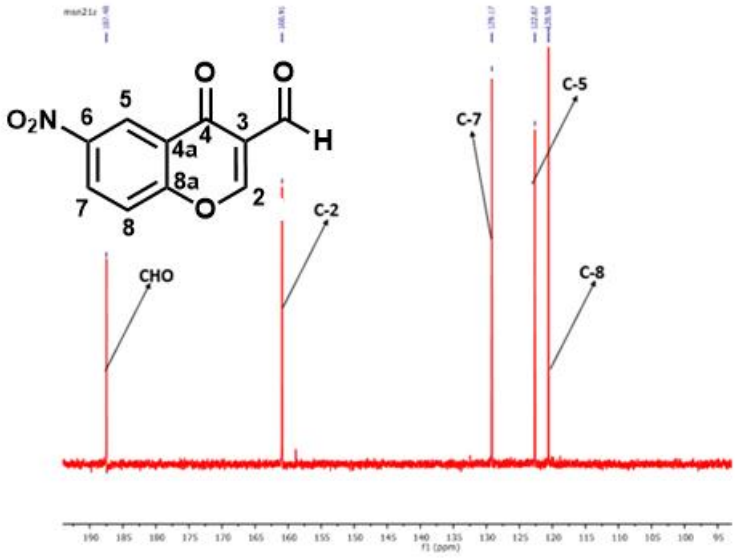


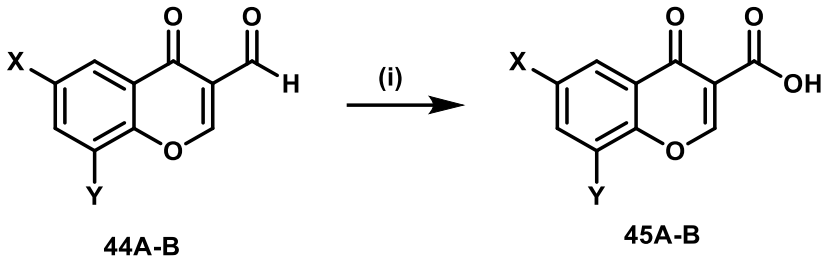
Figure 25: DEPT 135 spectrum of 6-nitrochromone-3-carbaldehyde **44E**.

4.1.9 Synthesis of substituted/unsubstituted chromone-3-carboxylic acids 45A-B

Subsequently, aldehydes were converted to carboxylic acids as carboxylic acids are more reactive toward anime in amidation. 6,8-Disubstituted/unsubstituted chromone-3-carbaldehydes **44A-B** were subjected to Lindgren oxidation by treating the appropriate 6,8-disubstituted/unsubstituted chromone-3-carbaldehydes **44A-B** with sulfamic acid and sodium chlorite solution in water and DCM as a solvent at room temperature for 2 h (Scheme 14). The chromone-3-carboxylic acid **45A-B** derivatives were obtained by quenching the resulting mixture with water and extracting with DCM, drying, and concentrating under reduced

© University of Venda

pressure to afford chromone-3-carboxylic acids **45A-B**.[28] Table 9 shows mass yield and melting point values of synthesized chromone-3-carboxylic acids **45A-B**.



44A-B **45A-B**

Conditions: (i) Sulfamic acid, NaOCl, DCM, 0 – 25 °C, 2 h.

Scheme 15: Synthesis of substituted/unsubstituted chromone-3-carboxylic acid derivatives **45A-B.**

Table 9: Synthesized substituted/unsubstituted chromone-3-carboxylic acid derivatives **45A-B**.

Compound 45	**X**	**Y**	**% Yield**	**Melting point (℃)**	**Lit. melting point (℃)**
A	H	H	38	199 - 201	202 - 205[28]
B	Cl	Br	15	320 - 321	-

^{1}H NMR spectra of **45A-B** revealed a downfield shift of the chromone proton 2-H, this observation is due to the deshielding effect of the acidic group. The remaining protons on the ring resonate in similar chemical regions as their corresponding aldehydes and the disappearance of the signal above 10 ppm confirms the conversion of the aldehyde to carboxylic acid. ^{13}C NMR spectra or **45A-B** (Table 10) revealed 10 carbon signals, C-4 resonating at 180.1 - 179.97 ppm and COOH resonating at 165.2 - 164.20 ppm. In addition, the signal for C-4 has shifted downfield whereas the carbon atom of the carboxylic acid group resonated upfield in comparison to the carbon atom of the aldehyde. FT-IR spectra (Figure 29) revealed a hydroxyl group at around 3226.1 and 3264.6 cm^{-1}, further confirming the conversion of the aldehydes to corresponding acids. Figures 24 – 27 show spectra for **45B**. Figures 61 and 62 in the appendix show ^{1}H NMR and ^{13}C NMR spectra, respectively.

© University of Venda

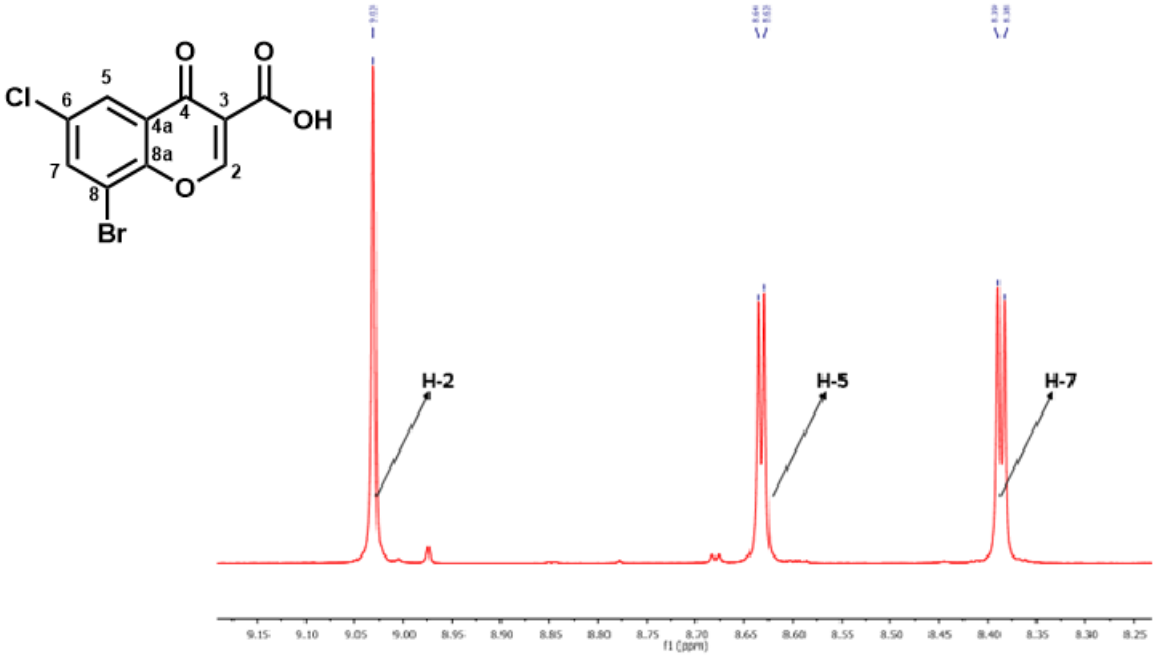


Figure 26: ^{1}H NMR spectrum of compound **45B** in $CDCl_3$ (at 400 MHz).

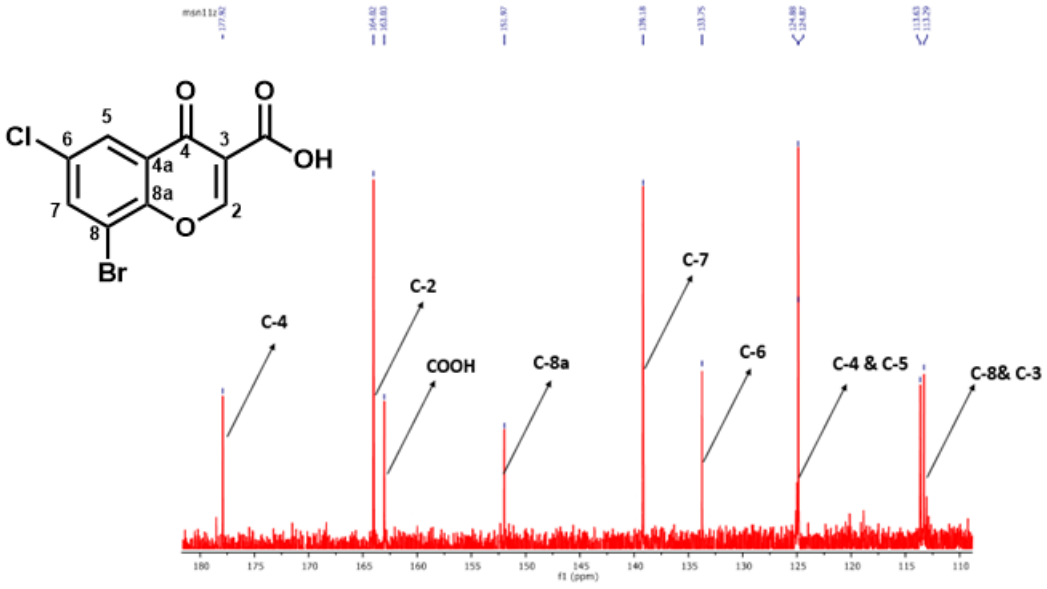


Figure 27: ^{13}C NMR spectrum of compound **45B** in $CDCl_3$ (at 100 MHz).

© University of Venda

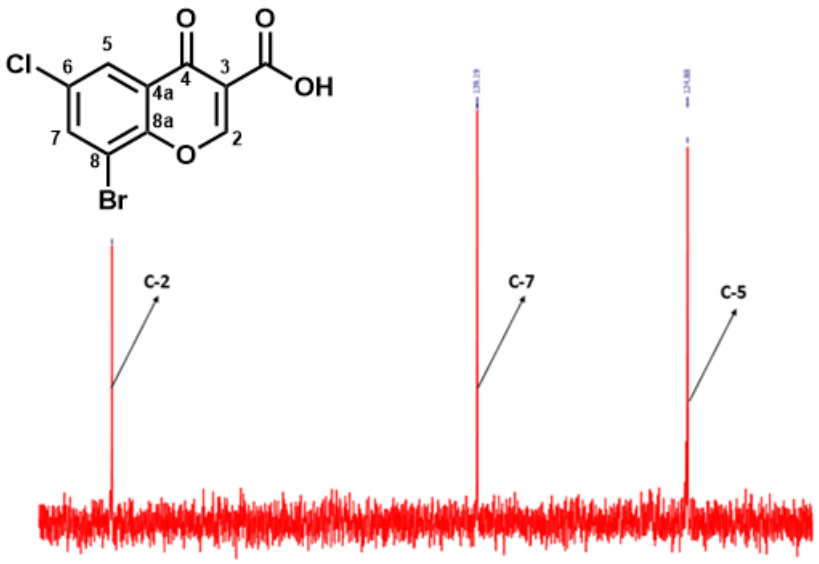


Figure 28: DEPT 135 spectrum of compound **45B** in $CDCl_3$.

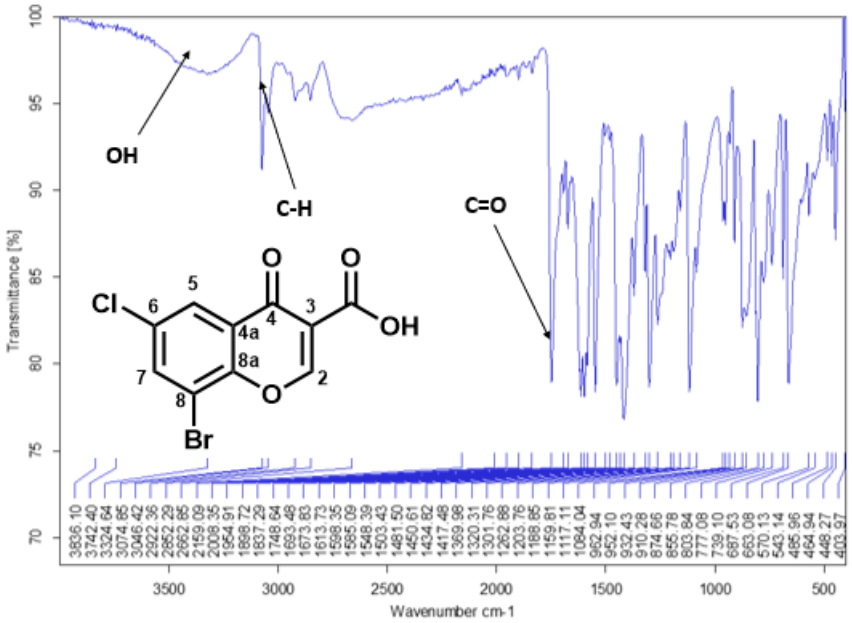


Figure 29: FTIR spectrum of compound **45B**.

© University of Venda

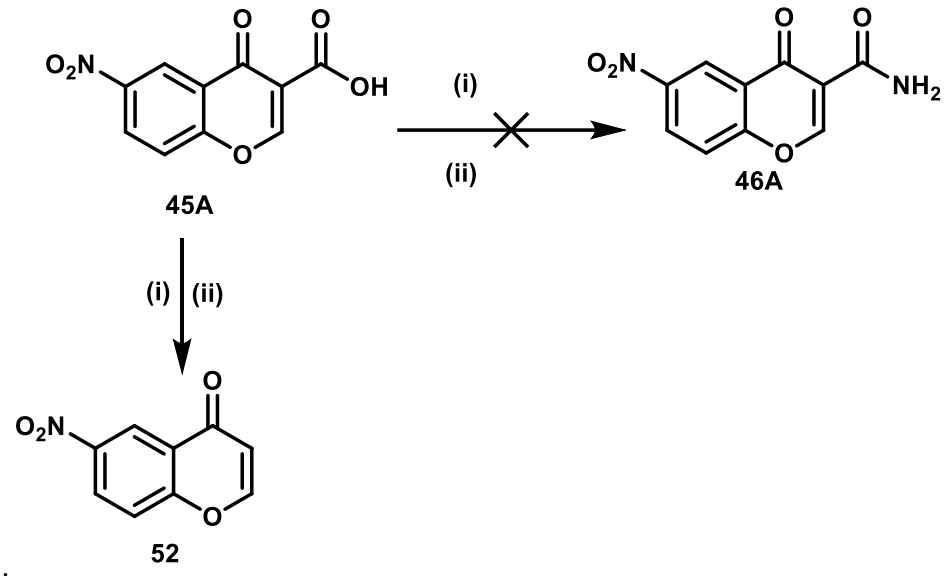
Table 10: ^{13}C NMR chemical shift values (ppm) of substituted/unsubstituted chromone-3-carboxylic acid derivatives **45A-B** in $CDCl_3$ (at 100 MHz).

NUCLEUS	45A	45B
C-2	163.9	164.0
C-3	112.9	113.3
C-4	179.3	177.9
C-4a	122.9	124.9
C-5	127.3	124.9
C-6	126.1	133.6
C-7	136.1	139.2
C-8	118.8	113.6
C-8a	156.6	151.9
COOH	164.2	165.0

4.1.10 Synthesis of 6-nitrochromone-3-carboxamide 46A

Next, in an attempt to synthesize 6-nitrochromone-3-carboxamide **46A** (Scheme 15), 6-nitrochromone-3-carboxylic acid **45A** was stirred with thionyl chloride under reflux for 1 hour at 80 ℃ to obtain the corresponding acid chloride. The resulting mixture was concentrated under reduced pressure to remove thionyl chloride.[70] The solid obtained was stirred with aqueous ammonia solution in DCM for 2 hours at 0 °C. A white precipitate was collected by suction filtration, washed with water and *n*-hexane, and dried under reduced pressure at 50 °C. After considering the ^{1}H NMR, ^{13}C NMR, DEPT, and FT-IR spectroscopy, the reaction was deemed unsuccessful, as the actual reaction that took place was decarboxylation to chromone **52**.

© University of Venda



Conditions: (i) $SOCl_2$, 80 °C, 3 h. (ii) DCM, NH_3 (aq), 0 – 25 °C, 2 h.

Scheme 16: Attempted synthesis of 6-nitrochromone-3-carboxamide **46A**.

Five proton signals were detected by ^{1}H NMR (Figure 28), all of which were in the aromatic region. The one-proton doublet for 5-H appeared at 8.54 ppm, while the one-proton doublet for 7-H appeared at 8.32 ppm. A new singlet integrating to two protons for NH_2 should have been present if compound **45A** was transformed into the intended 6-nitrochromone-3-carboxamide. This was not the case, however, as a new one-proton doublet appeared at 6.22 ppm, coupled with 2-H (supported by their *J* values), showing that the carboxylic acid group was removed. If the acid group or freshly produced carboxamide group was still attached to C-3, the 2-H proton should have appeared as a singlet; instead it appeared as a doublet at 8.11 ppm.

^{13}C NMR (Figure 29) analysis also showed one missing carbonyl group signal in regions where carbamates and carboxylic acids are predicted to resonate. The development of a new signal at 112.7 ppm in the aromatic region also indicates decarboxylation of the carbonyl group. Finally, we expected a total of 10 carbon signals, but only 9 were detected. The DEPT 135 spectrum (Figure 30) revealed a new signal in the aromatic region, which appears as a CH. The decarboxylation might have occurred during high-temperature heating during the conversion of carboxylic acid to acid chloride, or during amide synthesis due to the presence of HCl as a by-product. Figures 28 – 30 show spectra for **52**.

© University of Venda

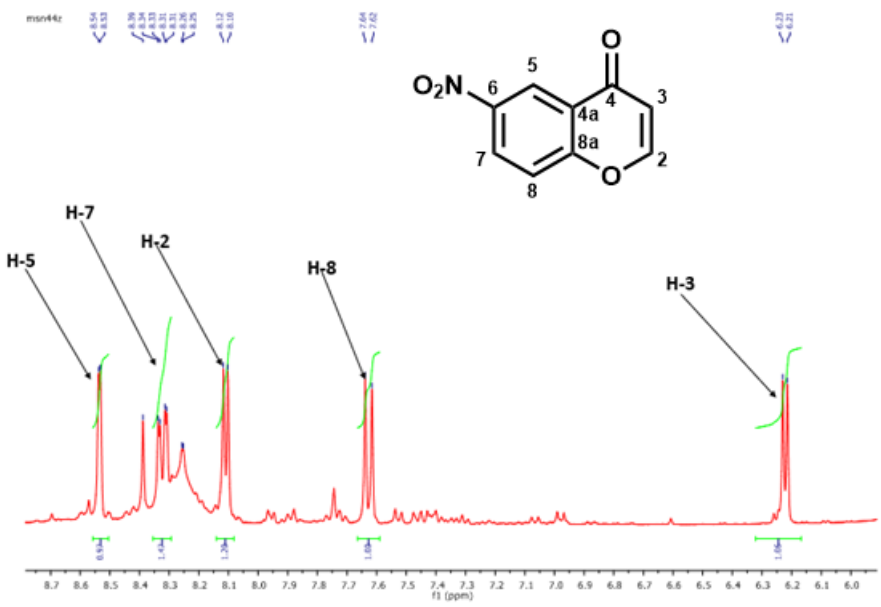


Figure 30: ^{1}H NMR spectrum of compound **52** in C_5D_5N (at 400 MHz).

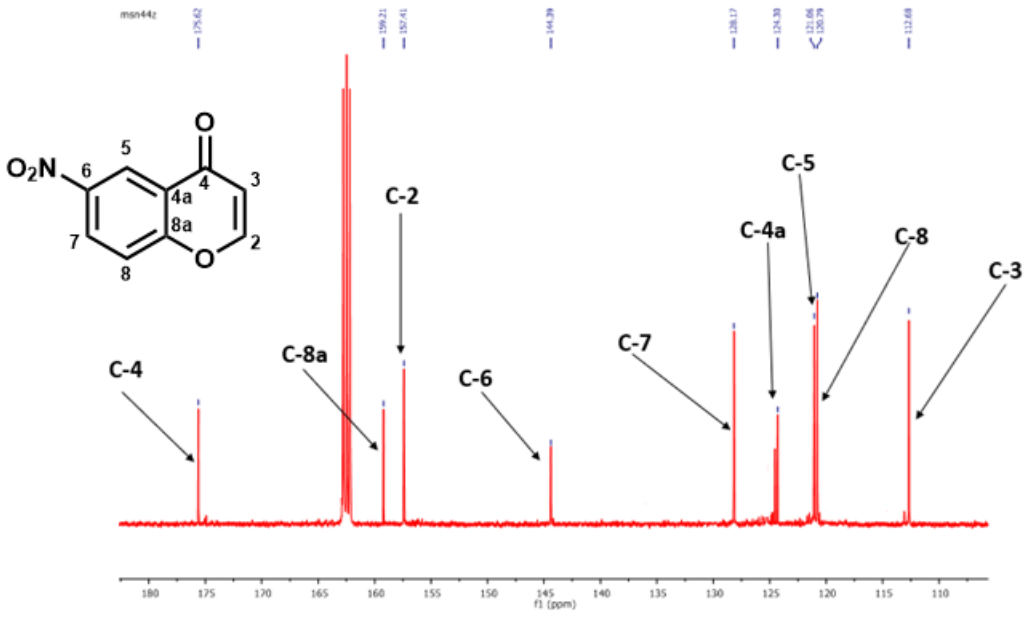


Figure 31: ^{13}C NMR spectrum of compound **52** in C_5D_5N (at 100 MHz).

© University of Venda

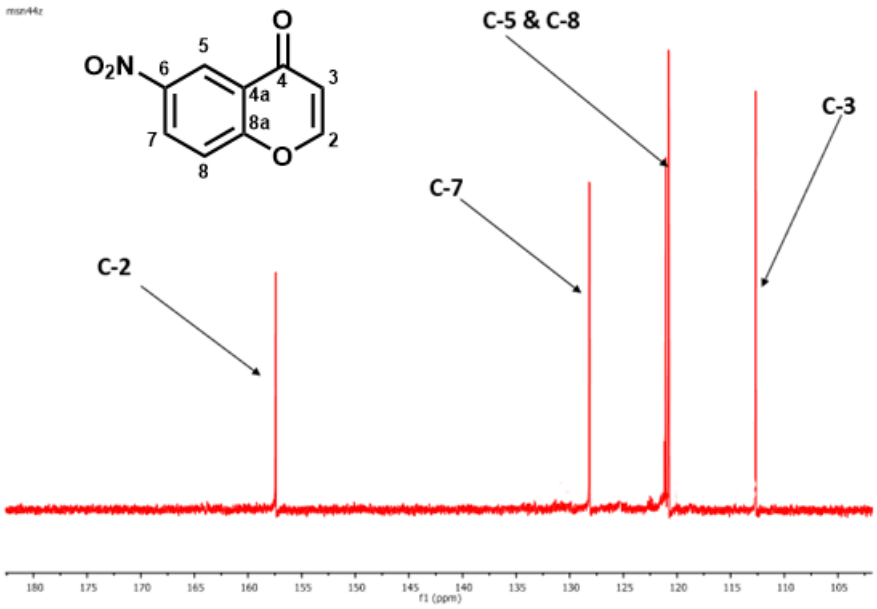
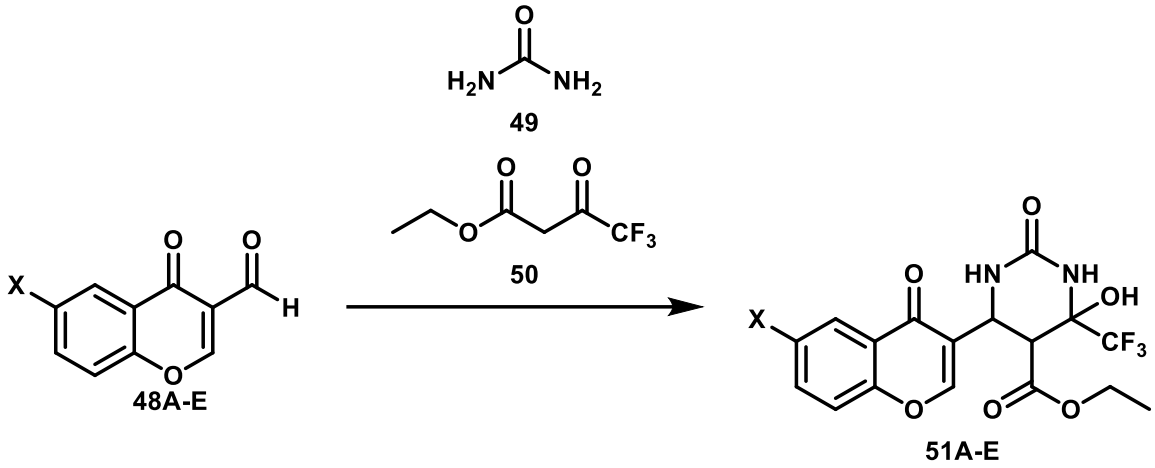


Figure 32: DEPT 135 spectrum of compound **52** in C_5D_5N.

4.1.11 Synthesis of ethyl 6-hydroxy-4-(chromon-3-yl)-2-oxo-6-trifluoromethyl-1,2,3,4-tetrahydropyrimidine-5-carboxylate derivatives 51A-E

Finally, to synthesize the target compounds, the previously synthesized chromone-3-carbaldehydes **51A-E** (see 4.1.5 and 4.1.6) were reacted with β-ketoester **50** and urea **49** in the presence of a catalytic amount of sulfamic acid in ethanol under reflux conditions for 3 - 6 h (Scheme 16). The synthesized compounds were well characterized by spectral data. Literature melting points for these compounds were not available since they are novel compounds.

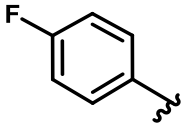
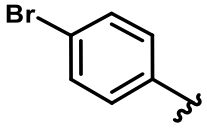
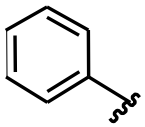
© University of Venda



Reagents and conditions: (i) EtOH, NH_2SO_3H, 80 °C, 3 h.

Scheme 17: Synthesis of ethyl 6-hydroxy-4-(chromon-3-yl)-2-oxo-6-trifluoromethyl-1,2,3,4-tetrahydropyrimidine-5-carboxylate derivatives **51A-E**.

Table 11: Synthesized ethyl 6-hydroxy-4-(chromon-3-yl)-2-oxo-6-trifluoromethyl-1,2,3,4-tetrahydropyrimidine-5-carboxylate derivatives **51A-E.**

Compound 51	X	Mass yield (g)	% Yield	Calculated m/z	Actual m/z $[M+H]^+$
A		3.6	67	476.1	495.1
B		0.9	53	536.0 and 538.0	555.0 and 557.0
C		1.0	74	458.1	477.1
D	**H**	3.7	60	382.1	401.0
E	**Br**	2.9	74	460.0	481.0

It was observed on the LC-MS (Table 11) that the mass to charge ratio (*m/z*) of the target compounds read 18 units higher than the theoretically expected. ^{1}H NMR spectra revealed two extra proton signals around 7.2 - 7.05 ppm singlet, and 3.79 – 3.47 ppm doublet. Upon

© University of Venda

close inspection of the mechanism and material used in the procedure, it was determined that the compounds still had the hydroxyl group (OH) where a double bond was anticipated, accounting for the two extra signals in the ^{1}H NMR spectrum. This indicated that the final step, which would have been dehydration, had not occurred. This was confirmed by both LC-MS and proton NMR that the dehydration did not occur. FT-IR also confirmed the presence of a weak OH signal at 3389 - 3467.8 cm^{-1} (Figure 34). The cyclization of urea was successful; this was confirmed by two new NH signals around 8.71 - 8.43 ppm and 7.81 - 7.44 ppm in the ^{1}H NMR spectrum. The disappearance of the aldehyde proton at around 10.4 – 10.2 ppm also confirmed his formation of the desired compound. The ester functional group attached to the newly cyclized pyrimidine was confirmed by the appearance of a quartet at 3.93 ppm – 3.83 ppm and a triplet at 0.90 ppm – 0.86 ppm, confirming both the OCH_2 and CH_3 groups, respectively.

Carbon-13 NMR and DEPT NMR were also employed to characterize the newly formed compounds (Table 12). The disappearance of the aldehyde (CHO) signal around 190 ppm in the ^{13}C NMR and DEPT 135 NMR was diagnostic, and the ester functional group was confirmed by the appearance of signals at 78.7 ppm and 14.0 ppm in the ^{13}C NMR spectrum, confirming both the OCH_2 and CH_3 groups, respectively. The presence of the OCH_2 group was further confirmed by DEPT 135. Figures 31 – 35 show spectra for **51D** , figures 63 – 78 in the appendix show spectra for **51A-C** and **51E.**

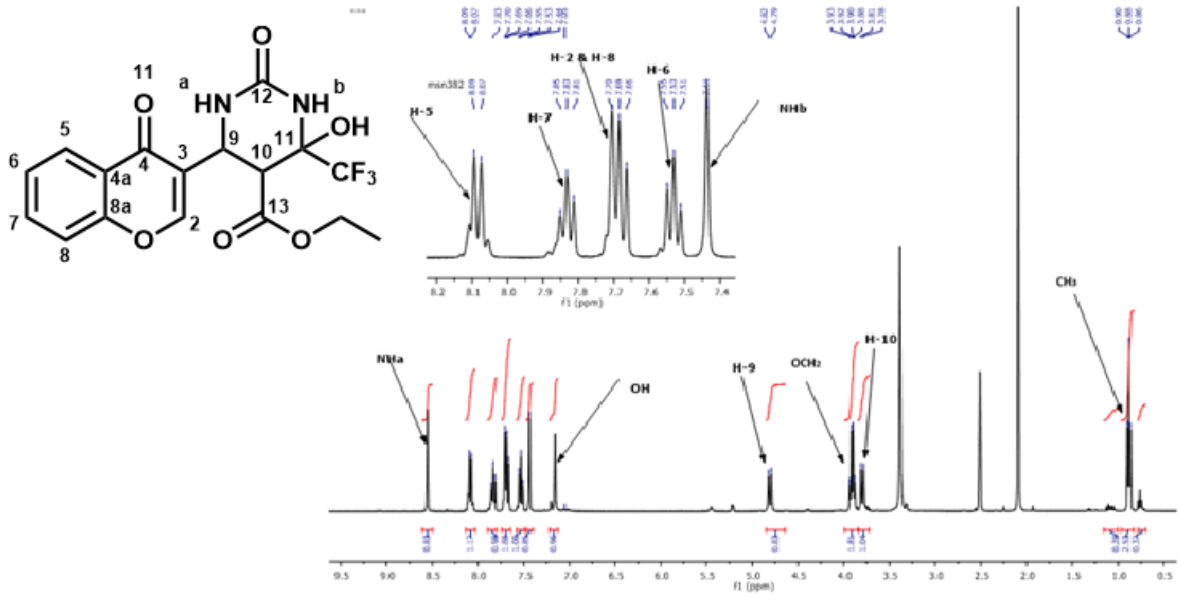


Figure 33: ^{1}H NMR spectrum of ethyl 6-hydroxy-4-(chromon-3-yl)-2-oxo-6-trifluoromethyl-1,2,3,4-tetrahydropyrimidine-5-carboxylate derivatives **51D**.

© University of Venda

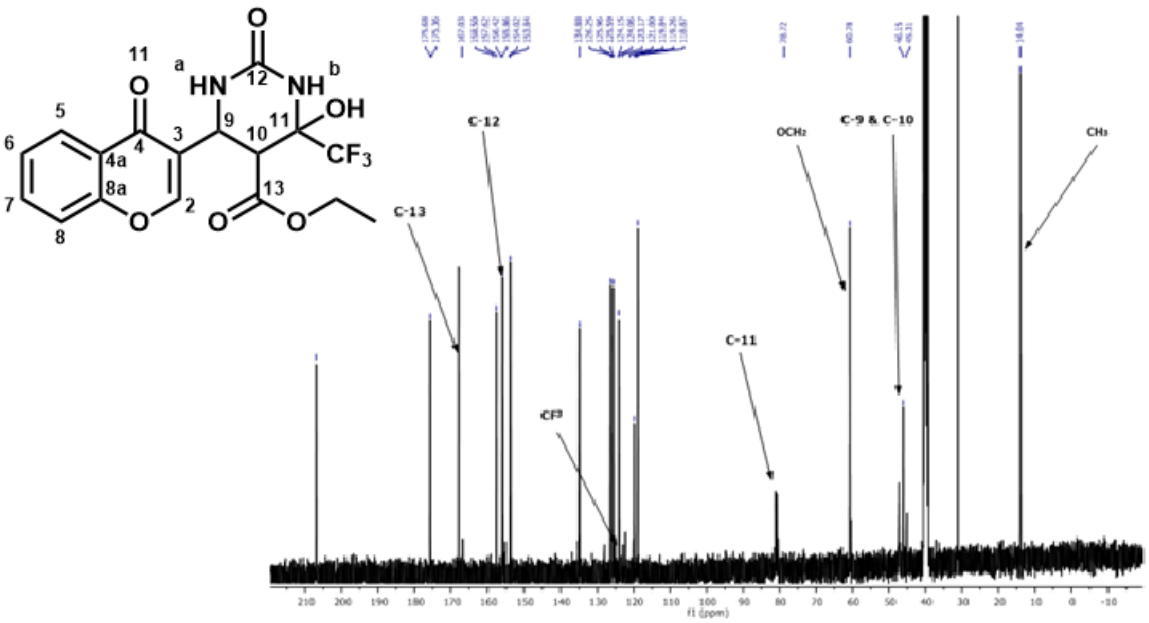


Figure 34: ^{13}C NMR spectrum of ethyl 6-hydroxy-4-(4-ochromon-3-yl)-2-oxo-6-trifluoromethyl-1,2,3,4-tetrahydropyrimidine-5-carboxylate derivative **51D**.

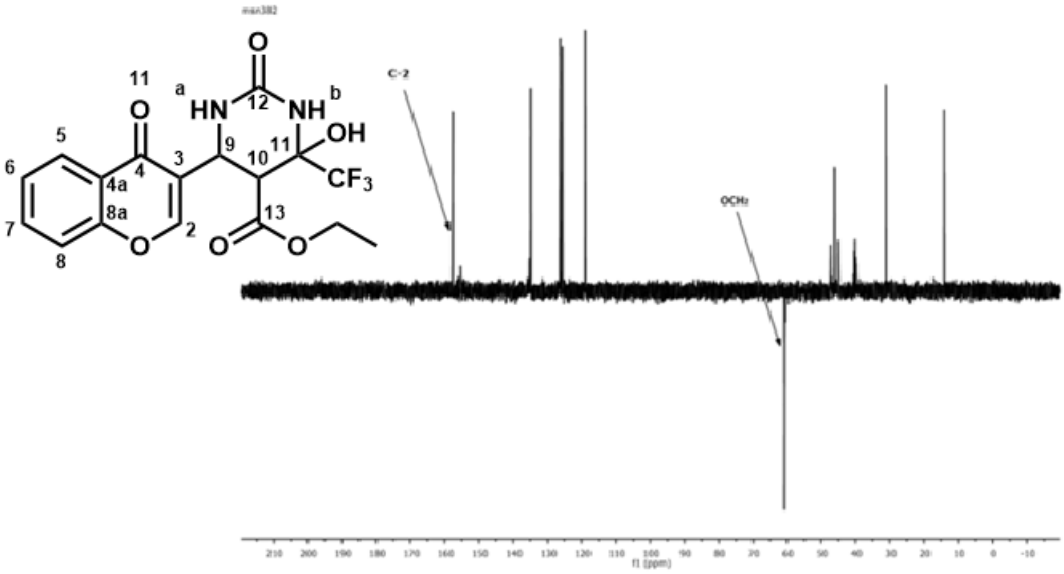


Figure 35: DEPT 135 spectrum of ethyl 6-hydroxy-4-(chromon-3-yl)-2-oxo-6-trifluoromethyl-1,2,3,4-tetrahydropyrimidine-5-carboxylate derivative **51D**.

© University of Venda

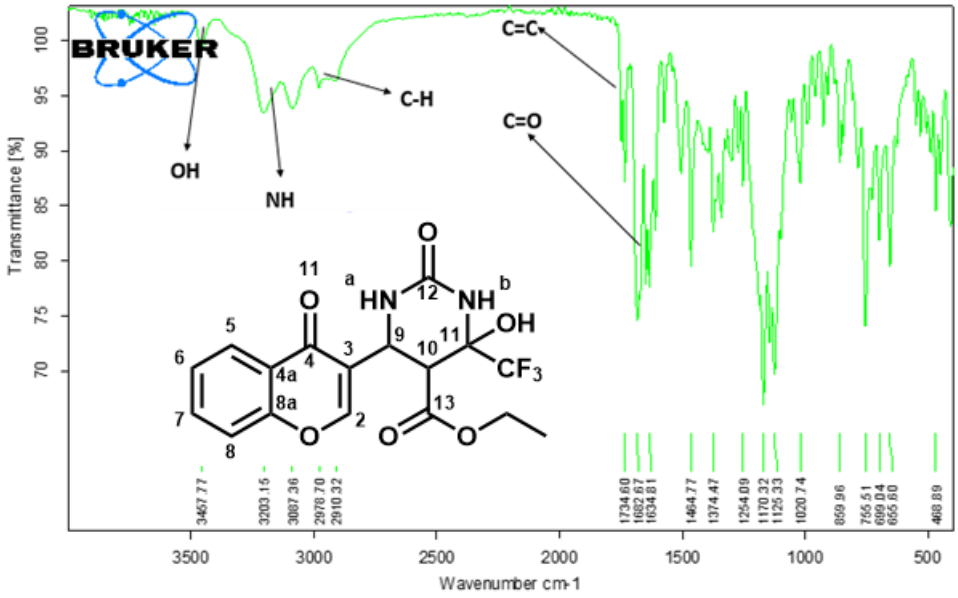


Figure 36: FT-IR spectrum of compound **51D**.

© University of Venda

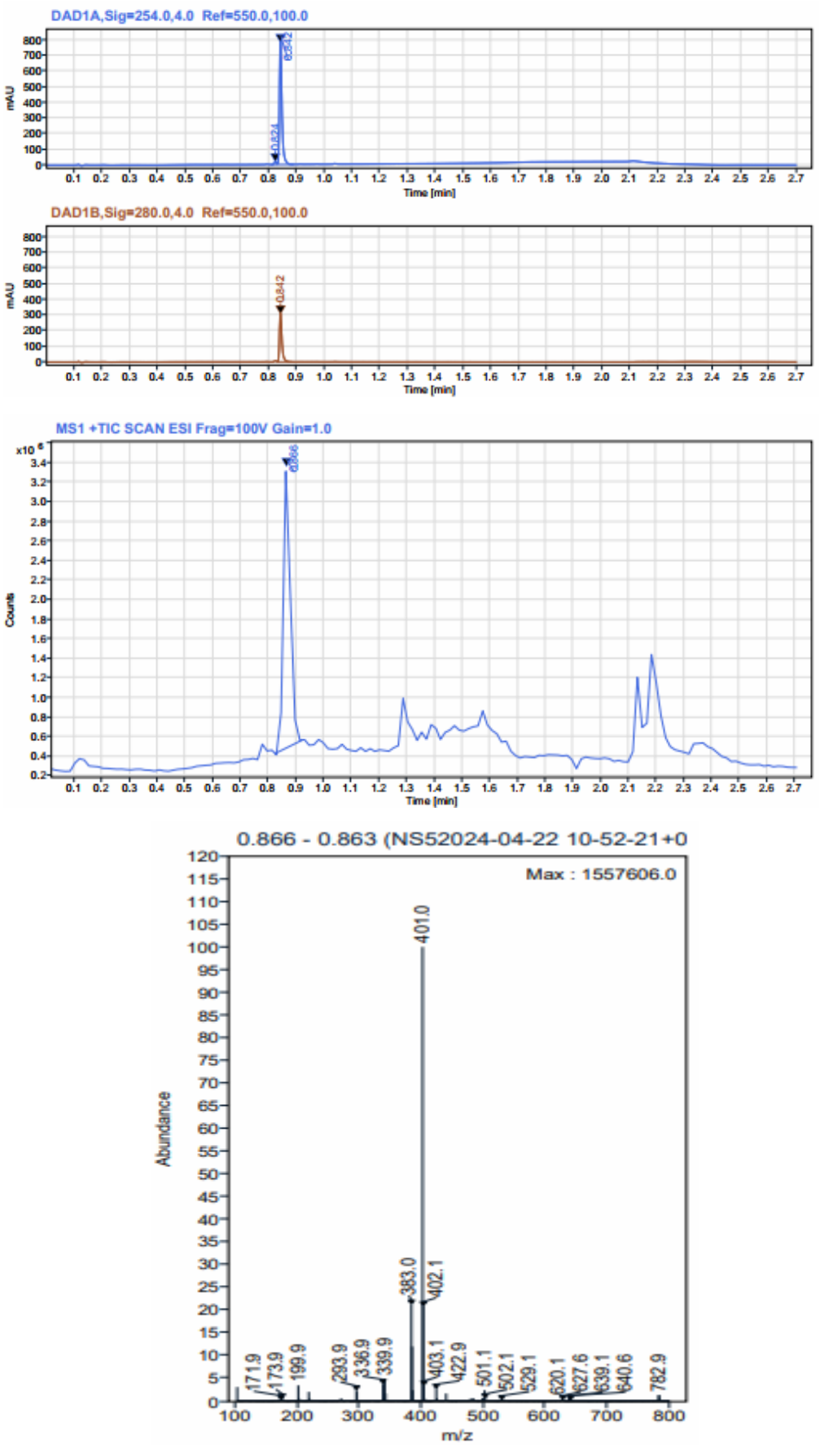


Figure 37: LC-MS of compound **51D**.

© University of Venda

Table 12: ^{13}C NMR chemical shift values (ppm) of ethyl 6-hydroxy-4-(chromon-3-yl)-2-oxo-6-trifluoromethyl-1,2,3,4-tetrahydropyrimidine-5-carboxylate derivatives **51A-E** (at 400 MHz).

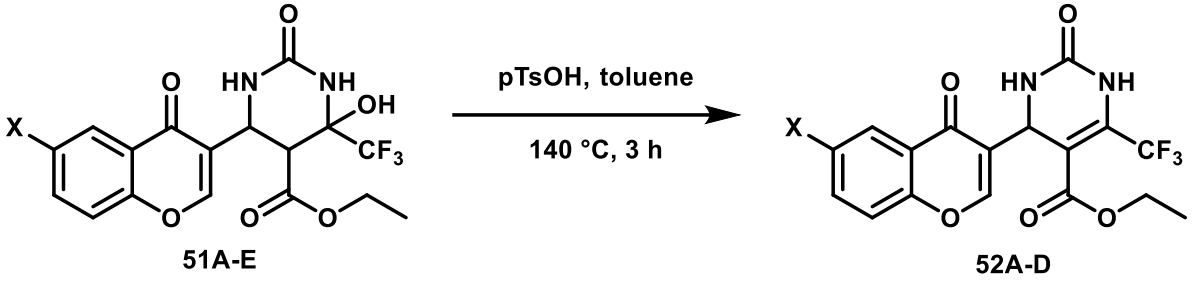
NUCLEUS	51A	51B	51C	51D	51E
C-2	153.9	153.71	153.9	153.8	153.8
C-3	119.9	120.6	119.4	120.8	120.1
C-4	175.6	174.9	175.7	175.7	174.5
C-4a	122.7	125.9	124.3	125.6	125.5
C-5	124.3	127.1	127.4	126.3	127.5
C-6	133.3	130.6	129.7	120.9	127.7
C-7	137.1	135.5	135.3	134.9	137.6
C-8	119.7	119.8	119.7	118.9	118.7
C-8a	155.3	156.8	155.4	155.9	154.8
C-9	47.4	52.0	46.2	47.2	47.2
C-10	46.2	45.3	45.4	46.2	46.2
C-11	81.1	80.8	82.8	80.9	80.8
C-12	157.7	157.8	157.7	157.6	157.9
C-13	167.9	167.4	167.9	167.9	167.8
OCH_2	60.9	60.8	60.8	60.7	60.8
CH_3	14.1	14.1	14.1	14.0	14.1
C-1'	135.3	140.3	133.7	-	-
C-2'	129.5	128.5	128.5	-	-
C-3'	116.6	128.6	128.6	-	-
C-4'	163.8	122.3	122.7	-	-
CF_3	116.7	116.2	113.5	111.0	116.2

4.1.12 Ethyl 4-(6-substituted chromone-3-)-2-oxo-6-trifluoromethyl-1,2,3,4-tetrahydropyrimidine-5-carboxylate derivatives 52A-D

To obtain the desired compounds, the partially reacted compounds from section 4.1.10 above were further reacted to dehydrate the OH group and form a double bond. Target compounds **52A-D** were synthesized via a thermal reaction employing compounds **51A-D**, para-toluene sulfonic acid as a catalyst in toluene at 140 °C for 3 hours, utilizing a Dean-Stark apparatus to

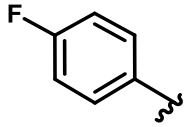
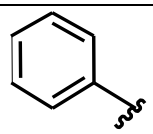
© University of Venda

facilitate continuous water removal (Scheme 17). The resultant compounds were thoroughly characterized using various spectroscopic techniques. Table 13 below depicts mass yield, percentage yield, and mass ratios of 4-(chromon-3-yl)-2-oxo-6-trifluoromethyl-1,2,3,4-tetrahydropyrimidine-5-carboxylate derivatives **52A-D**



Scheme 18: Synthesis of ethyl 4-(chromon-3-yl)-2-oxo-6-trifluoromethyl-1,2,3,4-tetrahydropyrimidine-5-carboxylate derivatives **52A-D**

Table 13: Synthesis of ethyl 4-(chromon-3-yl)-2-oxo-6-trifluoromethyl-1,2,3,4-tetrahydropyrimidine-5-carboxylate derivatives **52A-D**.

Compound 52	**X**	**Mass yield (g)**	**% Yield**	**Calculated *m/z***	**Actual *m/z* $[M+H]^+$**
A		0.094	23	476.1	477.0
B		0.012	24	458.1	459.1
C	**H**	0.200	38	382.1	383.0
D	**Br**	0.240	43	460.0	462.9

© University of Venda

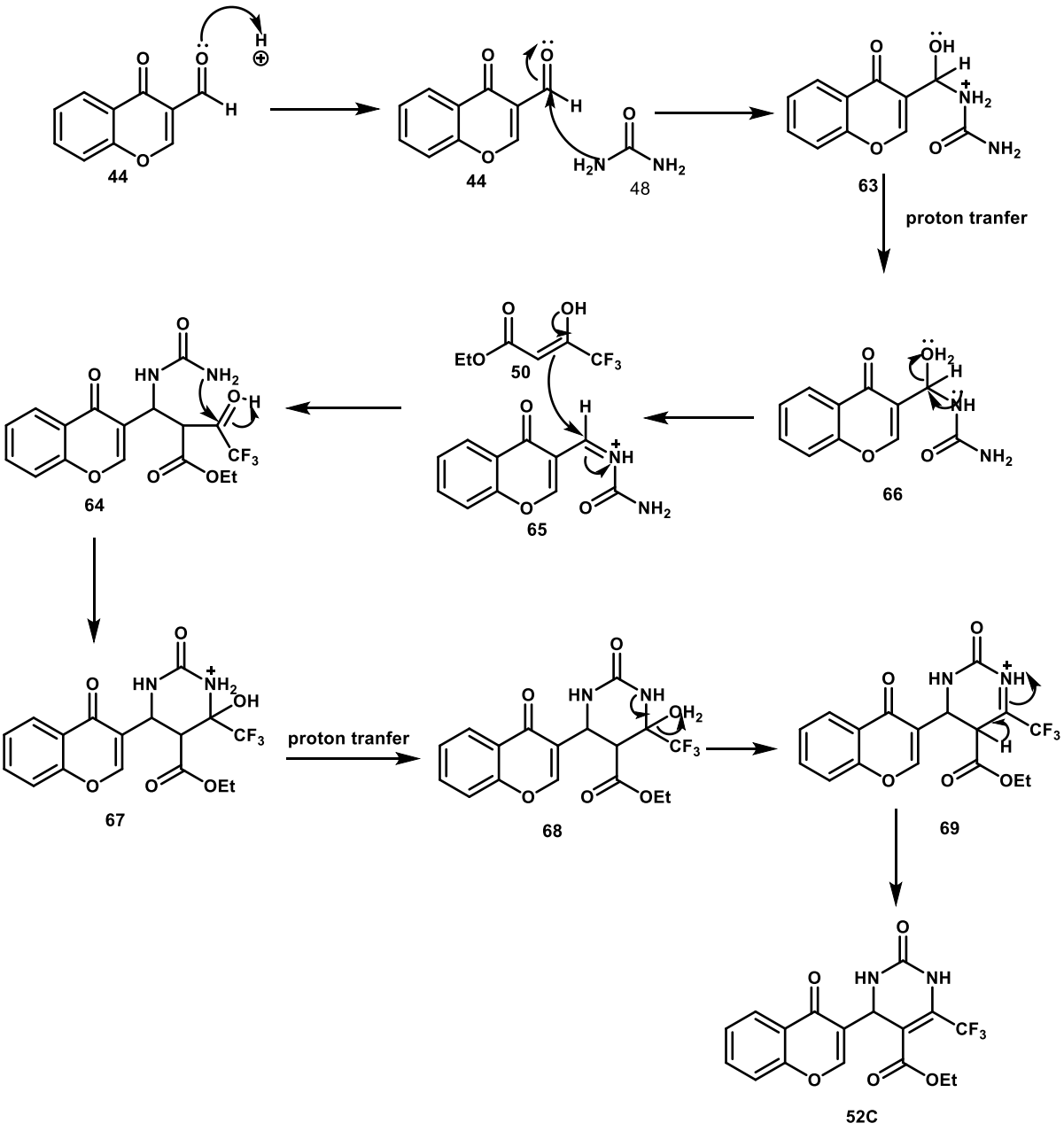
Analysis of ^{1}H NMR spectra of compounds **52A-D** revealed the disappearance of two signal peaks that were previously presence in compounds **51A-E**. The hydroxyl (OH) signal that previously appeared at around 7.03 ppm was not observed on newly formed targets. The H proton signals adjacent to the ester group previously observed between 3.5 - 4.0 ppm in compounds **51A-E**, were also no longer present. This was sufficient to confirm the success of cyclodehydration to afford compounds **52A-D**. The remaining proton signals appeared largely unchanged, with all other resonances maintaining their chemical shift values, indicating no unexpected changes in the molecular structure. The presence of the ester functional group was further confirmed on DEPT 135 (figure 39) by the presence of the OCH_2 group. Figures 36, 37 and 38 depict the expanded^{1}H NMR, ^{1}H NMR and ^{13}C MNR spectra of compound **52C**.

FTIR analysis of compound **52C** (Figure 39) showed the disappearance of OH which was previously appearing at 3457.77 cm^{-1} on the precursor compound **51C** (Figure 34). Other functional groups that confirmed the success of dehydration reaction to compounds **52A-D** include NH of the amide at 3216.96 cm^{-1}, C-H aromatic at 3091.58 cm^{-1} and C=O at 1686.72 cm^{-1}. HRMS (Figure 41) and LC-MS (Table 13) also confirmed the success of dehydration reaction to compounds **52A-D**. Table 14 below shows ^{13}C NMR chemical shift values (ppm) of ethyl 4-(chromon-3-yl)-2-oxo-6-trifluoromethyl-1,2,3,4-tetrahydropyrimidine-5-carboxylate derivatives **52A-E** (at 400 MHz). Figures 79-89 in the appendix show spectra for **52A-B** and **52D.**

4.1.12 Mechanism for synthesis of Ethyl 4-(6-substituted chromone-3-)-2-oxo-6-trifluoromethyl-1,2,3,4-tetrahydropyrimidine-5-carboxylate derivatives 52A-D

The rate-determining nucleophilic addition of urea to the aldehyde is the first step in this strategy. The condensation process that follows is catalysed by the addition of acid, resulting in imine nitrogen. The ketoester then contributes to the imine bond, and the ring is completed by the amine's nucleophilic assault on the carbonyl group. This final step results in a second condensation and the Biginelli compound (Scheme 18).[71]

© University of Venda



Scheme 19: Mechanism for the synthesis of ethyl 4-(chromon-3-yl)-2-oxo-6-trifluoromethyl-1,2,3,4-tetrahydropyrimidine-5-carboxylate derivatives **52A-E.**

© University of Venda

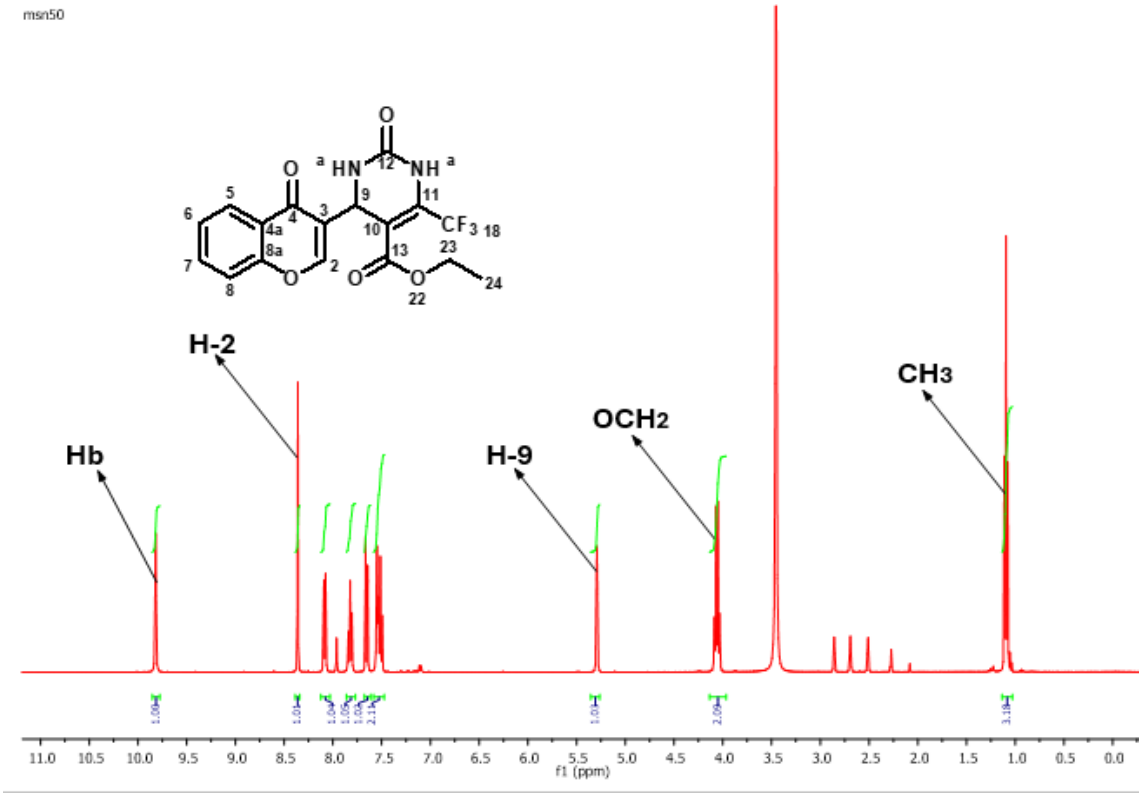


Figure 38: [1]H NMR spectrum of ethyl 2-oxo-4-(4-oxo-4*H*-chromen-3-yl)-6-(trifluoromethyl)-1,2,3,4-tetrahydropyrimidine-5-carboxylate **52C** in DMSO-DMF.

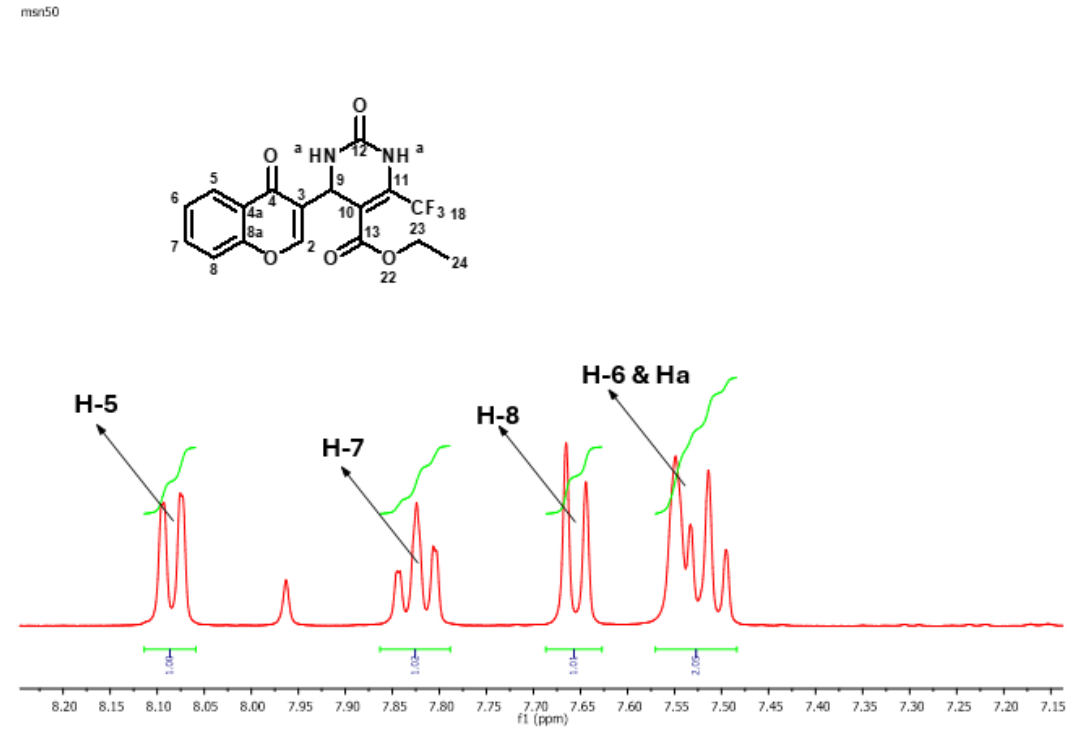


Figure 39: Expanded [1]H NMR spectrum of ethyl 2-oxo-4-(4-oxo-4*H*-chromen-3-yl)-6-(trifluoromethyl)-1,2,3,4-tetrahydropyrimidine-5-carboxylate **52C** in DMSO-DMF.

© University of Venda

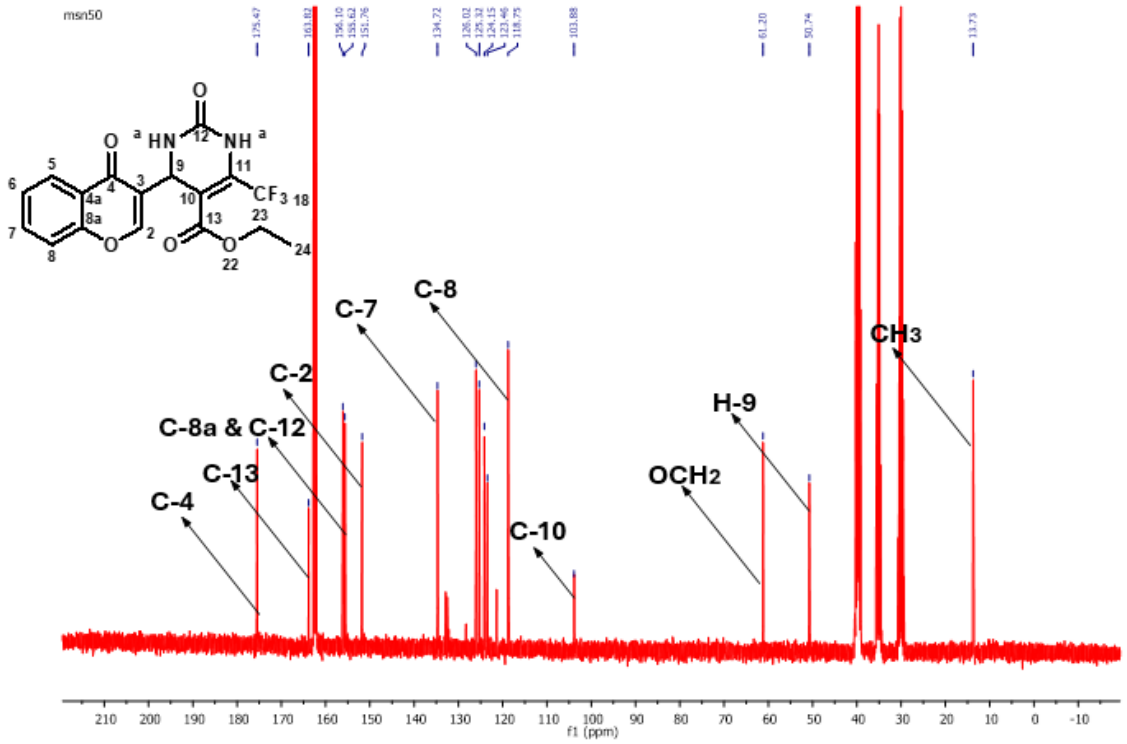


Figure 40: ^{13}C NMR spectrum of ethyl 2-oxo-4-(4-oxo-4*H*-chromen-3-yl)-6-(trifluoromethyl)-1,2,3,4-tetrahydropyrimidine-5-carboxylate **52C** in DMSO-DMF.

© University of Venda

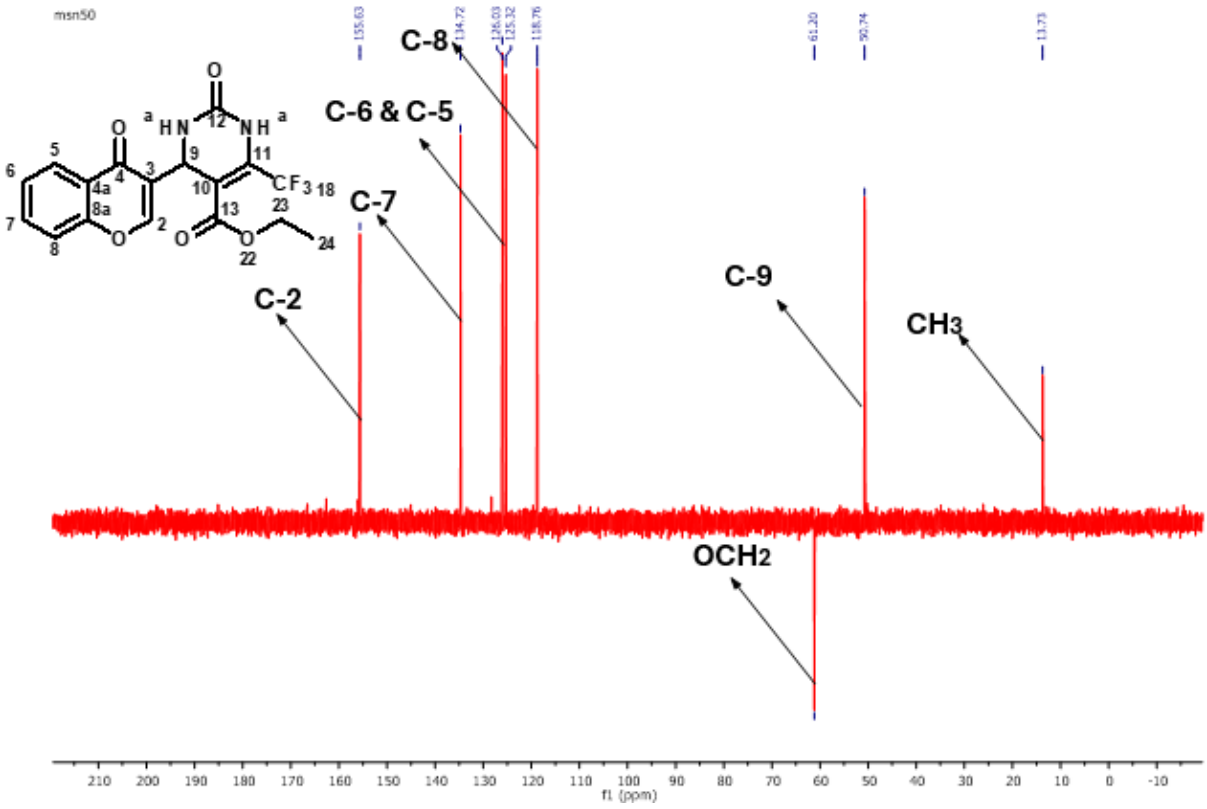


Figure 41: DEPT 135 NMR spectrum of ethyl 2-oxo-4-(4-oxo-4*H*-chromen-3-yl)-6-(trifluoromethyl)-1,2,3,4-tetrahydropyrimidine-5-carboxylate **52C** in DMSO-DMF.

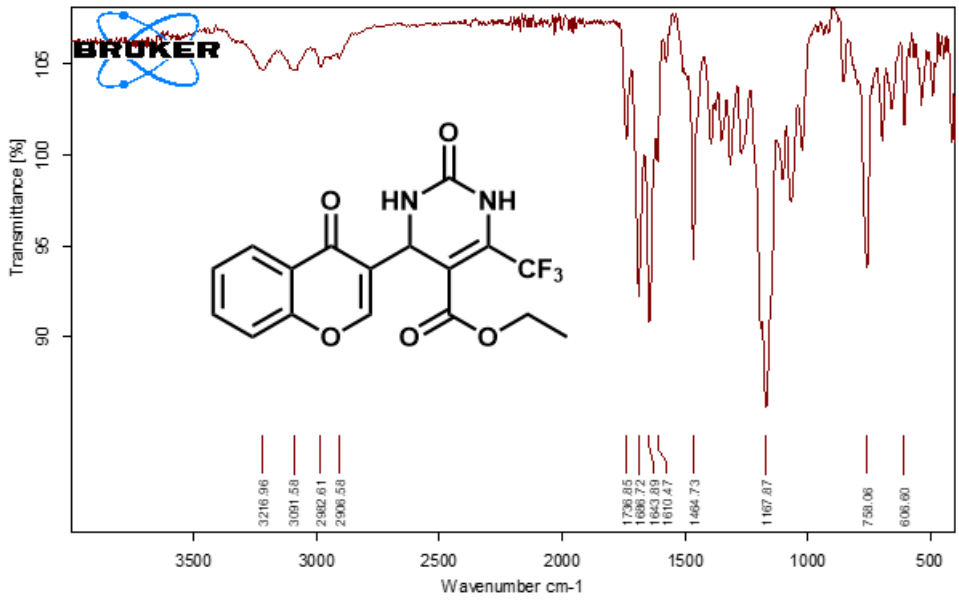


Figure 42: FT-IR spectrum of compound **52C.**

© University of Venda

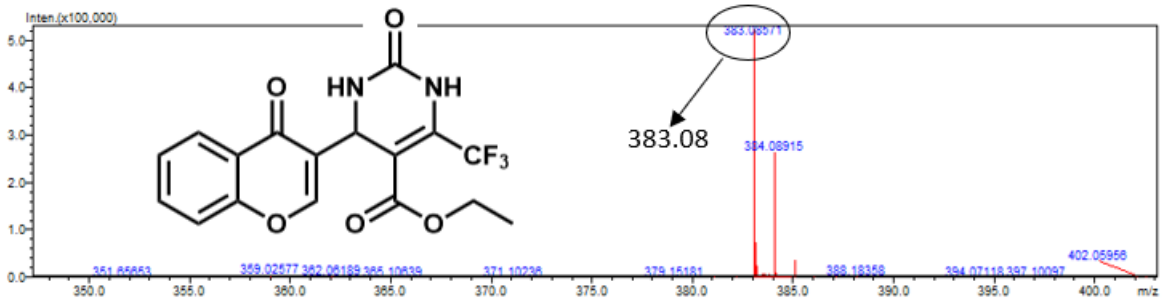


Figure 43: HRMS spectrum of compound **52C**.

© University of Venda

Table 14: ^{13}C NMR chemical shift values (ppm) of ethyl 4-(chromon-3-yl)-2-oxo-6-trifluoromethyl-1,2,3,4-tetrahydropyrimidine-5-carboxylate derivatives **52A-E** (at 400 MHz).

NUCLEUS	52A	52B	52C	52D
C-2	151.8	151.8	155.6	156.0
C-3	119.8	119.8	123.5	121.5
C-4	175.5	175.5	175.5	174.3
C-4a	122.7	124.5	124.2	125.6
C-5	124.4	126.0	126.0	127.5
C-6	133.3	129.7	123.3	127.7
C-7	137.1	138.1	134.7	137.4
C-8	118.6	118.6	118.9	118.5
C-8a	155.5	155.6	155.6	151.2
C-9	50.9	50.9	50.7	50.7
C-10	103.7	103.8	103.8	103.5
C-11	132.6	132.6	131.0	131.5
C-12	155.8	155.9	156.1	155.1
C-13	163.9	163.9	163.8	163.7
OCH_2	61.4	60.4	61.2	61.2
CH_3	14.1	14.1	13.7	13.7
C-1'	135.3	145.8	-	-
C-2'	129.6	128.6	-	-
C-3'	116.5	125.9	-	-
C-4'	161. 4	122.6	-	-
CF_3	121.4	121.4	120.0	120.5

© University of Venda

4.2 Biological Results

After successful synthesis, purification, and full characterization of the desired chromone target compounds, *in vitro* antimicrobial studies against the *Mtb* H37Rv strain were carried out at the University of Cape Town's H3D group. A modified microplate Alamar blue assay (MABA) was implemented to measure the MIC of each target molecule.[74]. For this study, the MIC is defined as the minimum concentration at which growth is inhibited 90%.

For all target compounds three different media were used. The composition of media in which MIC testing is performed has been shown to influence the behavior of some compounds.[75] Specifically, the presence of the detergent Tween 80 and of serum albumin has been shown to affect the activity of compounds.[75-77] Therefore, each compound was screened in media with three different compositions to determine if the supplements mentioned would modulate compound activity. The media used, were 7H9_ADC_GLU_TW: Middlebrook 7H9 media (Difco) supplemented with 0.2% glucose, Middlebrook albumin-dextrose- catalase (ADC) enrichment (Difco) and 0.05% Tween 80, 7H9_ADC_GLU_TX: Middlebrook 7H9 media (Difco) supplemented with 0.2% glucose, Middlebrook albumin-dextrose-catalase (ADC) enrichment (Difco) and 0.05% tyloxapol and 7H9_CAS_GLU_TX: Middlebrook 7H9 media (Difco) supplemented with 0.4% glucose, 0.03% Casitone (Gibco Bacto) and 0.05% tyloxapol. [75-77]

Qualitative as well as quantitative growth inhibition was determined. Qualitative scores were determined by visual observation of a bacterial pellet, where the visual MIC refers to the lowest concentration at which no bacterial pellet was observed. For the quantitative/calculated MIC, Alamar Blue, a resazurin-based, fluorescent and redox-responsive dye was chosen as a commercially available reagent providing a spectroscopic measure of the metabolic activity of bacterial cells. The MIC value was obtained after the addition of the resazurin dye and subsequent measurement of fluorescence. The anti-TB drugs isoniazid (INH) and moxifloxacin were used as reference standards in this study.

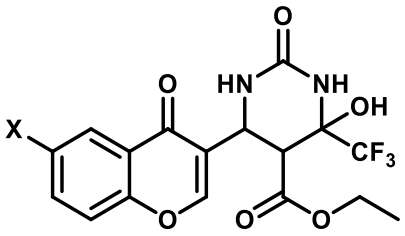
When determining the antimycobacterial activity, compounds with MIC_{90} < 15 µM would be considered active towards the inhibition of *Mtb*, compounds with MIC_{90} 15-35 µM moderately active, while those in the range MIC_{90} 35 to 62.5 µM were considered poorly active. Compounds with MIC_{90} >62.5 µM would be considered inactive. Unfortunately, all tested compounds were inactive against the *Mtb* H37Rv strain with MIC_{90} >62.5 µM (Table 15). The results suggest that the presence of the OH group yields inactive compounds. Reducing the OH group to form a double bond as reported in the literature is therefore critical for activity.

All tested compounds were evaluated for solubility at pH 7.4 in DMSO. Unsubstituted chromone (**51D**) and bromo-substituted chromone (**51E**) both exhibited high solubility of 200 µM. The addition of phenyl ring on chromone (**51C**) resulted in low solubility of 45 µM.

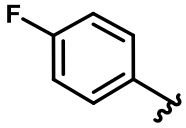
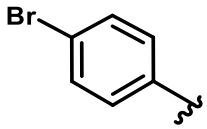
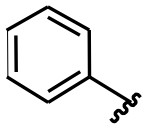
© University of Venda

Substituting a phenyl ring with fluorine (**51A**) and bromine (**51B**) on chromone resulted in an insoluble compound. These results revealed that the addition of a phenyl ring to chromone reduces the solubility.

Table 15: *In vitro* biological assays for synthesized ethyl 6-hydroxy-4-(chromon-3-yl)-2-oxo-6-trifluoromethyl-1,2,3,4-tetrahydropyrimidine-5-carboxylate derivatives 51A-E against *Mtb* H37Rv strain.



51A'-E'

Compound 51	**X**	**MIC_{90} (μM)[a]**	**MIC_{90} (μM)[b]**	**MIC_{90} (μM)[c]**	**Solubility (μM)**
A		>62.5	>62.5	>62.5	5
B		>62.5	>62.5	>62.5	<5
C		>62.5	>62.5	>62.5	45
D	**H**	>62.5	>62.5	>62.5	200
E	**Br**	>62.5	>62.5	>62.5	200
Isoniazid		4.35	5.97	1.66	
Moxifloxacin		0.24	0.16	0.35	

Media[a,b,c] used for screening: a = 7H9_ADC_GLU_TW, b = 7H9_ADC_GLU_TX and c = 7H9_CAS_GLU_TX.

The target compounds, ethyl 6-hydroxy-4-(chromon-3-yl)-2-oxo-6-trifluoromethyl-1,2,3,4-tetrahydropyrimidine-5-carboxylate derivatives **51A-E**, were successfully dehydrated to yield ethyl 4-(6-substituted/unsubstituted chromone-3-)-2-oxo-6-trifluoromethyl-1,2,3,4-

© University of Venda

tetrahydropyrimidine-5-carboxylate derivatives **52A-D**. Notably, these derivatives are analogous to those previously reported by Raju and co-workers, which exhibited potent activity against the *Mtb* H37Rv strain.[70] The results in Table 16 show that none of the target compounds were active against *Mtb* H37Rv in three different media. Additionally, converting the hydroxyl group to a double bond had no significant effect on the compounds' biological activity.

Compound **52B**, which was employed as a reference compound in this study, was previously reported by Raju and co-workers to exhibit a minimum inhibitory concentration (MIC) of 3.4 µM.[70] However, upon re-synthesis, compound **52B** was found to be inactive, with an MIC value exceeding 62.5 µM. This discrepancy may be attributable to differences in the testing media utilized. The media used for the reference compound (Middlebrook 7H11 agar) and experimental compounds (Middlebrook 7H9 broth) differed, which may have impacted the results.

Middlebrook 7H11 agar is a selective solid medium containing malachite green, which inhibits gram-positive bacteria and enhances the growth of M. tuberculosis.[81] However, malachite green can also lead to false positives by inhibiting contaminating bacteria and masking compound toxicity.[82] In contrast, Middlebrook 7H9 broth is a non-selective liquid medium that supports the growth of a wider range of microorganisms.[83] While it offers faster growth rates and is suitable for studying bacterial physiology, it may not support all mycobacterial species and is more prone to contamination.[83] The liquid nature of 7H9 broth and the presence of Tween 80 can cause bacterial clumping, leading to false negative results.[83-85] Variations in incubation conditions, such as temperature, time, and atmosphere, may have contributed to the differences in minimum inhibitory concentrations (MICs) between the literature compound and the re-synthesized compound.

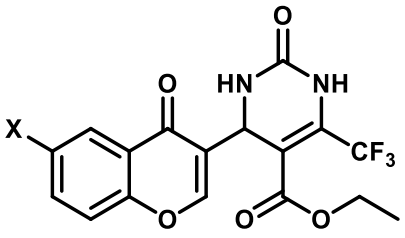
The target compounds **52A-D** exhibited poor solubility, with compounds **52C** and **52D** showing solubility values of 15 µM and 10 µM, respectively. Compounds **52A** and **52B** were insoluble, with values below 5 µM. Removal of the hydroxyl (OH) group from compounds **51D-E** significantly reduced their solubility, decreasing from 200 µM to 15 µM and 10 µM for compounds **52C** and **52D**, respectively. These results emphasize the importance of the OH group in maintaining solubility.

Cytotoxicity assays were conducted on the inactive compounds **52A-D** against the HepG2 cell line to distinguish between genuine inactivity and false negative caused by cell death. This helps to determine whether the inactivity stems from lack of biological activity or cytotoxic effects. Understanding the cytotoxicity profile also informs future compound development and modification. Results revealed no cytotoxic effects, with all compounds exhibiting values

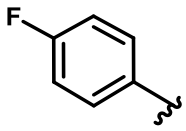
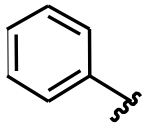
© University of Venda

above 50 µM. Emetine, used as a control, showed a value below 0.016 µM, within the expected range for this cell line.

Table 16: *In vitro* biological assays for synthesized Ethyl 4-(6-substituted/unsubstituted chromone-3-)-2-oxo-6-trifluoromethyl-1,2,3,4-tetrahydropyrimidine-5-carboxylate derivatives **52A-D** against *Mtb* H37Rv strain and cytotoxicity.



52A-D

Compound 52	**X**	**MIC_{90} (µM)[a]**	**MIC_{90} (µM)[b]**	**MIC_{90} (µM)[c]**	**Cytotoxicity (µM)**	**Solubility (µM)**
A		>62.5	>62.5	>62.5	>50	<5
B		>62.5	>62.5	>62.5	>50	<5
C	**H**	>62.5	>62.5	>62.5	>50	15
D	**Br**	>62.5	>62.5	>62.5	>50	10
Isoniazid		4.35	5.97	1.66		
Moxifloxacin		0.24	0.16	0.35		

Media[a,b,c] used for screening: a = 7H9_ADC_GLU_TW, b = 7H9_ADC_GLU_TX and c = 7H9_CAS_GLU_TX.

© University of Venda

CHAPTER 5: CONCLUSION AND PERSPECTIVE

5.1 Conclusions

This study investigated the synthesis of two series of chromone-based compounds as potential anti tubercular agents. Despite the challenges in synthesizing the first series due to decarboxylation during amidation, the second service was successfully prepared. Although the latter series showed no activity against tuberculosis; its lack of cytotoxicity is noteworthy.

Firstly, the investigation of 6,8-disubstituted/unsubstituted chromone-3-carbamates was conducted for the evaluation of potential antituberculosis activity. The syntheses of the 6,8-disubstituted/unsubstituted chromone-3-carbaldehydes **44A-E** were synthesized by subjecting 3,5-disubstituted/unsubstituted 2-hydoxyacetophenones **43A-C** to a Vilsmeier-Haack reaction and converted to 6,8-disubstituted/unsubstituted chromone-3-carboxylic acid analogues **45A-B** by the Lindgren oxidation. The amidation of the 6,8-disubstituted/unsubstituted chromone-3-carboxylic acids was unsuccessful.

Also, a series of new ethyl 6-hydroxy-4-(6-substituted/unsubstituted chromone-3-)-2-oxo-6-trifluoromethyl-1,2,3,4-tetrahydropyrimidine-5-carboxylate derivatives **51A-E** were synthesized to enhance the efficacy and physicochemical properties of the previously discovered analogue **40A**. Our desired substituted chromone target compounds were successfully synthesized from 3,5-disubstituted/unsubstituted-2-hydroxyacetophenones using a literature reported method. Six new 6-substituted/unsubstituted chromone-3-carbaldehydes **48A-F** were synthesized and transformed into ethyl 6-hydroxy-4-(6-substituted/unsubstituted chromone-3-)-2-oxo-6-trifluoromethyl-1,2,3,4-tetrahydropyrimidine-5-carboxylate derivatives **51A-E**.

The synthesized products **51A-E** were obtained in moderate to high yields, characterized using NMR, FTIR, LC-MS, HRMS and melting point determination. The fully characterized synthesized compounds were screened against the *Mtb* H37Rv clinical strain. Three media were used for screening and MABA was used to obtain quantitative results. Unfortunately, compounds **51A-E** were inactive. Tested compounds with phenyl ring attached to the chromone (**51A-C**) resulted in low solubility, whereas compounds (**51D-E**) without a phenyl ring showed high solubility of 200 µM. After successful removal of the OH group on compounds **51A-E** by dehydration, compounds **52A-D** were also screened against *Mtb* H37Rv clinical strain under similar conditions. Conversely, the tested compounds were still inactive indicating that the presence of OH does not affect the activity but improves solubility as the solubility for compounds **51D-E** was greatly decreased. The *Mtb* results were not in line with the one reported by Raju and co-workers, compound **52C** with MIC of 3.4 µM. The discrepancies in

© University of Venda

the results could be due to differences media used, incubation conditions, bacteria, contaminations, or others.

5.2 Future work

I. To conduct biological studies for synthesized target compounds using 7H11 media condition

II. Further investigation and method modifications for the synthesis of 6,8-disubstituted/unsubstituted chromone-3-carbamates.

III. CHN analysis of all synthesized compounds.

© University of Venda

CHAPTER 6: EXPERIMENTAL

6.1 General methods

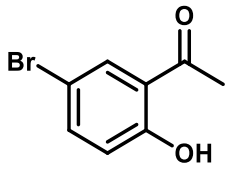
All reactions were performed in an oven-dried round-bottom flask with a magnetic stirring bar. Melting points were determined using a BÜCHI Melting point B-540 apparatus. A Fourier transform infrared spectrometer was used to capture IR spectra. ^{1}H NMR (400 MHz) spectra were obtained using $CDCl_3$ as solvent ($CHCl_3$ = 7.26 ppm) on a Bruker 400 MHz spectrometer. ^{13}C NMR (100 MHz) spectra were also recorded on the Bruker NMR spectrometer using $CDCl_3$ as solvent ($CHCl_3$ = 77.0 ppm). Chemical shifts for ^{1}H and ^{13}C NMR are given in parts per million (ppm). NMR signals are abbreviated as follows: s = singlet, d = doublet, t = triplet, q = quartet, m = multiplet. Coupling constants, *J*, were recorded in hertz (Hz).

6.2 Syntheses

6.2.1 General synthesis of 5-bromo-2-hydroxyacetophenone 42B

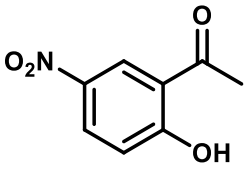
2-Hydroxyacetophenone **42A** 29 mmol) was treated with NBS (29 mmol) in acetic acid (30 mL). The mixture was heated under reflux while stirring for 2 hours. The mixture was then quenched with ice-cold water (100 mL), dried, then recrystallized with ethanol to afford the expected 5-bromo-2-hydroxyacetophenone **42B** as a brown precipitate.

5-Bromo-3-iodo-2-hydroxyacetophenone 42B (55%)



2-Hydroxyacetophenone **42A** (29 mmol), NBS (29 mmol), acetic acid (30 mL). m.p. 57- 61 °C, lit.[70] 58 – 61 °C, IR ν_{max}/cm^{-1} 3064.41 (CH, aromatic), 2998.69 (CH), 1645.83 (C=O). ^{1}H NMR (400 MHz, $CDCl_3$) δ 12.09 (s, 1H), 7.75 (d, *J* = 2.4 Hz, 1H), 7.46 (dd, *J* = 8.9, 2.4 Hz, 1H), 6.80 (d, *J* = 8.9 Hz, 1H), 2.55 (s, 3H) ppm. ^{13}C NMR (101 MHz, $CDCl_3$) δ 203.6 (C=O), 161.3 (C-2), 139.1 (C-4), 132.9 (C-6), 120.9 (C-1), 120.5 (C-3), 110.4 (C-5), 26.7 (CH_3) ppm.

6.2.2 Synthesis of 5-nitro-2-hydroxyacetophenone 42C (56%)



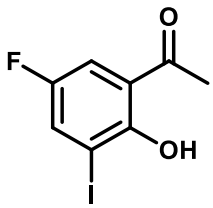
© University of Venda

A mixture of nitric acid (4 eq) and sulphuric acid (4 eq) was added dropwise at 0 °C into a round bottom flask containing 2-hydroxyacetophenone **42A** (29 mmol). The mixture was stirred for 6 hours. The reaction mixture was quenched with ice-cold water (100 mL), dried then recrystallized with ethanol to afford the expected 5-nitro-2-hydroxyacetophenone **42C** as a yellow precipitate, m.p. 57 - 61 °C, lit.[73] 58 – 61 °C, IR ν_{max}/cm^{-1} 3063.81 (CH, aromatic), 2999.66 (CH), 1641.27 (C=O). ^{1}H NMR (400 MHz, $CDCl_3$) δ 12.87 (s, 1H), 8.71 (d, *J* = 2.7 Hz, 1H), 8.34 (dd, *J* = 9.2, 2.7 Hz, 1H), 7.08 (d, *J* = 9.3 Hz, 1H), 2.76 (s, 3H) ppm. ^{13}C NMR (100 MHz, $CDCl_3$) δ 204.1 (C=O), 167.1 (C-2), 139.5 (C-5), 131.1 (C-4), 127.4 (C-6), 119.5 (C-1), 118.5 (C-3), 26.7 (CH_3) ppm.

6.2.3 General synthesis of 3,5-disubstituted/unsubstituted 2-hydroxyacetophenones 43A-D

The corresponding 2-hydroxyacetophenones **42A-E** (29 mmol) were treated with NIS (29 mmol) in acetic acid (30 mL). The mixture was heated under reflux while stirring for 2 hours. The mixture was quenched with ice-cold water (100 ml), dried then recrystallized with ethanol to afford the expected 3,5-disubstituted/unsubstituted 2-hydroxyacetophenone derivatives **43A-E**

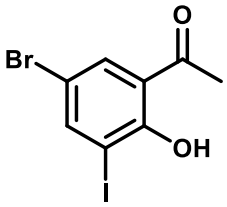
5-Fluoro-2-hydroxy-3-iodoacetophenone 43A (78%)



5-Fluoro-2-hydroxy-3-iodoacetophenone **42 C** (29 mmol), NIS (29 mmol), acetic acid (30 ml). Dark brown solid, m.p. 90-98 °C, IR ν_{max}/cm^{-1} 3066.71 (CH, aromatic), 1650.26 (C=O). ^{1}H NMR (400 MHz, $CDCl_3$) δ 12.86 (s, 1H), 7.73 (dd, *J* = 7.3, 3.0 Hz, 1H), 7.46 (dd, *J* = 8.4, 3.0 Hz, 1H), 2.65 (s, 3H) ppm. ^{13}C NMR (100 MHz, $CDCl_3$) δ 203.3 (C=O), 203.2 (C=O), 157.7 (C-2), 157.7 (C-2), 155.7 (C-5), 153.3 (C-5), 133.3 (C-4), 133.1 (C-4), 118.3 (C-1), 118.2 (C-1), 116.2 (C-6), 116.0 (C-6), 86.3 (C-3), 86.2 (C-3), 26.5 (CH_3) ppm.

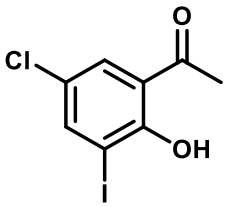
5-Bromo-3-iodo-2-hydroxyacetophenone 43B (78%)

© University of Venda



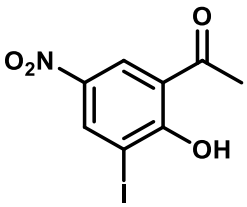
5-Bromo-2-hydroxyacetophenone (29 mmol),**42B** NBS (29 mmol), acetic acid (30 mL). Brown solid, m.p. 90 - 93 °C, lit.[70] 89 °C, IR ν_{max}/cm^{-1} 3064.34 (CH, aromatic), 2999.66 (CH), 1643.76 (C=O). ^{1}H NMR (400 MHz, $CDCl_3$) δ 13.06 (s, 1H), 8.04 (d, *J* = 2.2 Hz, 1H), 7.84 (d, *J* = 2.3 Hz, 1H), 2.65 (s, 4H) ppm. ^{13}C NMR (100 MHz, $CDCl_3$) δ 203.2 (C=O), 160.2 (C-2), 147.3 (C-4), 133.1 (C-6), 120.2 (C-1), 111.1 (C-5), 87.7 (C-3), 26.5 (CH_3) ppm.

5-Chloro-3-iodo-2-hydroxyacetophenone 43C (80%)



5-Chloro-2-hydroxyacetophenone **42D** (29 mmol), NBS (29 mmol), acetic acid (30 mL). Yellow solid, m.p. 108 -111 °C, lit.[70] 105 °C. IR ν_{max}/cm^{-1} 3066.71 (CH, aromatic), 1650.26 (C=O). ^{1}H NMR (400 MHz, DMSO) δ 12.95 (s, 1H), 8.09 (d, *J* = 2.1 Hz, 1H), 8.03 (d, *J* = 2.2 Hz, 1H), 2.69 (s, 3H) ppm. ^{13}C NMR (100 MHz, DMSO) δ 205.2 (C=O), 159.4 (C-2), 144.4 (C-4), 131.4 (C-6), 124.0 (C-5), 120.3 (C-1), 88.4 (C-3), 27.4 (CH_3) ppm.

2-Hydroxy-3-iodo-5-nitroacetophenone 43D (65%)



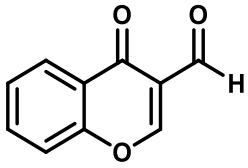
2-Hydroxy-5-nitroacetophenone **42C** (29 mmol), NIS (29 mmol), acetic acid (30 mL). Black solid, m.p. 132-136 °C, IR ν_{max}/cm^{-1} 3066.71 (CH, aromatic), 1650.26 (C=O). ^{1}H NMR (400 MHz, $CDCl_3$) δ 12.87 (s, 1H), 8.83 (d, *J* = 2.6 Hz, 1H), 8.71 (dd, *J* = 2.6, 1H), 2.18 (s, 3H) ppm. ^{13}C NMR (101 MHz, $CDCl_3$) δ 203.98(C=O), 167.2 (C-2), 144.7 (C-5), 140.2 (C-4), 119.6 (C-6), 118.5 (C-1), 86.7 (C-3), 26.5 (CH_3) ppm.

© University of Venda

6.2.4 General synthesis of 6,8-disubstituted/unsubstituted chromone-3-carbaldehyde derivatives 44A-C

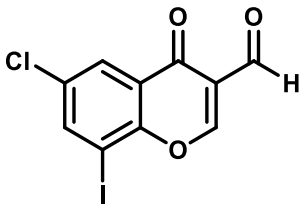
To an oven-dried round-bottom flask, the corresponding 3,5-disubstituted/unsubstituted 2-hydroxyacetophenone **42A-D** (3.30 mmol) in DMF (15 mL) was added. $POCl_3$ (3 mL) was added dropwise at 0 °C and left to stir at room temperature for 12 – 18 h. The reaction mixture was quenched with ice-cold water (100 mL) to yield crude solid product, which was then recrystallized using hot ethanol to afford the expected 6,8-disubstituted/unsubstituted chromone-3-carbaldehyde derivatives **44A-D**.

Chromone-3-carbaldehyde 44A (95%)



2-Hydroxyacetophenone **42A** (2 g, 18.36 mmol), DMF (15 mL), $POCl_3$ (3 mL). Yellow, solid, m.p.154 - 160 °C, lit.[70] 151 – 153 °C, IR ν_{max}/cm^{-1} 1691.27 (C=0), 1643.94 (C=O). ^1H NMR (400 MHz, $CDCl_3$) δ 10.38 (1H, s), 8.56 (1H, s), 8.39 (1H, d, *J* = 2.3 Hz), 7.79 - 7.75 (1H, m, *J* = 8.9, 2.4 Hz), 7.56 - 7.49 (2H, m) ppm. ^{13}C NMR (101 MHz, $CDCl_3$) δ 188.5 (CHO), 175.9 (C-4), 160.7 (C-2), 156.2 (C-8a), 134.9 (C-7), 126.6 (C-6), 126.1 (C-5), 125.3 (C-3), 120.3 (C-4a), 118.6 (C-8) ppm.

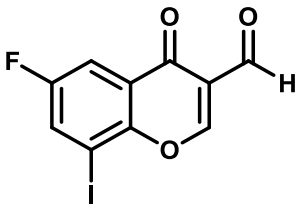
6-Chloro-8-iodo-chromone-3-carbaldehyde 44C (86%)



5-Chloro-3-iodo-2-hydroxyacetophenone **43C** (3 g, 13.88 mmol), DMF (15 mL), $POCl_3$ (3 mL). Brown solid, m.p. 200 - 206 °C, IR ν_{max}/cm^{-1} 3071.22 (CH, aromatic), 2972.28 (CH),1692.28 (C=O), 1651.28 (C=O). ^1H NMR (400 MHz, $CDCl_3$) δ 10.26 (1H), 8.53 (1H, s), 8.14 (1H. d, *J* = 2.3 Hz), 8.08 (1H, d, *J* = 2.3 Hz ppm. ^{13}C NMR (101 MHz, $CDCl_3$) δ 187.8 (CHO), 174.5 (C-4), 160.7 (C-2), 153.9 (C-8a), 144.0 (C-7), 133.4 (C-5), 126.5 (C-3), 125.9 (C-6), 120.0 (C-4a). 88.9 (C-8) ppm.

© University of Venda

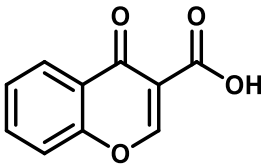
6-Fluoro-8-iodochromone-3-carbaldehyde 44B (98%)



6-Fluoro-8-iodo-2-hydroxyacetophenone **43A** (1 g, 2.56 mmol), DMF (15 mL), $POCl_3$ (3 mL). Brown, solid, m.p. 198-205 °C, IR ν_{max}/cm^{-1} 3066.71 (CH, aromatic), 1763.81 (C=0), 1643.81 (C=O). ^1H NMR (400 MHz, $CDCl_3$) δ 10.35 (1H, s), 8.62 (1H, s), 7.94 (2H, d, *J* = 1.63 Hz) ppm. ^{13}C NMR (101 MHz, $CDCl_3$) δ 187.9 (CHO), 174.9 (C-4), 160.8 (C-2), 159.5 (C-6), 152.0 (C-8a), 132.7 132.5 (C-7), 126.8 (C-3), 119.3 (C-4a), 111.8 (C-5), 86.0 (C-8) ppm.

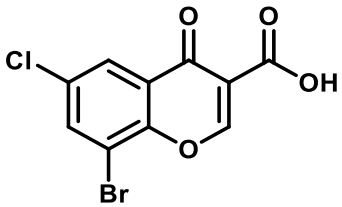
6.2.5 General synthesis of 6,8-disubstituted/unsubstituted chromone-3-carboxylic acid derivatives 45A-B

Chromone-3-carboxylic acid 45A (38%)



Chromone-3-carbaldehyde **44A** (1 g, 17.46 mmol), sulfamic acid (4 g), sodium chlorite (2 g). Yellow, solid, m.p. 199 -201 °C, lit.[10] 202 – 205 °C, IR ν_{max}/cm^{-1} 3324.10 (OH), 3074.09 (CH, aromatic), 2922.62 (CH) 1748.57 (C=O), 1631.83 (C=O). ^1H NMR (400 MHz, $CDCl_3$) δ 9.03 (H, s), 8.40 (1H, dd, *J* = 1.7, 2,4 Hz), 7.92 - 7.87 (1H, m), 7.71 (1H, d, *J* = 1.7 Hz), 7.69 - 7.60 (2H, m) ppm. ^{13}C NMR: δ 179.4 (C-4), 164.2 (C-2), 163.9 (COOH), 156.6 (C-8a), 136.1 (C-7), 127.3 (C-6), 126.6 (C-5), 122.9 (C-4a), 118.8 (C-8), 113.1 (C-3) ppm.

6-Chloro-8-bromochromone-3-carboxylic acid 45B (15%)



6-Chloro-8-bromochromone-3-carbaldehyde **44D** (1.2 g, 13.88 mmol), acetic acid (15 mL), sodium acetate (3 mL). (2.7 g, 96.11%). Brown solid, m.p. 320 - 321 °C, IR ν_{max}/cm^{-1} 3324.10

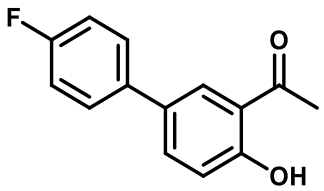
© University of Venda

(OH), 3074.09 (CH, aromatic), 2922.62 (CH) 1748.57 (C=O), 1631.83 (C=O). ^{1}H NMR (400 MHz, $CDCl_3$) δ 9.03 (H, s), 8.50 (1H, d, *J* = 1.7 Hz), 8.40 (1H, d, *J* = 1.7 Hz) ppm. ^{13}C NMR: δ 177.9 (C-4), 164.0 (C-2), 163.0 (COOH), 152.0 (C-8a), 139.8 (C-7), 133.6 (C-6), 124.9 (C-5), 124.9 (C-4a), 113.7 (C-8), 112.7 (C-3) ppm.

6.2.6 General synthesis of 5-(4-substituted/unsubstituted phenyl)-2-hydroxyacetophenones (42D-F)

$Pd(OAc)_2$ (0.07 g, 10 mol%) was added to a solution containing K_2CO_3 (2.76 g, 20 mmol), 4-substituted/unsubstituted phenylboronic acid (10 mmol), 5-bromo-2-hydroxyacetophenone **42B** (2.6 g, 10 mmol), water (0.7 mL), and TEA (3 mL) that had been agitated for 20 minutes at the same temperature. For 12 hours, the reaction mixture was gradually heated to reflux. After the reaction was completed, as monitored by TLC, the solvents were removed under reduced pressure, the reaction mixture was extracted with ethyl acetate (2 x 30 mL), and the organic layer was separated and dried over sodium sulphate. The obtained crude product was then purified by flash chromatography using silica gel and hexane: ethyl acetate (98:2) as the eluent, yielding 5-(4-substituted/unsubstituted phenyl)-2-hydroxyacetophenones **42D-F**.[73]

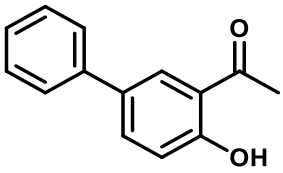
5-Phenyl-2-hydroxyacetophenone 42D (76%)



$Pd(OAc)_2$ (10 mmol), K_2CO_3 (2.76 g, 20 mmol), 4-fluorophenylboronic acid (10 mmol), 5-bromo-2-hydroxyacetophenone **42B** (2.6 g, 10 mmol), water (0.7 mL), and TEA (3 mL). Red-brown solid, m.p. 58 °C, IR ν_{max}/cm^{-1}, 3049.09 (CH, aromatic), 2791.62 (CH), 1670.26 (C=O), 1631.83 (C=O). ^{1}H NMR (400 MHz, $CDCl_3$) δ 7.89 (1H, d, *J* = 2,0 Hz), 7.68 (1H, d, *J* = 2.0 Hz), 7.52 (2H, d, *J* = 1.7, 2,4 Hz), 7.44 (2H, t, *J* = 1.7, 2,4 Hz), 7.36 (1H, t, *J* = 2, H-4'), 7.04 (1H, d, *J* = 1.7 Hz), 2.63 (3H, s) ppm. ^{13}C NMR: δ 204.6 (CH_3), 161.8 (C-2), 139.9 (C-1'), 135.3 (C-4), 132.4 (C-5), 128.0 (C-4'), 128.9 (C-3'), 127.4 (C-6), 126.7 (C-2'), 120.1 (C-1), 119.0 (C-3), 26.5 (CH_3) ppm.

© University of Venda

5-Phenyl-2-hydroxyacetophenone 42F (80%)

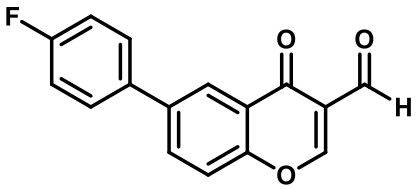


$Pd(OAc)_2$ (10 mmol), K_2CO_3 (2.76 g, 20 mmol), phenylboronic acid (10 mmol), 5-bromo-2-hydroxyacetophenone **42B** (2.6 g, 10 mmol), water (0.7 mL), and TEA (3 mL). Red-brown solid, m.p. 56 - 59 °C, lit[73] 57 - 59 °C. IR ν_{max}/cm^{-1}, 3049.09 (CH, aromatic), 2791.62 (CH) 1755.57 (C=O), 1670.26 (C=O), 1631.83 (C=O). ^{1}H NMR (400 MHz, $CDCl_3$) δ 7.89 (1H, d, *J* = 2.0 Hz), 7.68 (1H, d, *J* = 2.0 Hz), 7.52 (2H, dd, *J* = 1.7 Hz, 2,4 Hz), 7.44 (2H, dd, *J* = 1.7 Hz, 2,4 Hz), 7.34 (1H, t, *J* = 2.0 Hz), 7.04 (1H, d, *J* = 1.7 Hz), 2.63 (3H, s) ppm. ^{13}C NMR: δ 204.6 (CH_3), 161.8 (C-2), 139.9 (C-1'), 135.3 (C-4), 132.4 (C-5), 128.0 (C-4'), 12893 (C-3'), 127.4 (C-6), 126.7 (C-2'), 119.8 (C-1), 118.8 (C-3), 26.7 (CH_3) ppm.

6.2.7 General synthesis of 6-substituted/unsubstituted chromone-3-carbaldehydes (48A-E)

Phosphorus oxychloride was gently added to a well-stirred and cooled (0-5°C) mixture containing *N*,*N*-dimethylformamide and 1-(2-hydroxy)acetophenone for 30 minutes. The liquid was then stirred for 12-24 hours at room temperature. The orange-yellow organic compound was stirred with crushed ice (20 g), then extracted with chloroform (2 x 30 mL), and the layers separated. The organic layer was dried over anhydrous sodium sulphate, and the solvent was extracted using decreased pressure. The obtained residue was purified using column chromatography on silica gel to get chromone-3-carbaldehydes (**48A-E**) in 63 - 98% yield.

6-(4-Fuorophenyl)-chromone-3-carbaldehyde 48A (98%)

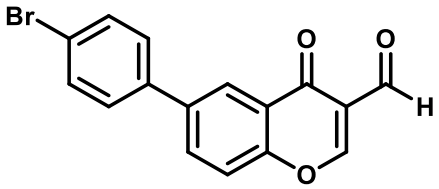


5-(4-Fluorophenyl)-2-hydroxyacetophenone **42D** (2 g, 18.36 mmol), DMF (15 mL), phosphoryl chloride (3 mL). Yellow solid, m.p. 119 °C, IR ν_{max}/cm^{-1} 3049.09 (CH, aromatic), 2791.62 (CH), 1670.26 (C=O), 1631.83 (C=O). ^{1}H NMR (400 MHz, $CDCl_3$) δ 8.79 (H, s), 8.11 (1H, dd, *J* = 1.7, 2.4 Hz), 7.89 - 7.84 (1H, m), 7.71 (1H, d, *J* = 1.7 Hz), 7.54 - 7.58 (2H, m) ppm. ^{13}C NMR:

© University of Venda

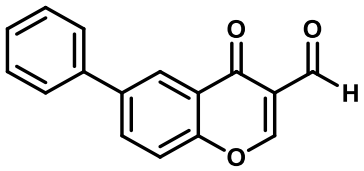
δ 161.0 (C-2), 124.4 (C-3), 175.2 (C-4), 123.4 (C-4a), 126.0 (C-5), 126.9 (C-6), 135.3(C-7), 119.0 (C-8), 155.6 (C-8a), 125.9 (C-1'), 118.2 (C-2'), 169.3 (C-3'), 168.2 (C-4') ppm.

6-(4-Bromophenyl)-chromone-3-carbaldehyde 48B (57%)



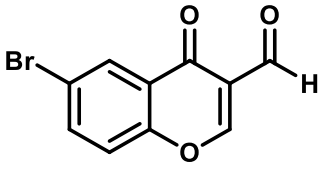
5-(4-Bromophenyl)-2-hydroxyacetophenone **42E** (2 g, 18.36 mmol), DMF (15 mL), phosphorus oxychloride (3 mL). Yellow solid, m.p. 120 °C, IR ν_{max}/cm^{-1}, 3100.9 (CH, aromatic), 2789.2 (CH) 1742.5 (C=O), 1639.3 (C=O). ^{1}H NMR (400 MHz, $CDCl_3$) δ 8.79 (H, s), 8.11 (1H, dd, *J* = 1.7, 2.4 Hz), 7.89 - 7.84 (1H, m), 7.71 (1H, d, *J* = 1.7 Hz), 7.54 - 7.58 (2H, m) ppm. ^{13}C NMR: δ 161.0 (C-2), 124.4 (C-3), 175.2 (C-4), 123.4 (C-4a), 126.0 (C-5), 126.9 (C-6), 135.3(C-7), 119.0 (C-8), 155.6 (C-8a), 125.9 (C-1'), 118.2 (C-2'), 169.3 (C-3'), 133.4 (C-4') ppm.

6-Phenylchromone-3-carbaldehyde 48C (96%)



5-Phenyl-2-hydroxyacetophenone **42F** (2 g, 18.36 mmol), DMF (15 mL), $POCl_3$ (3 mL). Yellow solid, m.p. 115, IR ν_{max}/cm^{-1} 3138.10 (NH), 3049.09 (CH, aromatic), 2791.62 (CH) 1755.57 (C=O), 1670.26 (C=O), 1631.83 (C=O). ^{1}H NMR (400 MHz, $CDCl_3$) δ 8.79 (H, s), 8.11 (1H, dd, *J* = 1.7, 2.4 Hz, H-4), 7.89 - 7.84 (1H, m), 7.71 (1H, d, *J* = 1.7 Hz), 7.54 - 7.58 (2H, m) ppm. ^{13}C NMR: δ 161.0 (C-2), 124.4 (C-3), 175.2 (C-4), 123.4 (C-4a), 126.0 (C-5), 126.9 (C-6), 135.3 (C-7), 119.0 (C-8), 155.6 (C-8a), 125.9 (C-1'), 118.2 (C-2'), 169.3 (C-3'), 168.2 (C-4') ppm.

6-Bromochromone-3-carbaldehyde 48E (63%)

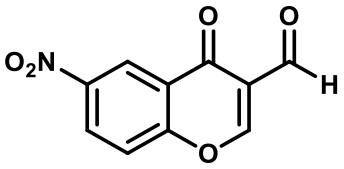


5-Bromo-2-hydroxyacetophenone **42B** (2 g, 18.36 mmol), DMF (15 mL), $POCl_3$ (3 mL), m.p. 191 – 196 °C, lit.[10] 190 – 193 °C, IR ν_{max}/cm^{-1} 3023.9 (CH, aromatic), 2791.6 (CH) 1723.6 (C=O), 1641.8 (C=O). ^{1}H NMR (400 MHz, DMSO-d_6) δ 9.92 (1H, s), 8.15 (1H, s), 7.95 (1H, d,

© University of Venda

J = 1.4 Hz), 7.57 (1H, dd, *J* = 7.5, 1.4 Hz), 6.96 (1H, d, *J* = 7.5 Hz) ppm. ^{13}C NMR (100 MHz, DMSO-d_6) δ 187.1 (CHO), 174.1 (C-4), 162.2 (C-2), 155.1 (C-8a), 137.8 (C-7), 127.5 (C-5), 126.3 (C-6), 121.1 (C-8), 120.1 (C-3), 119.2 (C-4a) ppm.

6.2.8 Synthesis of 6-nitrochromone-3-carbaldehyde 48F (53%)



A mixture of nitric acid (4 mL) and sulphuric acid (4 mL) was added dropwise at 0 °C into a round bottom flask containing chromone-3-carbaldehyde **44A** (29 mmol). The mixture was stirred for 6 hours. The reaction mixture was quenched with ice-cold water (100 mL) to afford the expected 6-nitrochromone-3-carbaldehyde **48F**.

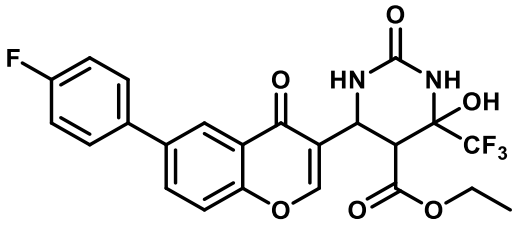
Chromone-3-carbaldehyde **44A** (29 mmol), sulphuric acid (4 mL), nitric acid (4 mL). (2 g, 18.36 mmol), DMF (15 mL), $POCl_3$ (3 mL). Yellow solid, m.p. 186 °C, lit.[31] 185 - 187 °C, IR ν_{max}/cm^{-1} 1691.27 (C=0), 1643.94 (C=O). ^{1}H NMR (400 MHz, $CDCl_3$) δ 10.38 (1H, s), 8.56 (1H, s), 8.39 (1H, d, *J* = 2.3 Hz), 7.76 (1H, dd, *J* = 8.9, 2.4 Hz), 7.57 (1H, d, *J* = 8.9 Hz) ppm. ^{13}C NMR (100 MHz, $CDCl_3$) δ 188.5 (CHO), 175.9 (C-4), 160.7 (C-2), 156.2 (C-8a), 134.9 (C-7), 144.6 (C-6), 126.1 (C-5), 125.3 (C-3), 120.3 (C-4a), 118.6 (C-8) ppm.

6.2.9 General synthesis of ethyl 6-hydroxy-4-(6-substituted/unsubstituted chromone-3-)-2-oxo-6-trifluoromethyl-1,2,3,4-tetrahydropyrimidine-5-carboxylate derivatives 51A-E

To sulfamic acid (0.67 g), a solution of urea **49** (0.72 g, 12 mmol), 6-substituted/unsubstituted chromone-3-carbaldehyde (10 mmol), and ethyl 4,4,4-trifluoroacetoacetates **48A-E** (1.62 g, 12 mmol) in ethanol (15 mL) was added and the mixture was refluxed for three hours. The reaction mixture was added to 120 g of crushed ice and stirred for five to ten minutes after it had cooled to room temperature. Ethyl 6-hydroxy-6-trifluorimethyl-2-oxo-4-(5-substituted/unsubstituted chromone-3-)-1,2,3,4-tetrahydropyrimidine-5-carboxylates **51A-E** were obtained by filtering the separated yellow solid, washing it with ice-cold water (20 mL), and then were purified using flash chromatography to afford a white precipitate.

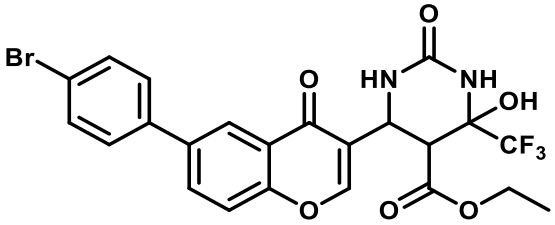
Ethyl 6-hydroxy-4-(6-[4-fluorophenyl]chromone-3-)-2-oxo-6-trifluoromethyl-1,2,3,4-tetrahydropyrimidine-5-carboxylate derivative 51A (67%)

© University of Venda



6-[4-Fluorophenyl]chromone-3-carbaldehyde **48A** (10 mmol), urea (0.72 g, 12 mmol mL), sulfamic acid (0.67 g), and 4,4,4-trifluoroacetoacetate (1.62 g, 12 mmol) in ethanol (15 mL). White solid, m.p. 324 - 325 °C, IR ν_{max}/cm^{-1} 3148.10 (NH), 3029.09 (CH, aromatic), 2790.92 (CH) 1755.57 (C=O), 1670.26 (C=O), 1631.83 (C=O). ^{1}H NMR (400 MHz, DMSO-d_6) δ 8.19 – 8.11 (m, 2H), 7.81 (s, 1H), 7.75 (1H, dd, *J* = 7.5, 1.4 Hz), 7.63 – 7.54 (2H, m), 7.24 – 7.13 (3H, m), 7.10 (1H, d, *J* = 0.9 Hz), 5.34 (1H, s), 4.81 (1H, dd, *J* = 12.0, 0.8 Hz), 4.17 (2H, q, *J* = 5.9 Hz), 3.76 (1H, d, *J* = 11.9 Hz), 1.38 (3H, t, *J* = 5.9 Hz) ppm. ^{13}C NMR (100 MHz, DMSO-d_6) δ 175.6 (C-4), 167.9 (C-13), 163.8 (C-4'), 157.7 (C-12), 155.3 (C-8a), 153.9 (C-2), 137.1 (C-7), 135.3 (C-1'), 133.3 (C-6), 129.5 (C-2'), 124.3 (C-5), 122.7 (C-4a), 119.9 (C-3), 119.7 (C-8), 116.7 (CF_3), 116.6 (C-3') 81.1 (C-11), 60.9 (OCH_2), 47.4 (C-9), 46.2 (C-10), 14.1 (CH_3) ppm. Mass (LC-MS): *m/z* calc: 494.1, found: 495.2 [M^+ +H]. HRMS: *m/z:* calc: 494.1, found: 495.1 [M^+ +H]

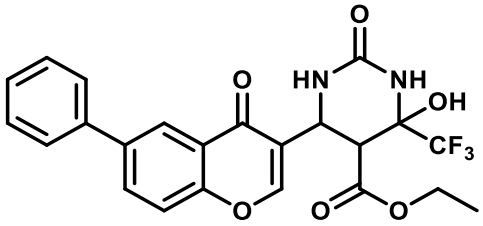
Ethyl 6-hydroxy-4-(6-[4-bromophenyl]chromone-3-)-2-oxo-6-trifluoromethyl-1,2,3,4-tetrahydropyrimidine-5-carboxylate derivative 51B (53%)



6-[4-Bromophenyl]chromone-3-carbaldehyde **48B** (10 mmol), urea (0.72 g, 12 mmol), sulfamic acid (0.67 g), and 4,4,4-trifluoroacetoacetate (1.62 g, 12 mmol) in ethanol (15 mL). White solid, 341-344 °C, IR ν_{max}/cm^{-1} 3138.10 (NH), 3049.09 (CH, aromatic), 2791.62 (CH) 1755.57 (C=O), 1670.26 (C=O), 1631.83 (C=O). ^{1}H NMR (400 MHz, DMSO-d_6) δ 8.24 (1H, s), 8.13 (1H, d, *J* = 1.6 Hz), 7.78 – 7.69 (2H, m), 7.62 (2H, d, *J* = 7.5 Hz), 7.49 (2H, d, *J* = 7.5 Hz), 7.21 (1H, d, *J* = 7.5 Hz), 7.10 (1H, d, *J* = 0.9 Hz), 5.66 (1H, s), 4.81 (2H, m), 0.96 (3H, t) ppm. ^{13}C NMR (100 MHz, DMSO-d_6) δ 174.9 (C-4), 167.4 (C-13), 157.8 (C-12), 156.7 (C-8a), 153.7 (C-2), 140.3 (C-1'), 135.5 (C-7), 130.6 (C-6), 128.6 (C-2'), 128.5 (C-3'), 127.1 (C-5), 126.0 (C-4a), 122.3 (C-4'), 120.6 (C-3), 119.8 (C-8), 116,2 (CF_3), 80.8 (C-11), 60.8 (OCH_2), 52.0 (C-9), 45.0 (C-10), 14.1 (CH_3) ppm. Mass (LC-MS): m/z: calc: 556.0, found: 557.1 [M^+ +H]. HRMS: *m/z:* calc: 556.0, found: 557.0 [M^+ +H]

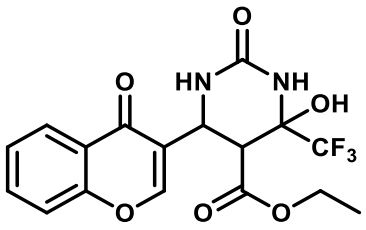
© University of Venda

Ethyl 6-hydroxy-4-(6-phenylchromone-3-)-2-oxo-6-trifluoromethyl-1,2,3,4-tetrahydropyrimidine-5-carboxylate derivative 51C (74%)



6-Phenylchromone-3-carbaldehyde **48C** (10 mmol), urea (0.72 g, 12 mmol), sulfamic acid (0.67 g), and ethyl 4,4,4-trifluoroacetoacetate (1.62 g, 12 mmol) in ethanol (15 mL). White, solid, m.p. 301-304, IR ν_{max}/cm^{-1} 3138.10 (NH), 3049.09 (CH, aromatic), 2791.62 (CH) 1755.57 (C=O), 1670.26 (C=O),1631.83 (C=O). ^{1}H NMR (400 MHz, DMSO-d_6) δ 8.60 (1H, s), 8.26 (1H, d, *J* = 1.7 Hz), 8.20 – 8.08 (1H, m), 7.87 – 7.70 (5H, m), 7.35 (3H, t, *J* = 8.7 Hz), 7.22 (1H, s), 4.87 (1H, d, *J* = 11.6 Hz), 3.94 (2H, q, *J* = 6.9 Hz), 3.85 (1H, d, *J* = 11.7 Hz), 0.93 (3H, t, *J* = 7.0 Hz) ppm. ^{13}C NMR (100 MHz, DMSO-d_6) δ: 175.7 (C-4), 167.9 (C-13), 157.7 (C-12), 155.4 (C-8a), 153.9 (C-2), 135.3 (C-7), 133.7 (C-1'), 129.7 (C-6), 128.6 (C-3'), 128.5 (C-2'), 127.4 (C-5), 124.3 (C-4a), 122.7 (C-4'), 119.9 (C-3), 119.7 (C-8), 113.5 (CF_3), 82.8 (C-11), 60.9 (OCH_3), 46.2 (C-9), 45.4 (C-10), 14.1 (CH_3) ppm, Mass (LC-MS): *m/z:* calc: 476.1, found: 477.0 [M^+ +H]. HRMS: *m/z:* calc: 476.1, found: 477.1 [M^+ +H]

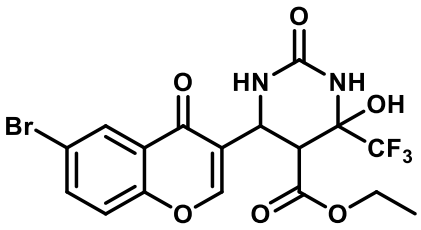
Ethyl 6-hydroxy-4-(chromone-3-)-2-oxo-6-trifluoromethyl-1,2,3,4-tetrahydropyrimidine-5-carboxylate derivative 51D (60%)



Chromone-3-carbaldehyde **48D** (10 mmol), urea (0.72 g, 12 mmol), sulfamic acid (0.67 g), and ethyl 4,4,4-trifluoroacetoacetate (1.62 g, 12 mmol) in ethanol (15 mL). White solid, 283 - 284 °C, IR ν_{max}/cm^{-1} 3138.10 (NH), 3049.09 (CH, aromatic), 2791.62 (CH) 1755.57 (C=O), 1670.26 (C=O), 1631.83 (C=O). ^{1}H NMR (400 MHz, DMSO-d_6): *δ* 8.30 - 8.15 (1H, m), 8.08 (s.1H), 7.82 - 7.74 (1H, m), 7.66 (1H, s), 7.56 (2H, d, *J* = 8.1 Hz), 7.52 - 7.46 (1H, m), 5.30 (d, 1H, *J* = 4.1 Hz), 3.98 - 3.75 (2H, m), 0.88 (t, 3H, *J* = 6.9 Hz) ppm. ^{13}C NMR (100 MHz, DMSO-d_6): *δ* 175.7 (C-4), 167.9 (C-13), 157.6 (C-12), 155.9 (C-8a), 153.8 (C-2), 134.9 (C-7), 126.3 (C-5), 125.6 (C-4a),120.9 (C-6), 120.8 (C-3), 120.0 (CF_3), 118.9 (C-8), 80.9 (C-11), 60.7 (OCH_2), 47.2 (C-9), 46.2 (C-10), 14.0 (CH_3) ppm. Mass (LC-MS): *m/z*: calc: 400.1, found: 401.0 [M^+ +H].

© University of Venda

Ethyl 6-hydroxy-4[-6-bromochromone-3-]-2-oxo-6-trifluoromethyl-1,2,3,4-tetrahydropyrimidine-5-carboxylate derivative 51E (74%)



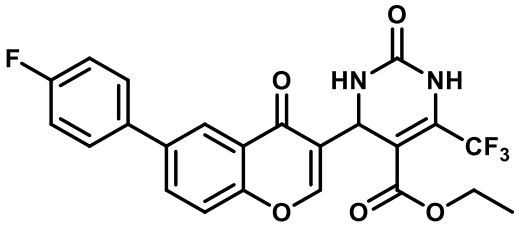
6-Bromochromone-3-carbaldehyde **48E** (10 mmol), urea (0.72 g, 12 mmol), sulfamic acid (0.67 g), and ethyl 4,4,4-trifluoroacetoacetate (1.62 g, 12 mmol) in ethanol (15 mL). White solid, m.p. 291-294 °C, IR ν_{max}/cm^{-1} 3131.10 (NH), 3100.09 (CH, aromatic), 2791.62 (CH) 1755.57 (C=O), 1670.26 (C=O), 1631.83 (C=O). ^{1}H NMR (400 MHz, $CDCl_3$ + DMSO-d_6) δ 8.20 (1H, s), 7.96 (1H, d, *J* = 1.6 Hz), 7.72 (1H, s), 7.59 (1H, dd, *J* = 7.5, 1.4 Hz), 7.10 (1H, d, *J* = 0.9 Hz), 6.93 (1H, d, *J* = 7.5 Hz), 5.33 (1H, s), 4.81 (1H, dd, *J* = 3.8, 0.6 Hz), 4.16 (2H, q, *J* = 5.9 Hz), 3.79 (1H, d, *J* = 3.8 Hz), 1.35 (3H, t, *J* = 5.9 Hz) ppm. ^{13}C NMR (100 MHz, DMSO-d_6): *δ* 174.5 (C-4), 167.8 (C-13), 157.9 (C-12), 154.8 (C-8a), 153.8 (C-2), 137.6 (C-7), 127.7 (C-6), 127.5 (C-5), 125.5 (C-4a), 120.1 (C-3), 118.7 (C-8), 116.2 (CF_3), 80.8 (C-11), 60.8 (OCH_2), 47.2 (C-9), 46.2 (C-10), 14.1 (CH_3) ppm. Mass (LC-MS): *m/z*: calc: 480.0, found: 479.5 [M^+ +H]. HRMS: *m/z:* calc: 480.0, found: 481.0 [M^+ +H]

6.2.10. General synthesis of ethyl 4-(chromon-3-yl)-2-oxo-6-trifluoromethyl-1,2,3,4-tetrahydropyrimidine-5-carboxylate derivatives 52A-E

Ethyl 6-hydroxy-4-(6-substituted/unsubstituted chromone-3-)-2-oxo-6-trifluoromethyl-1,2,3,4-tetrahydropyrimidine-5-carboxylate derivatives **51A-E** underwent a cyclodehydration reaction. To a round-bottom flask containing these derivatives, 1.5 equivalents of para-toluene sulfonic acid and 20 mL of toluene were added. The mixture was stirred at 140 °C for 3 hours under Dean-Stark conditions. After cooling, the crude product was filtered and washed with hexane. Subsequent recrystallization from hot ethanol yielded ethyl 4-(6-substituted/unsubstituted chromone-3-)-2-oxo-6-trifluoromethyl-1,2,3,4-tetrahydropyrimidine-5-carboxylate derivatives **52A-D**.

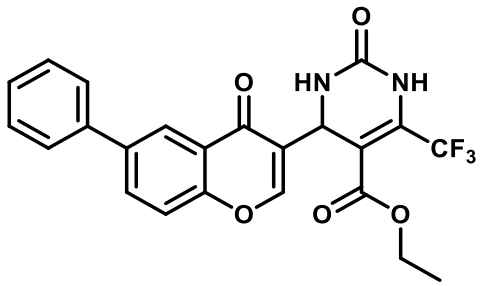
Ethyl 4-(6-(4-fluorophenyl)-4-oxo-*4H*-chromen-3-yl)-2-oxo-6-(trifluoromethyl)-1,2,3,4-tetrahydropyrimidine-5-carboxylate 52A

© University of Venda



Intermediate **51A** (10 mmol), *p*-TsOH (12 mmol) in toluene (10 mL). Brown, solid m.p. 301-304 °C, IR ν_{max}/cm^{-1} 3131.10 (NH), 3087.22 (NH), 3100.09 (CH, aromatic), 2791.62 (CH) 1735.57 (C=O), 1667.36 (C=O), 1631.95 (C=O). ^{1}H NMR (400 MHz, DMSO) δ 9.79 (s, 1H), 8.38 (s, 1H), 8.26 (d, *J* = 2.4 Hz, 1H), 8.12 (dd, *J* = 8.8, 2.4 Hz, 1H), 7.84 – 7,80 (m, 2H), 7.77 (d, *J* = 8.7 Hz, 1H), 7.55 (s, 1H), 7.33 (t, *J* = 8.8 Hz, 2H), 5.25 (s, 1H), 4.05 (q, *J* = 7.0 Hz, 2H), 1.09 (t, *J* = 7.1 Hz, 3H) ppm. ^{13}C NMR (100 MHz, DMSO-d_6) δ 175.5 (C-4), 163.9 (C-13), 161.4 (C-4'), 155.8 (C-12), 155.5 (C-8a), 151.8 (C-2), 137.1 (C-7), 135.3 (C-1'), 133.3 (C-6), 132.6 (C-11), 129.6 (C-2'), 124.4 (C-5), 122.7 (C-4a), 121.35 (CF_3), 119.8 (C-3), 118.6 (C-8), 116.5 (C-3') 103.7 (C-10), 61.4 (OCH_2), 50.9 (C-9), 14.1 (CH_3) ppm. Mass (LC-MS): *m/z:* calc: 476.1, found: 477.0 [M^+ +H].

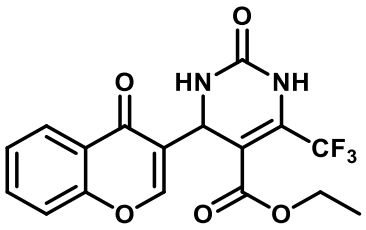
Ethyl 2-oxo-4-(4-oxo-6-phenyl-*4H*-chromen-3-yl)-6-(trifluoromethyl)-1,2,3,4-tetrahydropyrimidine-5-carboxylate 52B



Intermediate **51C** (10 mmol), *p*-TsOH (12 mmol) in toluene (10 mL). White solid, m.p. 244-246 °C, lit[70] 246-248 °C. IR ν_{max}/cm^{-1} 3091.10 (NH), 3072.22 (NH), 3009.25 (CH, aromatic), 2891.36 (CH) 1778.02 (C=O), 1670.26 (C=O), 1631.83 (C=O). ^{1}H NMR (400 MHz, DMSO-d_6) δ 9.79 (s, 1H), 8.38 (s, 1H), 8.28 (d, *J* = 2.4 Hz, 1H), 8.14 (dd, *J* = 8.8, 2.4 Hz, 1H), 7.79 – 7.76 (m, 2H), 7.57 – 7.39 (m, 3H), 7.12 (d, *J* = 7.8 Hz, 2H), 5.24 (s, 1H), 4.05 (q, *J* = 6.5 Hz, 2H), 2.29 (s, 3H), 1.09 (t, *J* = 7.1 Hz, 3H). . ^{13}C NMR (100 MHz, DMSO-d_6) δ 175.5 (C-4), 163.9 (C-13), 161.4, 155.9 (C-12), 155.6 (C-8a), 151.8 (C-2), 145.8 (C-1'), 138.1 (C-7), 129.7 (C-6), 128.6 (C-3'), 127.4 (C-2'), 126.0 (C-5), 124.5 (C-4a), 122.6 (C-4'), 121.35 (CF_3), 119.8 (C-3), 118.6 (C-8), 116.3 (C-3'), 103.8 (C-10), 61.4 (OCH_2), 50.9 (C-9), 14.1 (CH_3) ppm. Mass (LC-MS): *m/z:* calc: 458.1, found: 459.1 [M^+ +H].

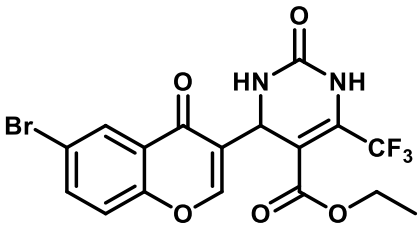
© University of Venda

Ethyl 2-oxo-4-(4-oxo-4*H*-chromen-3-yl)-6-(trifluoromethyl)-1,2,3,4-tetrahydropyrimidine-5-carboxylate 51C



Intermediate **51D** (10 mmol), *p*-TsOH (1.62 g, 12 mmol) in toluene (10 mL). White solid, m.p. 263-264 °C, IR ν_{max}/cm^{-1} 3216.96 (NH), 3091.58 (NH), 2982.61 (CH, aromatic), 2606.58 (CH), 1735.85 (C=C), 1698.72 (C=O) 1642.89 (C=O), 1610.47 (C=O).^{1}H NMR (400 MHz, DMSO-d_6) δ 9.81 (s, 1H), 8.35 (s, 1H), 8.07 (d, *J* = 6.4 Hz, 1H), 7.81 (t, *J* = 8.2 Hz, 1H), 7.64 (d, *J* = 8.4 Hz, 1H), 7.51 (dd, *J* = 14.5, 6.9 Hz, 2H), 5.28 (s, 1H), 4.05 (q, *J* = 7.1 Hz, 2H), 1.08 (t, *J* = 7.1 Hz, 3H) ppm. ^{13}C NMR (101 MHz, DMSO-d_6) δ 175.5(C-4), 163.8(C-13), 156.1(C-2), 155.6(C-12), 151.8(C-8a), 134.7(C-7), 131.0 (C-11), 126.0, 125.3, 124.2, 123.5(C-6), 121.4(C-3), 120.5(CF_3), 118.8(C-8), 103.9(C-10), 61.2(OCH_2), 50.7(C-9), 13.7(CH_3) ppm. Mass (LC-MS): *m/z:* calc: 382.1 found: 383.0 [M^+ +H]. HRMS: *m/z:* calc: 382.1, found: 383.1 [M^+ +H]

Ethyl 4-(6-bromo-4-oxo-4*H*-chromen-3-yl)-2-oxo-6-(trifluoromethyl)-1,2,3,4-tetrahydropyrimidine-5-carboxylate 52D



Intermediate **51E** (10 mmol), *p*-TsOH (12 mmol) in toluene (10 mL). White solid, m.p. 305-319 °C, IR ν_{max}/cm^{-1} 3296.16 (NH), 3025.98 (NH), 2981.91 (CH, aromatic), 2724.58 (CH), 1753.58 (C=C), 1692.27 (C=O) 1658.45 (C=O), 1647.10 (C=O). ^{1}H NMR (400 MHz, DMSO-d_6) δ 9.84 (s, 1H), 8.41 (s, 1H), 8.13 (s, 1H), 7.97 (d, *J* = 8.9 Hz, 1H), 7.66 (d, *J* = 9.0 Hz, 1H), 7.55 (s, 1H), 5.29 (s, 1H), 4.05 (q, *J* = 7.2 Hz, 2H), 1.09 (t, *J* = 7.1 Hz, 3H) ppm. ^{13}C NMR (101 MHz, DMSO-d_6) δ 174.3(C-4), 163.7(C-13), 156.0(C-2), 155.1(C-12), 151.7(C-8a), 137.4(C-7), 131.5 (C-11), 127.7(C-6), 127.5(C-5), 125.6(C-4a), 123.7(C-6), 121.5(C-3), 120.5(CF_3), 118.5(C-8), 103.5(C-10), 61.2(OCH_2), 50.7(C-9), 13.7(CH_3) ppm. Mass (LC-MS): *m/z:* calc: 462.0, found: 462.9 [M+H]$^+$. HRMS: *m/z:* calc: 460.0, found: 461.0 [M^+ +H]

© University of Venda

6.3. *In vitro* antimycobacterial assay

A 10 mM stock solution of each sample in pure DMSO (Sigma Aldrich) was prepared. Two-fold serial dilutions were made in growth medium placed in 96-well round bottom plates. A series of dilutions from 62.5 to 0.122 µM was prepared for every compound, with isoniazid and moxifloxacin as reference drugs over a concentration range of 62.5 to 0.122 µM and 6.25 to 0.012 µM, respectively. A maximum inhibition control (rifampicin 0.15 µM) and a minimum inhibition control (0.625% DMSO) were included on each test plate. A *M. tuberculosis* H37RvMA[78] culture in 7H9_ADC_GLU_TW was grown to an optical density (OD_{600}) of 0.5 - 0.7 and diluted down to OD_{600} of 0.001 in each medium. Fifty µL of the diluted culture was added to each well of each test plate, for a final volume of 100 µl per well.

Each compound was tested in duplicate. The assay plates were incubated at 37 °C with 5% CO_2 and humidification. The assay was scored visually on day 7, and the Visual MIC was recorded as the lowest concentration at which no bacterial pellet was observed. One tenth of the assay volume of resazurin (0.2 mg/ml prepared in PBS) was then added to each well of the assay plate and re-incubated for 24 h. The relative fluorescence units (RFU) (excitation 540 nm, emission 590 nm) of each well was measured using a SpectraMax i3x Plate reader on day 8 (Serial no. 36370 3271, Molecular Devices Corporation 1311 Orleans Drive Sunnyvale, California). Data analysis was performed using Dotmatics software (https://www.dotmatics.com/solutions/data- intelligence-lab-software). Briefly, raw RFU data was normalized to the minimum and maximum inhibition controls to generate a dose response curve (% inhibition), using the Levenberg-Marquardt damped least-squares method, from which the MIC is calculated using the 4-parameter curve fit protocol. The lowest concentration of drug that inhibits 90% of growth of the bacterial population is the Calculated MIC.

Media used

- 7H9_ADC_GLU_TW: Middlebrook 7H9 media (Difco) supplemented with 0.2% glucose, Middlebrook albumin-dextrose-catalase (ADC) enrichment (Difco) and 0.05% Tween 80
- 7H9_ADC_GLU_TX: Middlebrook 7H9 media (Difco) supplemented with 0.2% glucose, Middlebrook albumin-dextrose- catalase (ADC) enrichment (Difco) and 0.05% Tyloxapol
- 7H9_CAS_GLU_TX: Middlebrook 7H9 media (Difco) supplemented with 0.4% glucose, 0.03% Casitone (Gibco Bacto) and 0.05% Tyloxapol.

© University of Venda

6.4. Solubility assay

Using a modified shake-flask approach, solubility was measured in 96-well plates at pH 7.4.[80] A GeneVac system was used to evaporate 4 µl of a 10 mM stock in DMSO that had been put to a 96-well plate. After that, the wells were filled with phosphate buffer (pH 7.4), and the plate was incubated for 24 h at 25 °C with shaking. Following the incubation period, the samples were moved to an analytical plate and centrifuged for 15 minutes at 3500g. For every sample ranging from 10 to 220 µM, a calibration curve in DMSO was created and put on the analytical plate. The HPLC-UV (Agilent 1200 quick resolution HPLC connected to a diode) method was then used for analysis and the solubility of each sample determined from the corresponding calibration curve.

© University of Venda

REFERENCES

1. A.T. Gordon, I.D.I Ramaite, S.S. Mnyakeni-Moleele, Arkivoc, 2020, **v**, 148-160
2. J.R. Hoult, M.A. Moroney, M. Payá, Methods in Enzymology, 1994, **234**, 443-454.
3. D. Lin, Jiang, S, Zhang, A. et al. Natural Products Bioprospecting 2022, **12**, 8.
4. V.Y. Sosnovskikh, Chemistry Heterocyclic Compounds, 2020, **56**, 243–254.
5. B.C. Raju, R.N. Rao, P. Suman, P. Yogeeswari, D. Sriram, T.B. Shaik, S.V. Kalivendi, Bioorganic & Medicinal Chemistry Letters, 2011, **21**, 2855–2859.
6. S. S. Shatokhin, V. A. Tuskaev, S. Ch. Gagieva, É. T. Oganesyan, Russian Chemical Bulletin, 2021, **70**, 1011-1045.
7. S. Gagneux, Nature Reviews Microbiology, 2018, **16**, 202-218
8. R.R. Chowdhury, F. Vallania, Q. Yang, C.J.L. Angel, F. Darboe, A. Penn-Nicholson, V. Rozot, E. Nemes, S.T. Malherbe, K. Ronacher, and G. Walzl, Nature 2018, **560**, 644-648.
9. M.J. Mphahlele, T.J. Makhafola and M.M. Mmonwa, Bioorganic and Medicinal Chemistry, 2016, **24**, 4576-4586.
10. S. Guillou and Y.L. Janin, Journal of Heterocyclic Chemistry, 2008, **45**, 1377-1384.
11. F. Bousejra-ElGarah, B. Lajoie, J.P. Souchard, G. Baziard, J. Bouajila and S. El Hage, Medicinal Chemistry Research, 2016, **25**, 2547-2556.
12. X. Huang and J.W. Keillor, Tetrahedron Letters, 1997, **38**, 313-316.
13. Y. Liang, S. Luo, C. Liu, X. Wu, Y. Ma, Tetrahedron Letters, 2000, **56**, 2961-2965.
14. M.Hosseini-Sarvari, Canadian Journal of Chemistry, 2008, **86**, 65-71. 83.
15. D. Sriram, P. Yogeshwar, M. Dinakaran, D. Banerjee, P. Bhat, S. Gadhwal. European Journal of Medicinal Chemistry, 2010, **45**, 120-123.
16. V. Makarov, E. Salina, R.C. Reynolds, P.P. Kyaw Zin, S. Ekins, Journal of Medicinal Chemistry, 2020, **10**, 8917-8955.
17. S.R. Mase, T. Chorba, Clinics in Chest Medicine, 2020, **40**, 775-795.
18. R. S. Keri, B. S. Sasidhar, B. M. Nagaraja, M. A. Santos, European Journal of Medicinal Chemistry, 2015, **100**, 257-269.
19. T. Askun, Research & Reviews: Journal of Pharmacological and Toxicological Methods, 2016, **3**, 1-11.
20. M. C. Wu, C. F. Peng, I. S. Chen, I. L. Tsai., Journal of Natural Products, 2011, **74** 976-982.
21. P. Tuntiwachwuttikul, P. Phansa, O. Y. Pootaeng, Chemical and Pharmaceutical Bulletin, 2006, **54**, 44-47.
22. U. Namdaung, N. Aroonrerk, S. Suksamrarn, K. Danwisetkanjana, J. Saenboonrueng, et al. Chemical and Pharmaceutical Bulletin (Tokyo), 2006, **54**: 1433-1436.

© University of Venda

23. J. Golus, R. Sawicki, J. Widelski, G. Ginalska, Journal of Applied Microbiology, 2016, **121**, 1291-1299.
24. V. Nalla, A. Shaikh, S. Bapat, R. Vyas, M. Karthikeyan M, et al., Royal Society Open Science, 2018, **5,** 171750-171764.
25. V. S. Laxmi, T. Y. Reddy, B. S. Kuarm, N. P. Reddy, P. A. Crooks, et al., Bioorganic & Medicinal Chemistry Letters, 2011, **21**, 4329-4331.
26. D. D. Haveliwala, N. R. Kamdar, P. T. Mistry, S. K. Patel, Helvetica Chimica Acta, 2014, **33**, 80-91.
27. D. D. Haveliwala, N. R. Kamdar, P. T. Mistry, S. K. Patel, Helvetica Chimica Acta, 2013 **96**, 897-905.
28. P. Li, B. Wang, X. Zhang, S. M. Batt, G. S. Besra, et al., European Journal of Medicinal Chemistry, 2018, **160**, 157-170.
29. S. Ananthan, E. R. Faaleolea, R. C. Goldman, J. V. Hobrath, C. D. Kwong CD, et al., Tuberculosis (Edinb), 2009, **89**, 334-353.
30. B. S. Sandile, T. M. Paseka, W. M. Raban, Organic & Medicinal Chemistry International Journal, 2020, **10**, 555784.
31. H.S. Roopadevi, Journal of Postgraduate Medicine, 2014, **60**, 300-302.
32. U. Manjunatha, H. I. L. Boshoff, C. E. Barry, Communicative & Integrative Biology, 2009, **2**, 215-218.
33. T. Kawate, N Iwase, M Shimizu, S.A. Stanley, S. Wellington, et al., Bioorganic & Medicinal Chemistry Letters, 2013, **23**, 6052-6059.
34. C. Gao, C. Peng, Y Shi, X You, K Ran, et.al., Scientific Reports, 2016 **6**, 1-9.
35. A. K. Brown, A. Papaemmanouil, V. Bhowruth, A. Bhatt, L.G. Dover, et al., Microbiology, 2007, **153**, 3314-3322
36. A. Gaspar, M. J. O. Matos, J. Garrido, E. Uriarte, F. Borges, Chemical Reviews 2010, **114**, 4960–4992.
37. V. A. Mamedov, A. A. Kalinin, A. T. Gubaidullin, I. A. Litvinov, Ya. A Levin. Tetrahedron Letters, 2003, **39**, 96–100.
38. W. Baker, Journal of the Chemical Society, 1933, **84**, 1381–1389.
39. C. M. Santos, A, M. S. Silva, European Journal of Organic Chemistry, 2017, **22**, 3115–3133.
40. Q. L. Li, Q. L. Liu, Z. Y. Ge, Y. M. Zhu, Helvetica Chimica Acta 2011, **94**, 1304–1309.
41. Hoshino, Y. Miyaura, N. Suzuki, Bulletin of the Chemical Society of Japan, 1988, **61**, 3008–3010.
42. A. Vilsmeier, A. Haack, Berichte der Deutschen Chemischen Gesellschaft zu Berlin (in German), 1927, **60**, 119–122.
43. G.Jones, S. P. Stanforth, Organic Reactions. 2000, **56**, 355–686.

© University of Venda

44. World Health Organization, Global Tuberculosis Report, 2021.

45. E. Terracciano, F. Amadori, L. Zaratti, E. Franco, Igiene Sanita Pubblica 2020, **76**, 59-66.
46. T.P. Mbuh, I. Ane-Anyangwe, W. Adeline, B.D. Thumamo Pokam, H.D. Meriki, W.F. Mbacham, BMC Pulmonary Medicine, 2019, **19**, 17.
47. Z. Pan, J. Zhang, Q . Bu, H. He, L. Bai, J. Yang, Q. Liu, J. Lyu, Infection and Drug Resistance. 2020, **13**, 1281-1286.
48. G. Sandhu, Journal of Global Infectious Diseases, 2011, **3**, 143150.
49. G.W. Comstock, V.T. Livesay, S.F. Woolpert, American Journal of Epidemiology, 1974, **99**, 131-138.
50. P.L. Lin, J.L. Flynn, Journal of Immunology, 2010 ,**185**, 15-22.
51. S. Kiazyk, T.B. Ball, Canada Communicable Disease Report, 2017, **43**, 62-66
52. Y. Chen, J. Liu, Q. Zhang, Q. Wang, L. Chai, H. Chen, D. Li, Y Qiu, Y. Wang, N. Shen, J. Wang, X. Xie, S. Li, M. Li, BMJ Open, 2023, **13**, e07413
53. J.W. Ai, Q.L. Ruan, Q.H. Liu, W.H. Zhang, Emerging Microbes and Infections, 2016, **5**, e10.
54. P.L. Lin, J.L. Flynn, Journal of Immunology, 2010, **185**, 15-22.
55. R. Loddenkemper, M. Lipman, A. Zumla, Cold Spring Harbour Perspective Medicine, 2015, **6**, a017848.
56. P. Narasimhan, J. Wood, C.R. Macintyre, D. Mathai, Pulmonary Medicine 2013.
57. T. Hermansen, T. Lillebaek, A.B Hansen, P.H. Andersen, P. Ravn, Tuberculosis (Edinb), 2014, **94**, 616-621.
58. D. Menzies, M. Pai, G. Comstock, Annals of Internal Medicine, 2007, **146**, 340-354.
59. J.F. Murray, American Journal of Respiratory and Critical Care Medicine. 2003, **168**, 1029–1033.
60. S.C. Woolwine, W.R. Bishai, New York: Informal Healthcare, 2006, **68**, 101–116.
61. M.A. Behr, W.R. Waters. Lancet Infectious Diseases, 2014, **14**, 250–255.
62. J. Phelan, P.F. De Sessions, L. Tientcheu, J. Perdigao, D. Machado, R. Hasan, et al., Scientific Reports, 2018, **8**,1–7.
63. L. Zhang, X. Jiang, D. Pfau, Y. Ling, C.F. Nathan, Journal of Experimental Medicine, 2021, **218**, e20200887.
64. C.M. González-Domenech, I. Pérez-Hernández, C. Gómez-Ayerbe, I.V. Ramos, R Palacios Muñoz, J. Santos, Viruses, 2021, **13**, 931.
65. G. Weiss and U.E Schaible, Immunological Reviews, 2015, **264**, 182-203.
66. A. Alelign, A. Zewude, T. Mohammed, S. Tolosa, G. Ameni, B. Petros, BMC Infectious Diseases, 2019, **19**, 1–8.
67. S. Motamen and R.J. Quinn. ACS Omega, 2020**, 5**, 28529−28540.

© University of Venda

68. J. Lehmann, American Review of Respiratory Disease, 1964, **90**, 953-956.
69. M.C. Wu, C-F. Peng, I-S. Chen, and I-L. Tsai. Journal of Natural Products 2011, **74**, 976–982.
70. Raju CB, Nageswara R, Suman P, Yogeeswari P, Sriram D, et al. Bioorganic & Medicinal Chemistry Letters, 2011, **21**, 2855–2859.
71. K. Banerji, D. Poddar, ChemInform, 1979, **10**.
72. J. F. Queiroz, J. W. M. Carneiro, A. A. Sabino, R. Sparapan, M. N. Eberlin, P. M. Esteves, Journal of Organic Chemistry, 2006, **71** (16): 6192–6203.
73. G, A. Molander, B. Biolatto, Journal of Organic Chemistry, 2003, **68**, 4302–4314.
74. S.G. Franzblau, et al., Journal of Clinical Microbiology, 1998, **36**, 362-366.
75. S.G. Franzblau, et al., Tuberculosis (Edinb), 2012, **92**, 453-488.
76. R.D. Pietersen, et al., Journal of Microbiological Methods, 2020, **170**, 105795.
77. K. Pethe, et al., Nature Communications, 2010, **1**, 57.
78. T.R. Ioerger, et al., Journal of Bacteriology, 2010,. **192**, 3645-3653.
79. Y. J. Cheng, Z. Y. Liu, H. J. Liang, C. T. Fang, N. N. Zhang, T. Y. Zhang, M. Yan, Molecules. 2019, **24**, 2021.
80. E. H. Kerns, et al., Current drug metabolism, 2008. **9**, 879-885.
81. M.L. Joloba, et al., Tuberculosis, 2014, 94, 311e316.
82. Hu et al. AMB Expr, 2017, **7**, 69.
83. V.M. Marando, D.E. Kim, L.L. Kiessling, 2021, **665**, 0076-6879.
84. Y.M.J.A. Gonzalez, C.R. Zaragoza, M.R. Guadarrama, et al., J Microbiol 2012, **50**, 419e25.
85. G. Leisching, R.-D. Pietersen, I. Wiid, B. Baker,. Tuberculosis, 2016, **100**, 53e60.

© University of Venda

APPENDIX

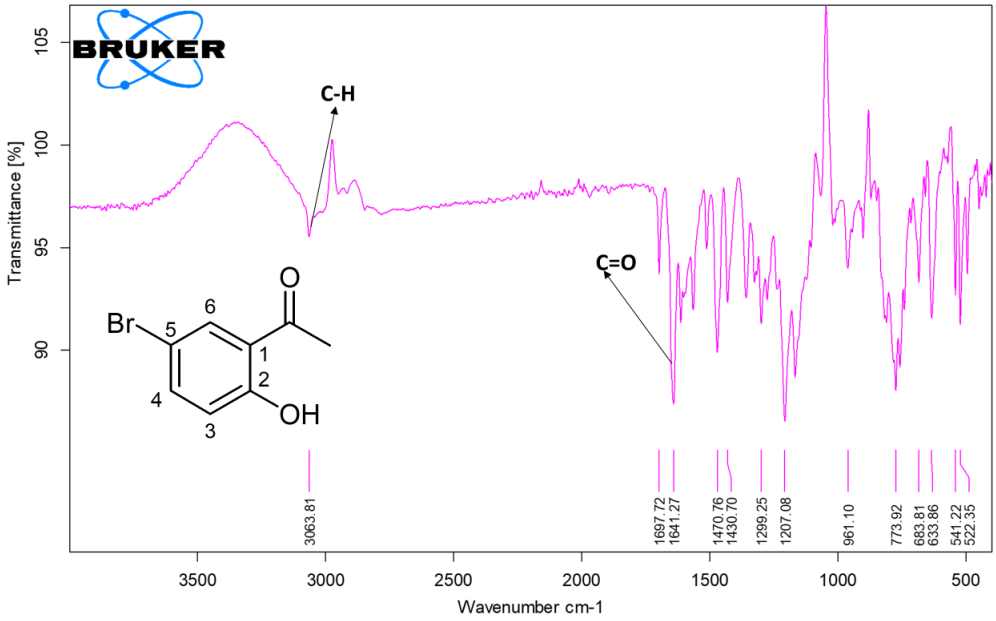


FIGURE 44: FT-IR spectrum of **44B**

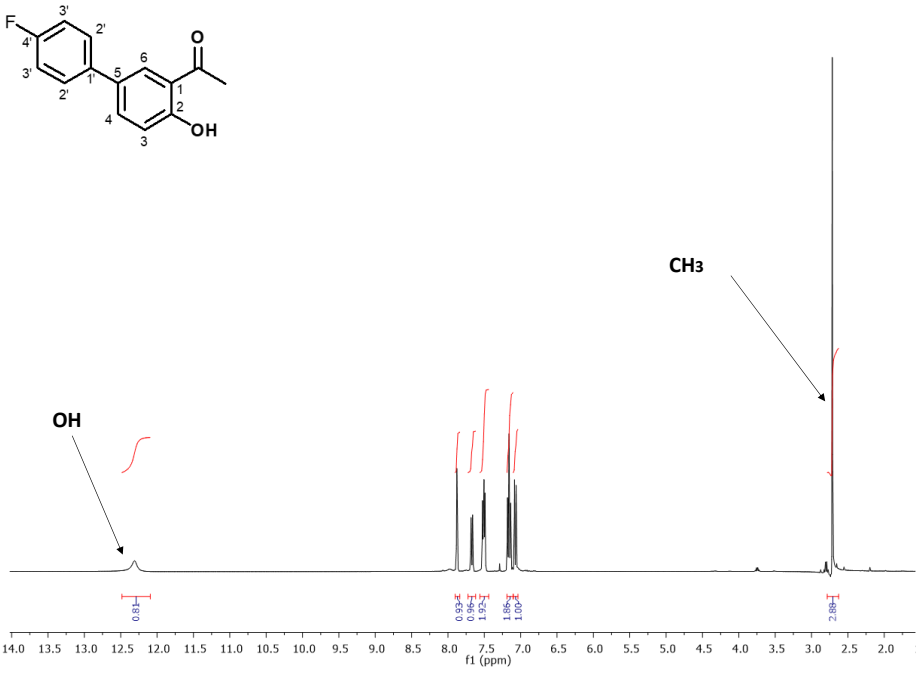
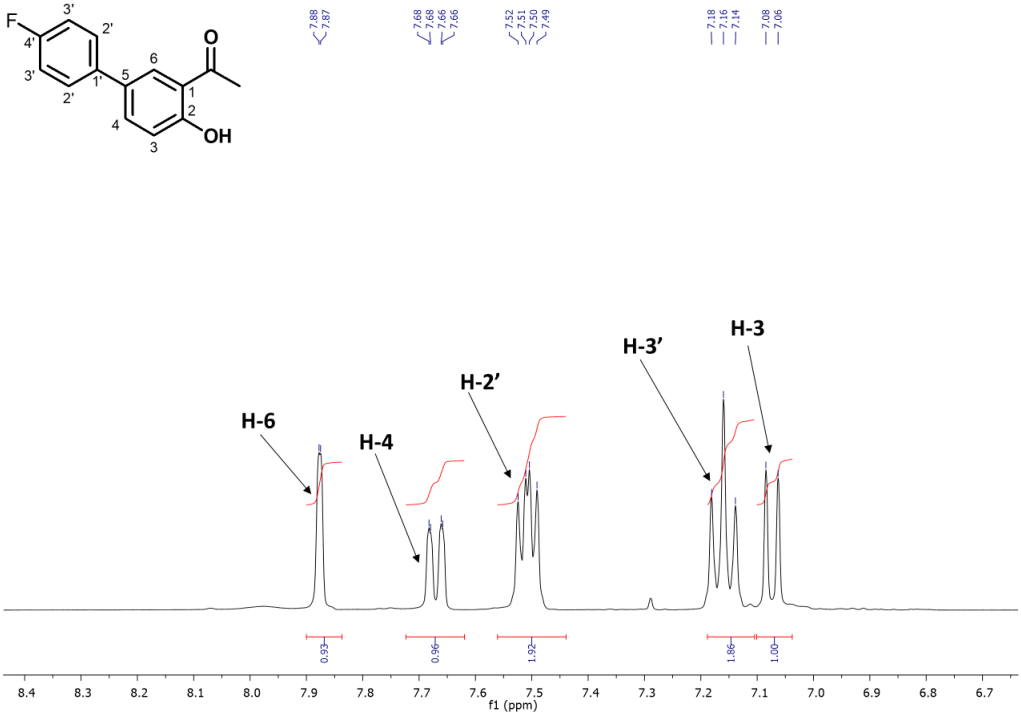


FIGURE 45: ^{1}H NMR spectrum of **42D** in $CDCl_3$ (at 100 MHz).

© University of Venda



FIGUR 46: Expanded ^{1}H NMR spectrum of **4D** in $CDCl_3$ (at 100 MHz).

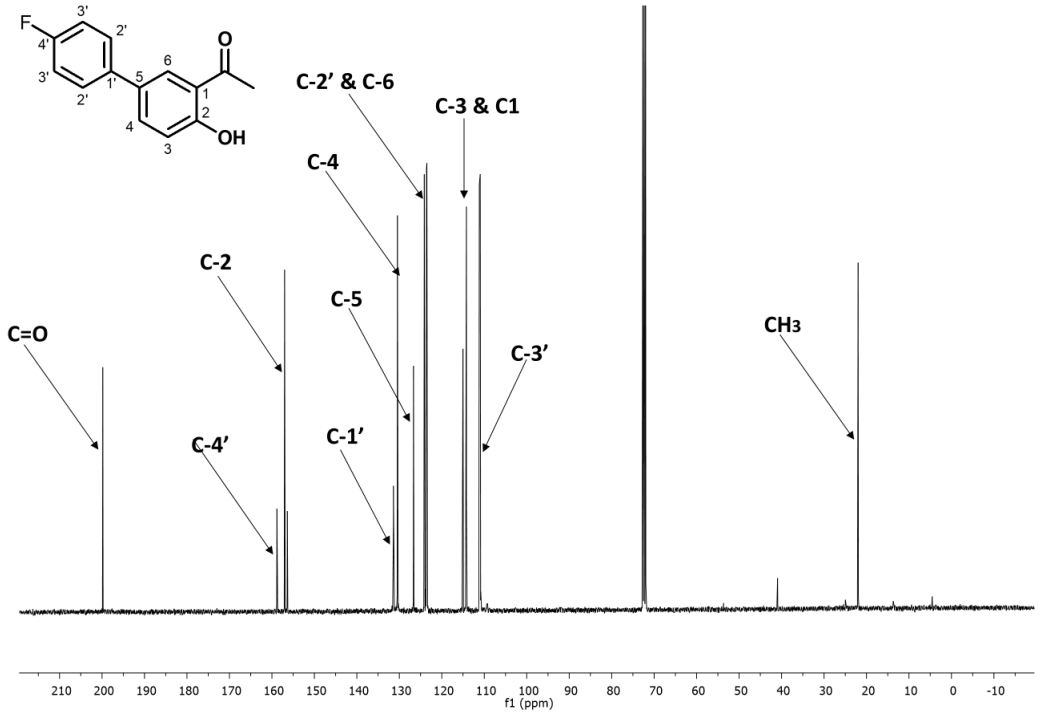


FIGURE 47: ^{13}C NMR spectrum of **4D** in $CDCl_3$ (at 100 MHz).

© University of Venda

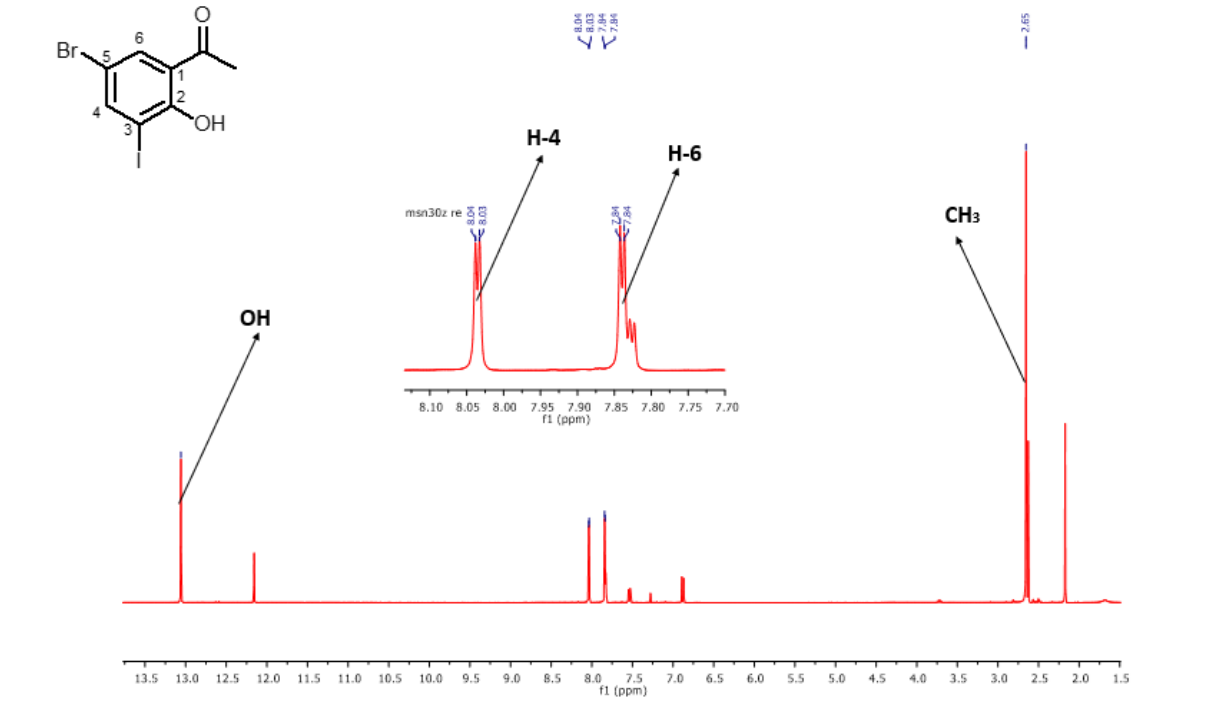


FIGURE 48: ^{1}H NMR spectrum of **43B** in $CDCl_3$ (at 100 MHz).

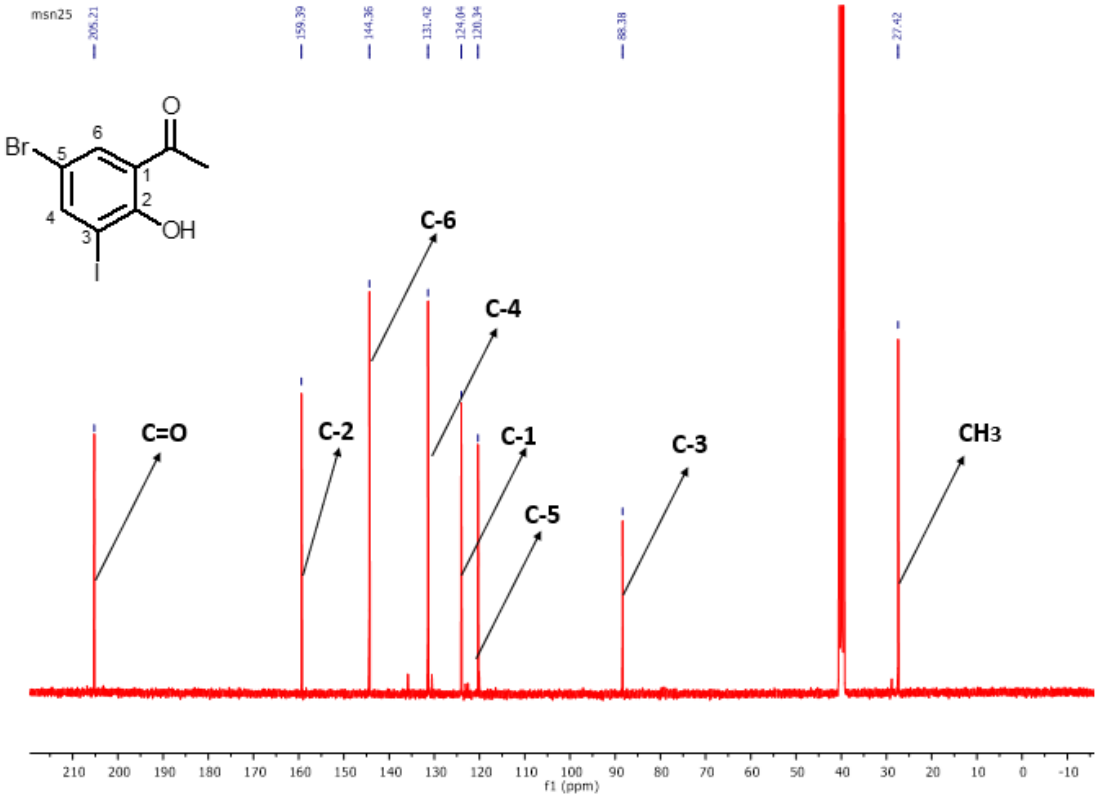


FIGURE 49: ^{13}C NMR spectrum of **43B** in $CDCl_3$ (at 100 MHz).

© University of Venda

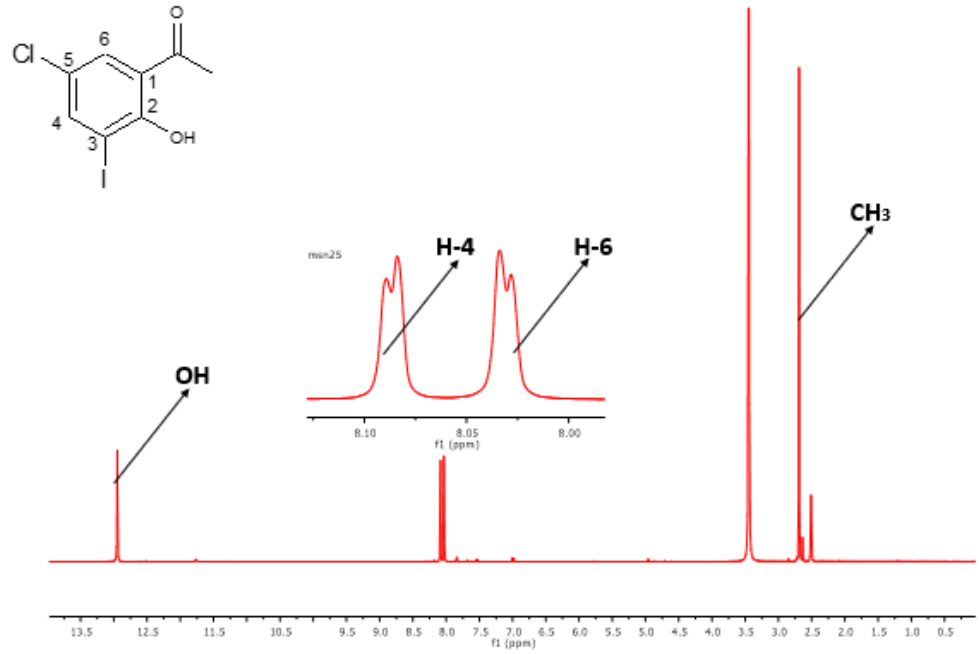


FIGURE 50: ^{1}H NMR spectrum of **43C** in $CDCl_3$ (at 100 MHz).

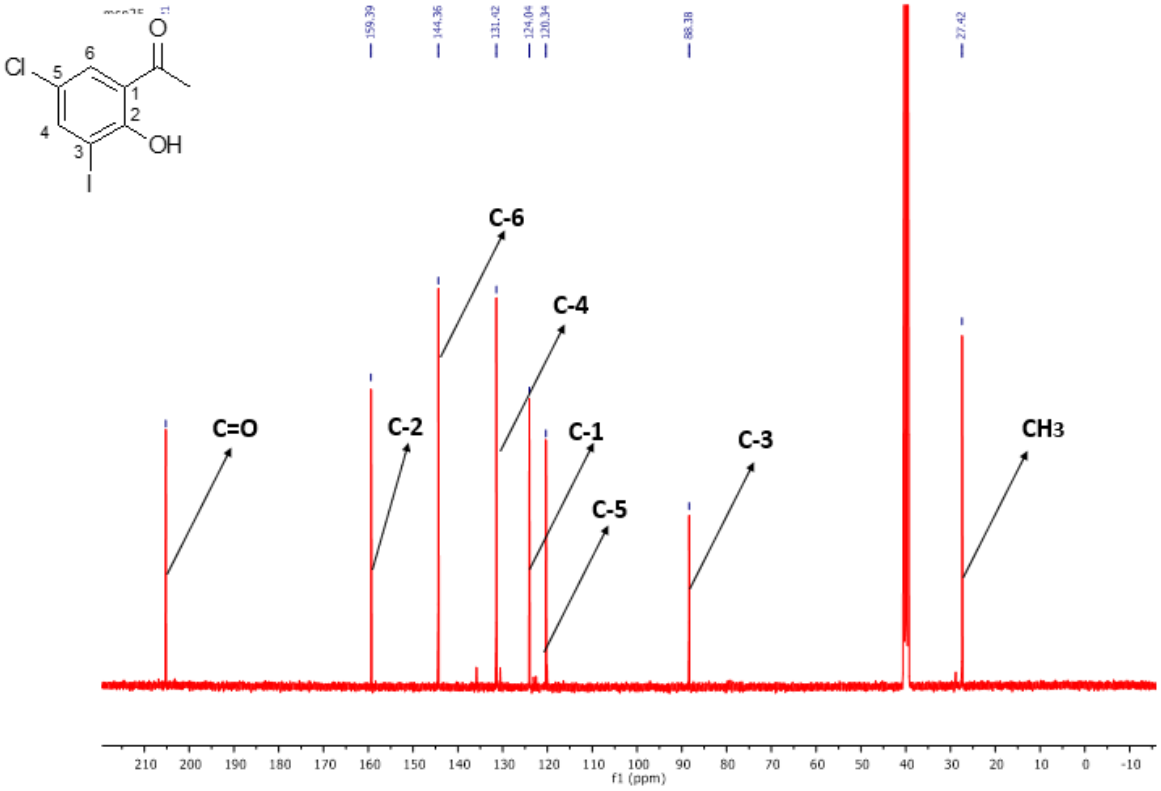


FIGURE 51: ^{13}C NMR spectrum of **43C** in $CDCl_3$ (at 100 MHz).

© University of Venda

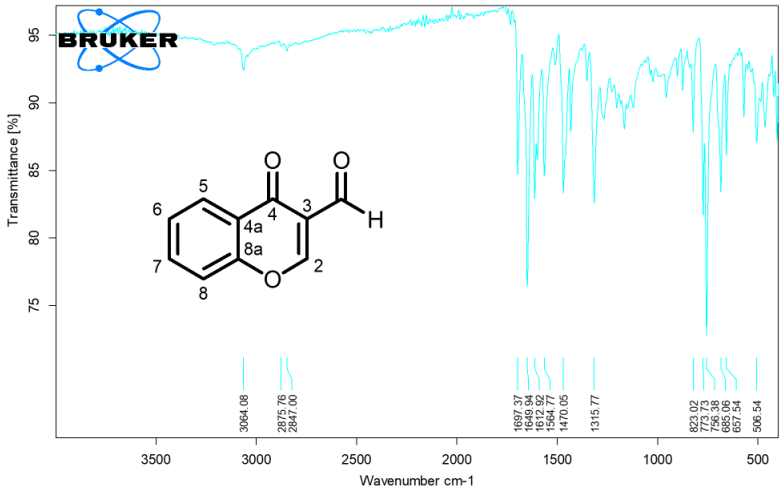


FIGURE 52: FT-IR spectrum of **44A**

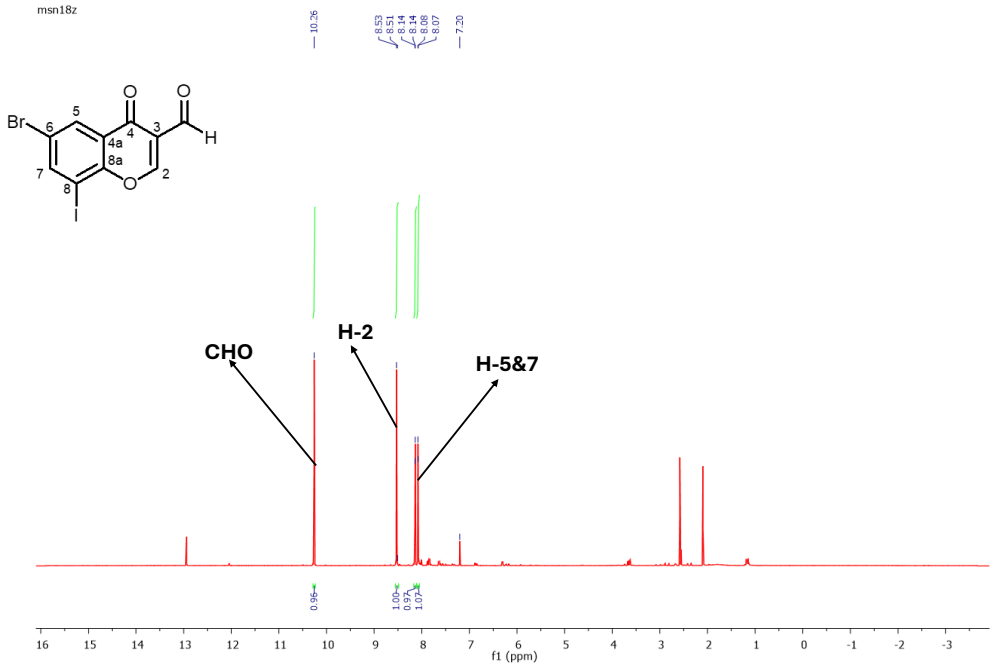


FIGURE 53: ^{1}H NMR spectrum of **44F** in $CDCl_3$ (at 100 MHz).

© University of Venda

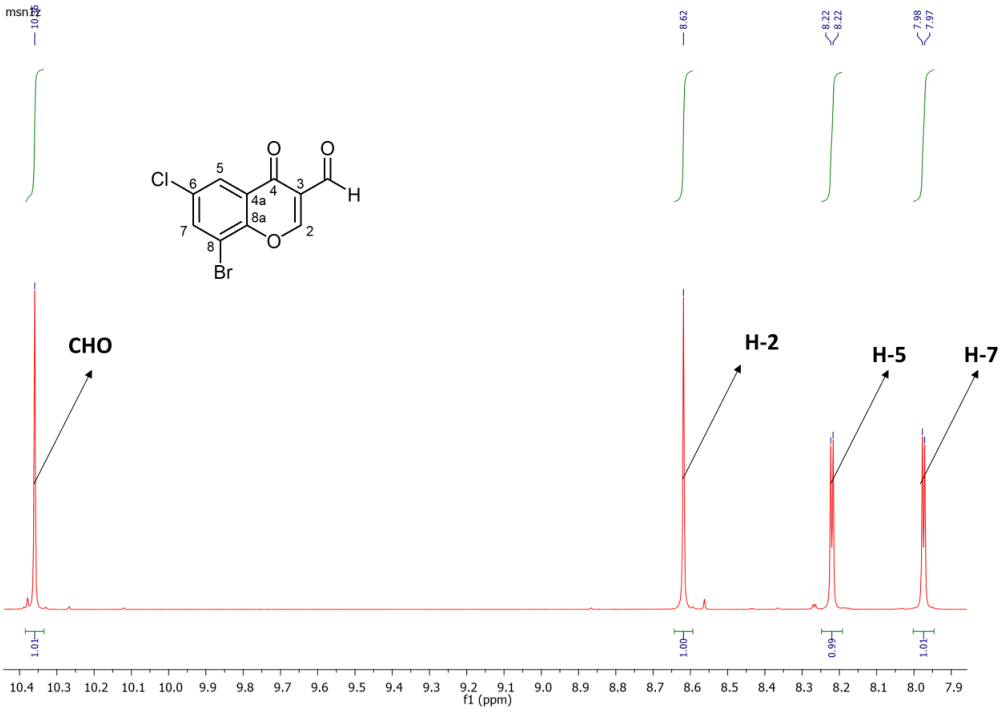


FIGURE 54: ^{1}H NMR spectrum of **44D** in $CDCl_3$ (at 100 MHz).

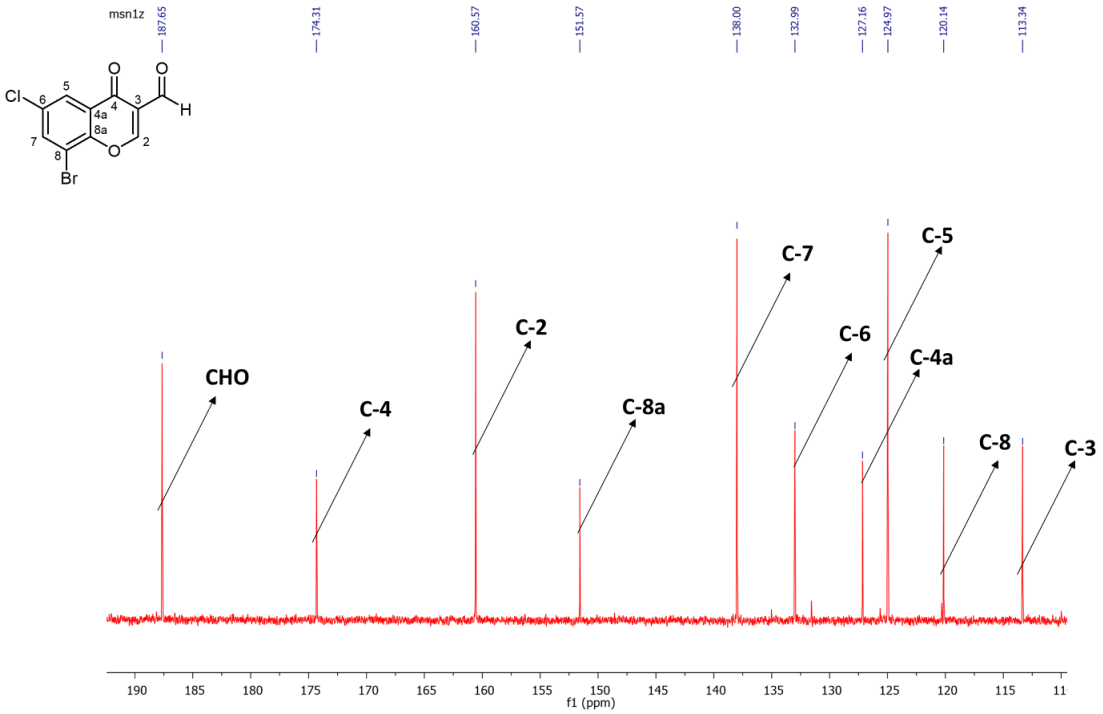


FIGURE 55: ^{13}C NMR spectrum of **44D** in $CDCl_3$ (at 100 MHz).

© University of Venda

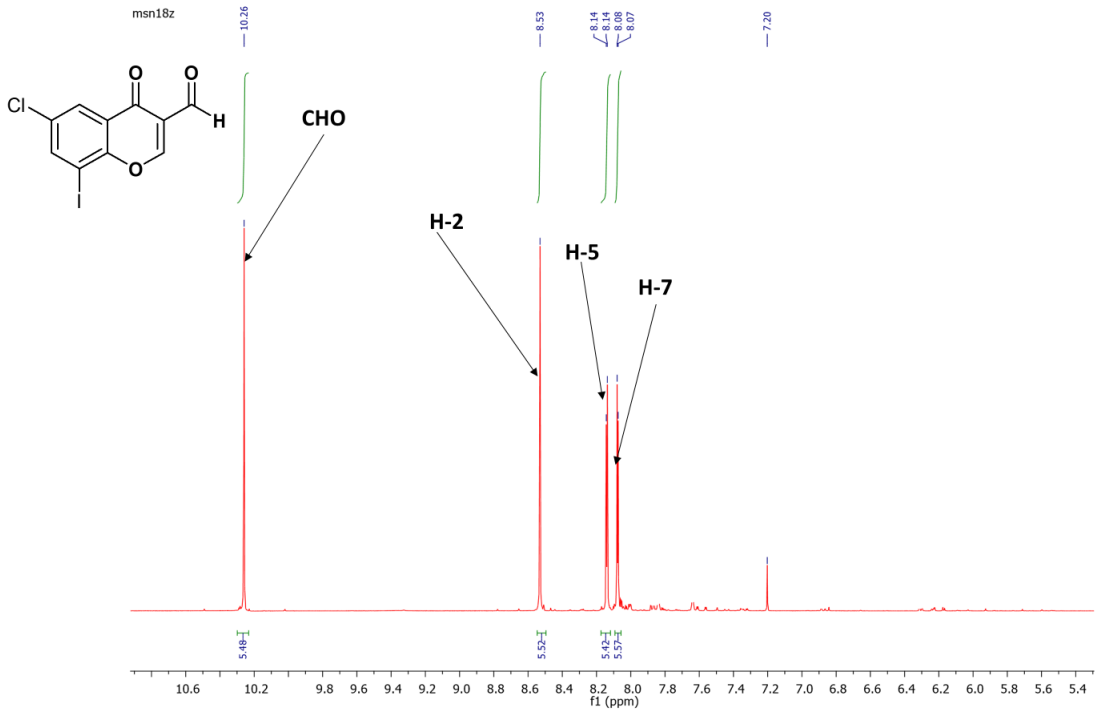


FIGURE 56: ^{1}H NMR spectrum of **44C** in $CDCl_3$ (at 100 MHz).

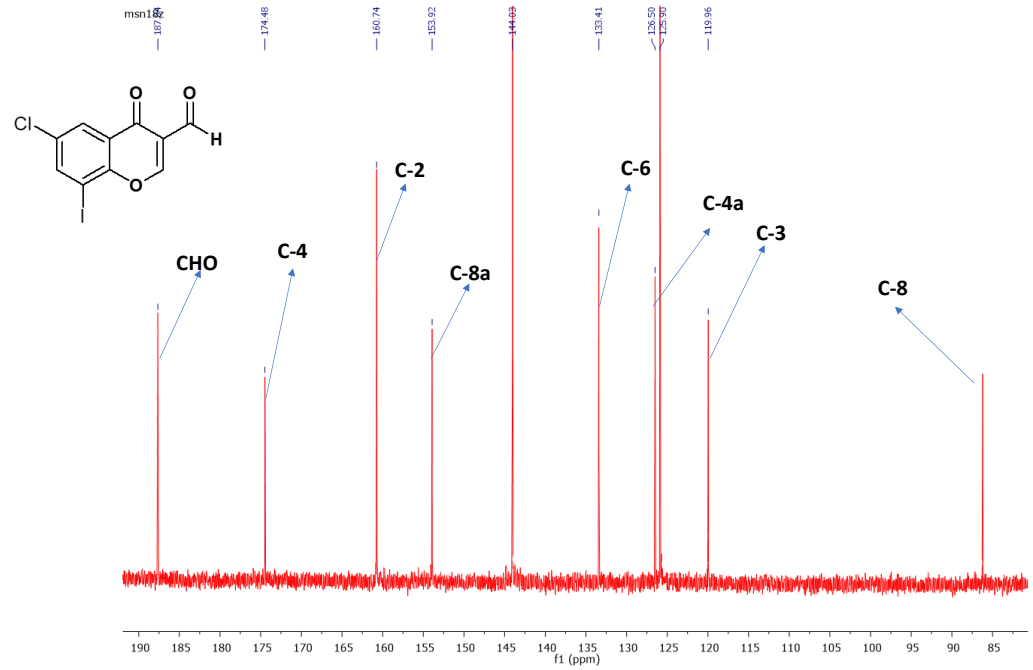


FIGURE 57: ^{1}H NMR spectrum of **44C** in $CDCl_3$ (at 100 MHz).

© University of Venda

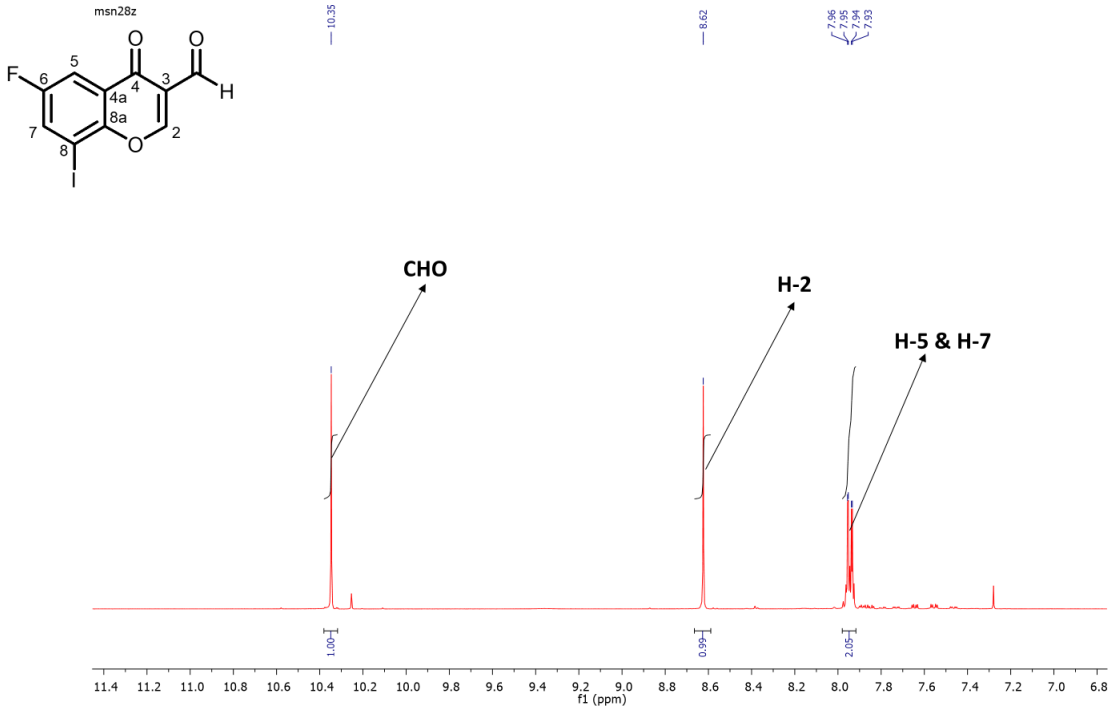


FIGURE 58: ^{1}H NMR spectrum of **44B** in $CDCl_3$ (at 100 MHz).

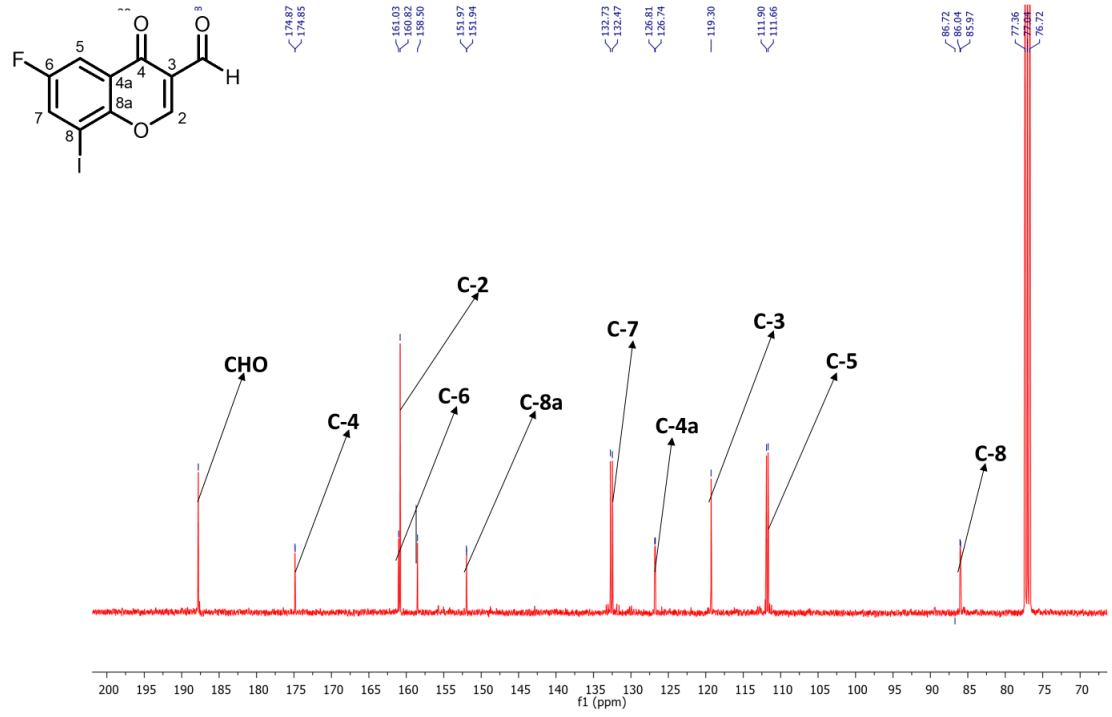


FIGURE 59: ^{13}C NMR spectrum of **44B** in $CDCl_3$ (at 100 MHz).

© University of Venda

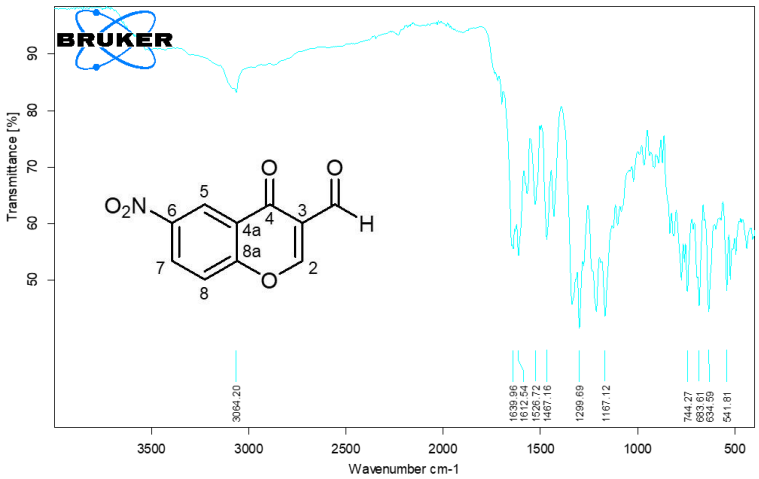


FIGURE 60: FT-IR spectrum of **44E**.

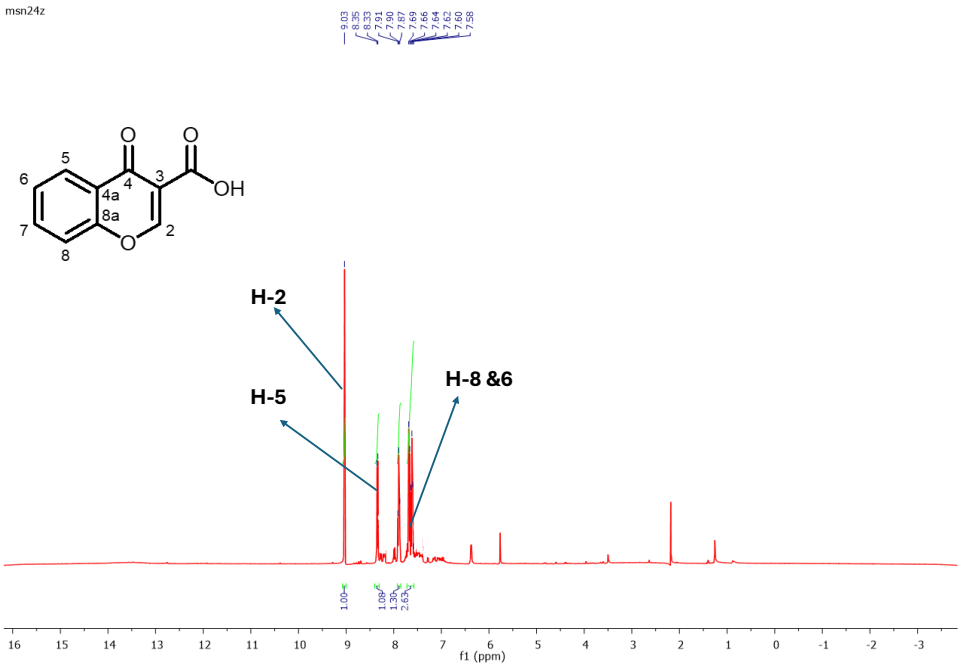


FIGURE 61: ^{1}H NMR spectrum of **45A** in DMSO (at 100 MHz).

© University of Venda

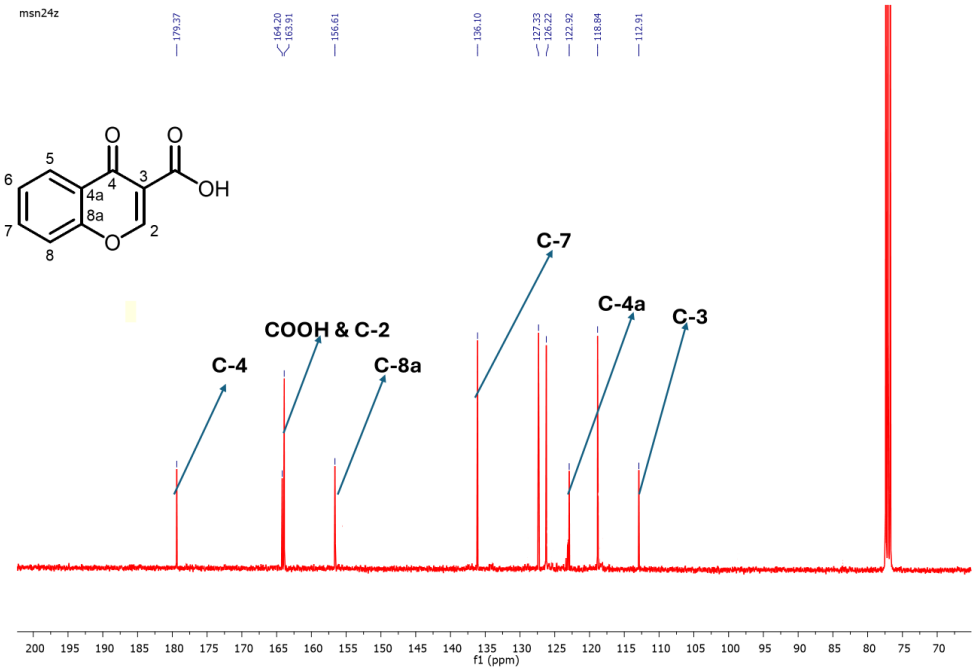


FIGURE 62: ^{13}C NMR spectrum of **45A** in DMSO (at 100 MHz).

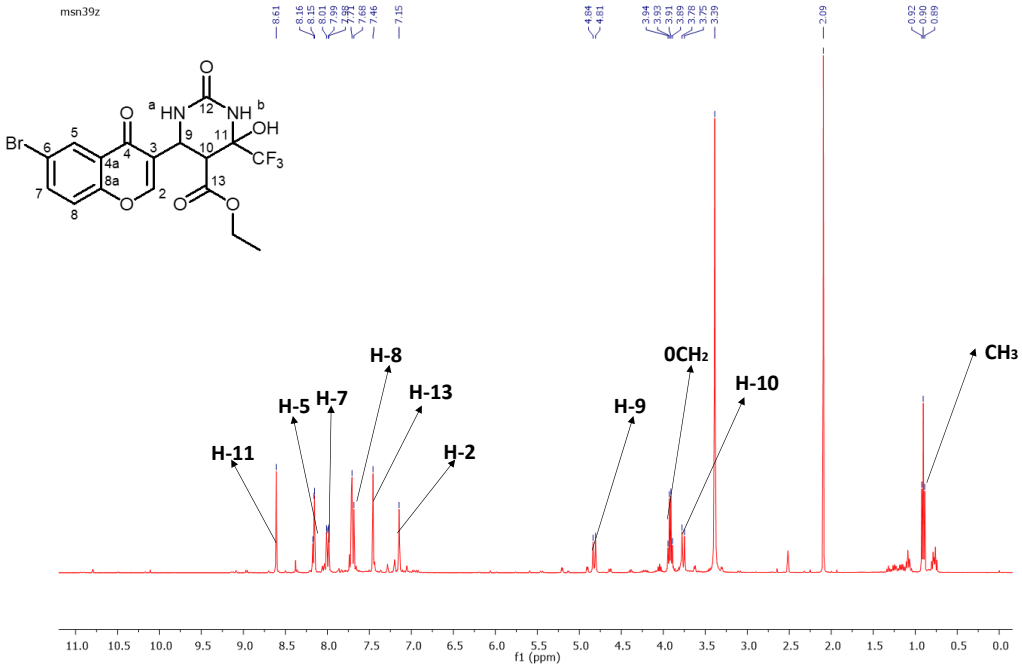


FIGURE 63: ^{1}H NMR spectrum of **51E** in DMSO (at 100 MHz).

© University of Venda

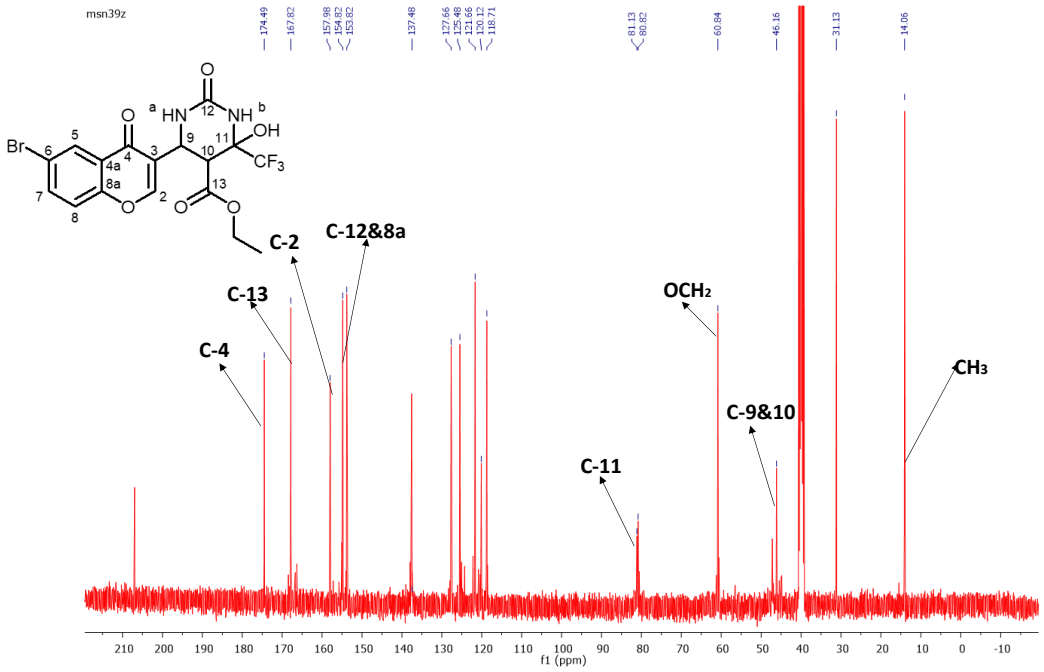


FIGURE 64: ^{13}C NMR spectrum of **51E** in DMSO (at 100 MHz).

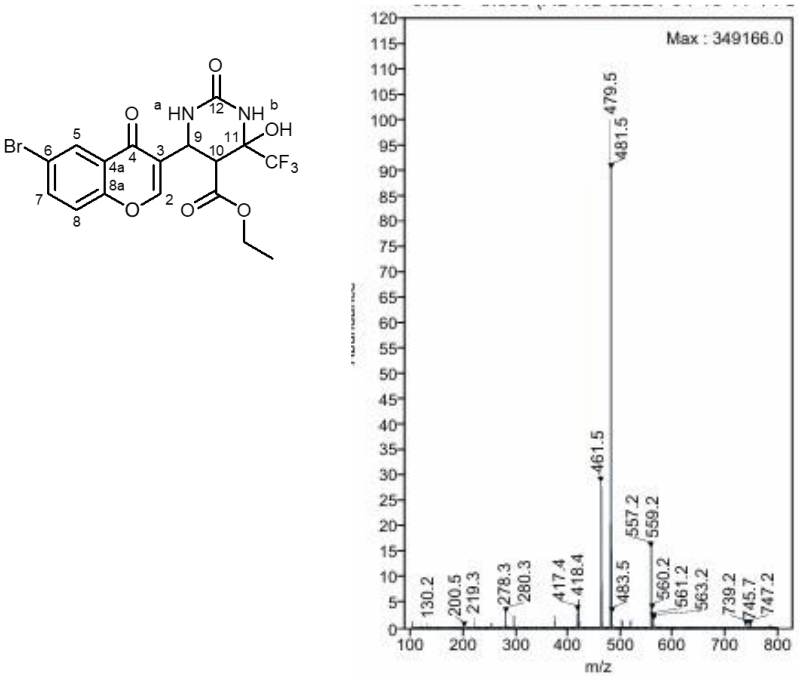


FIGURE 65: LC-MS spectrum of **51E.**

© University of Venda

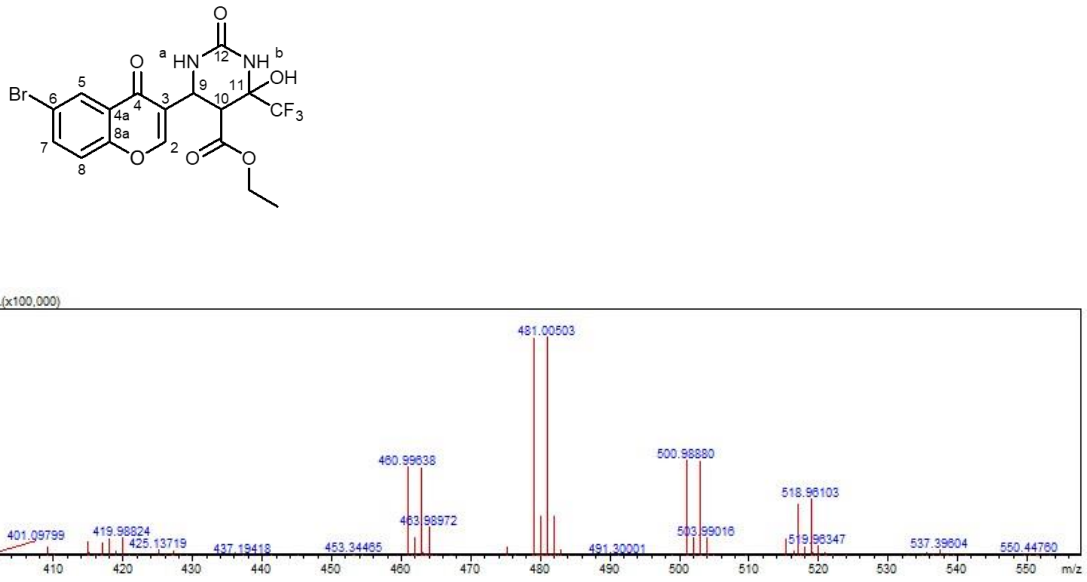


FIGURE 66: HR-MS spectrum of **51E.**

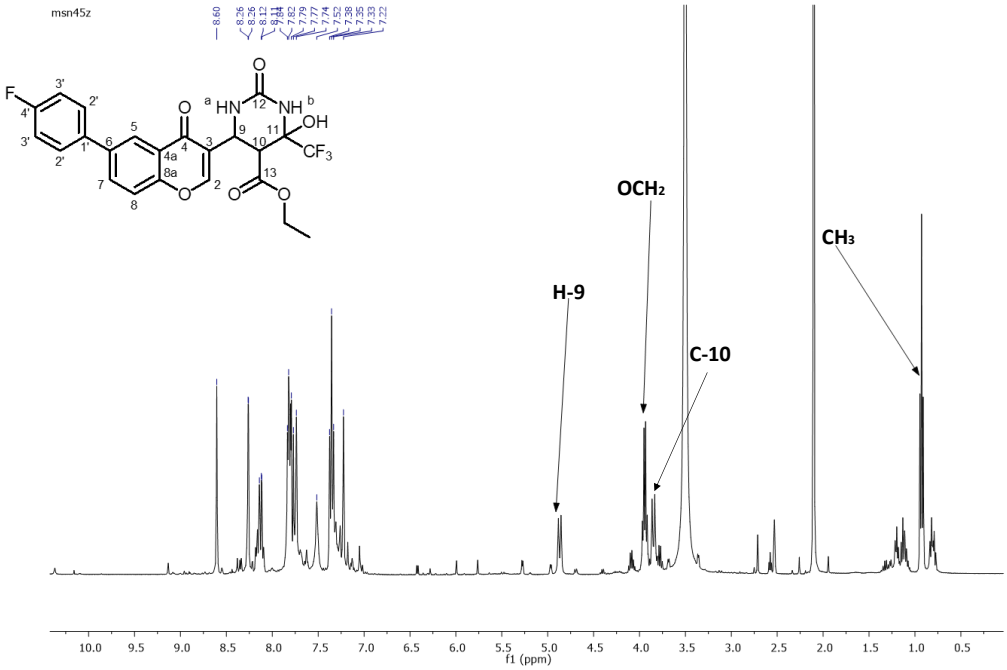


FIGURE 67: ^{1}H NMR spectrum of **51A** in $CDCl_3$ (at 100 MHz).

© University of Venda

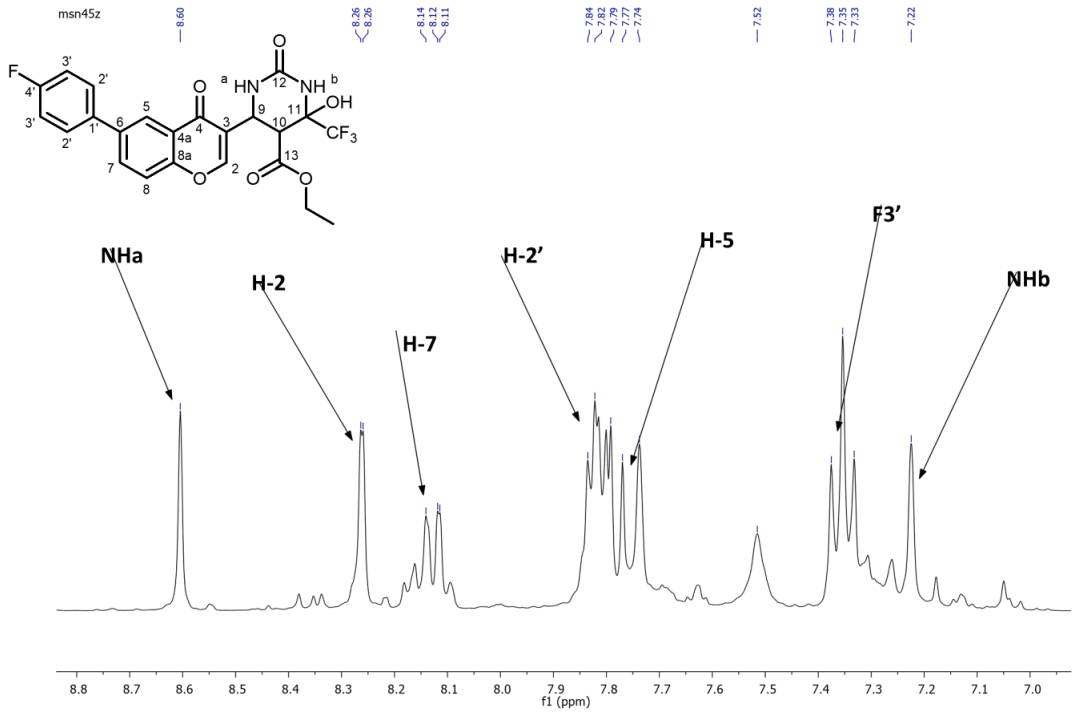


FIGURE 68: Expanded ^{1}H NMR spectrum of **51A** in $CDCl_3$ (at 100 MHz).

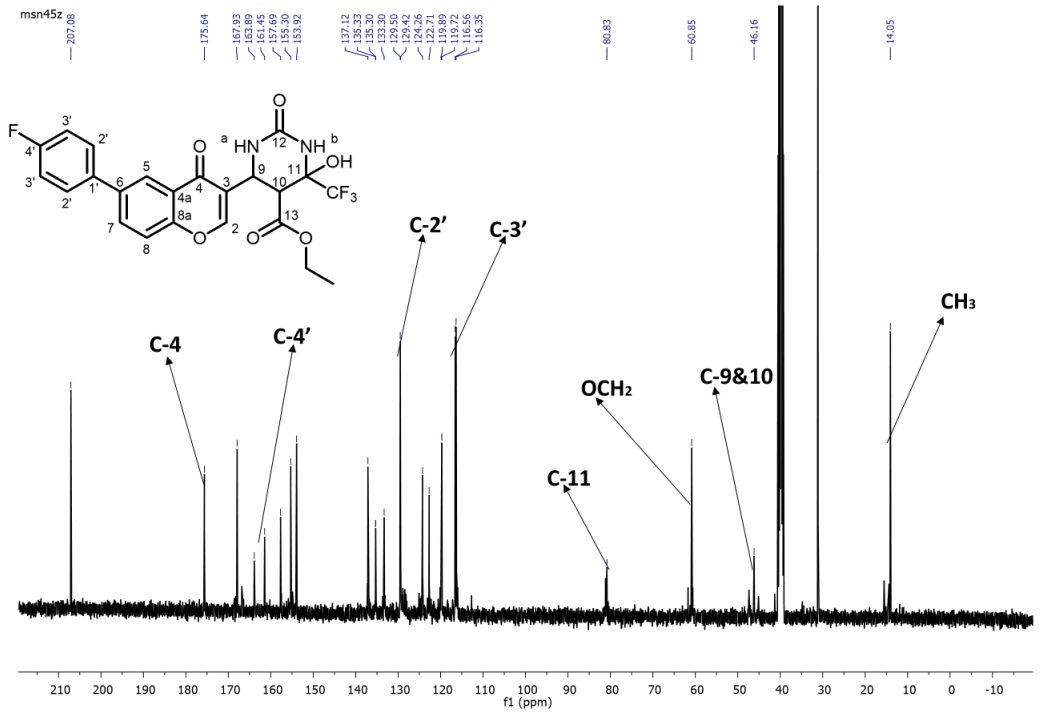


FIGURE 69: ^{13}C NMR spectrum of **51A** in $CDCl_3$ (at 100 MHz).

© University of Venda

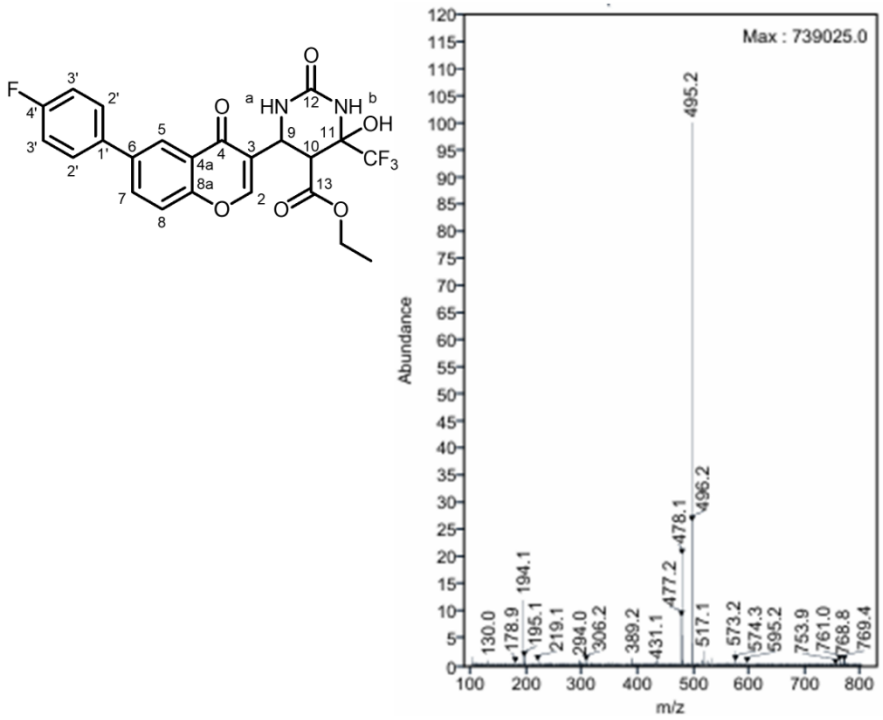


FIGURE 70: LC-MS spectrum of **51A.**

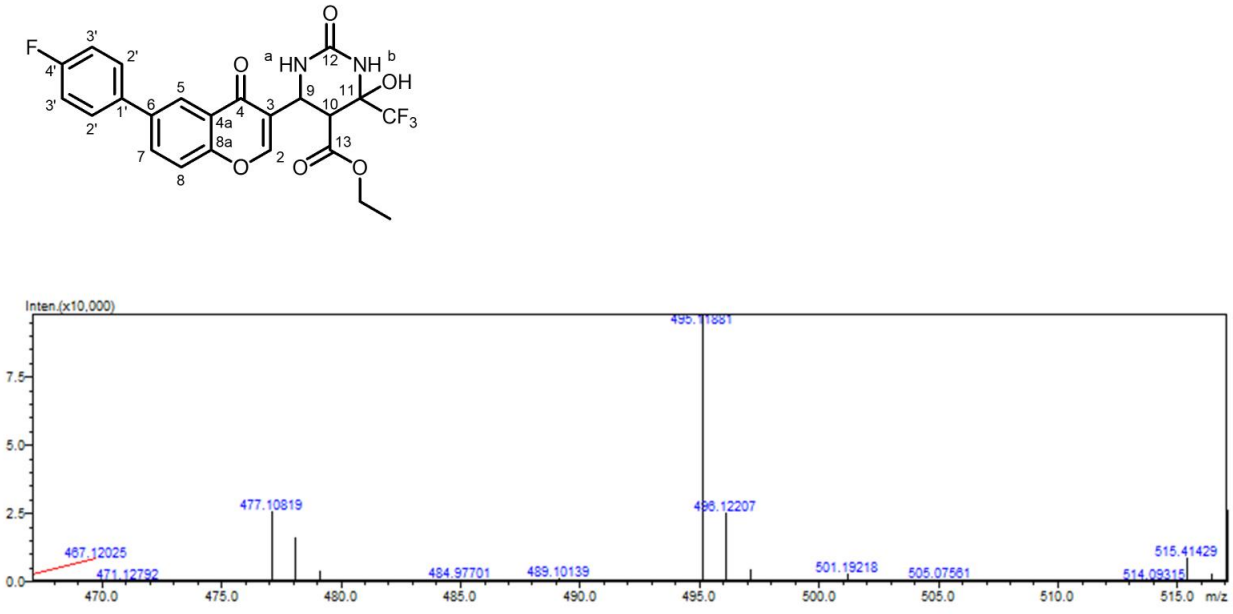


FIGURE 71: LC-MS spectrum of **51A.**

© University of Venda

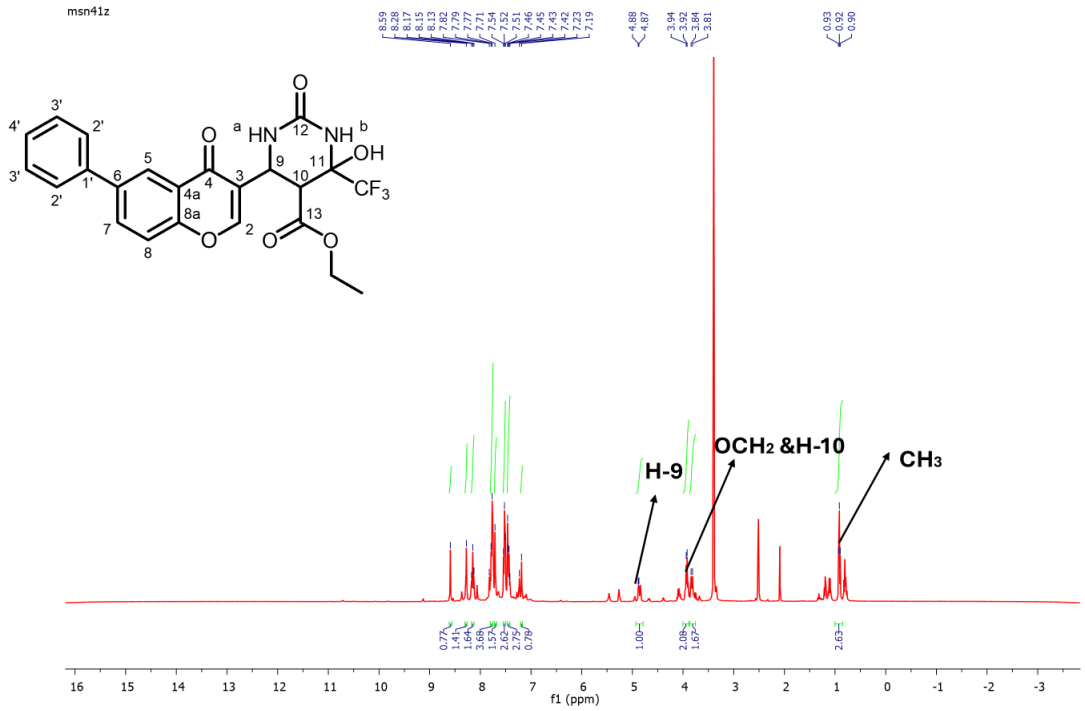


FIGURE 72: ^{1}H NMR spectrum of **51C** in $CDCl_3$ (at 100 MHz).

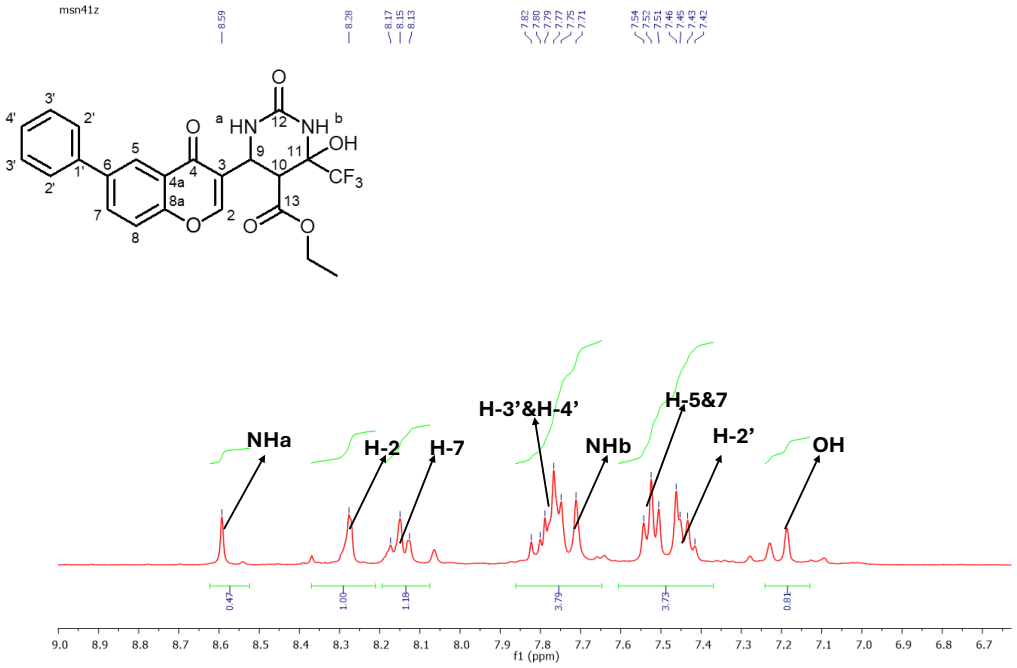


FIGURE 73: Expanded ^{1}H NMR spectrum of **51C** in $CDCl_3$ (at 100 MHz).

© University of Venda

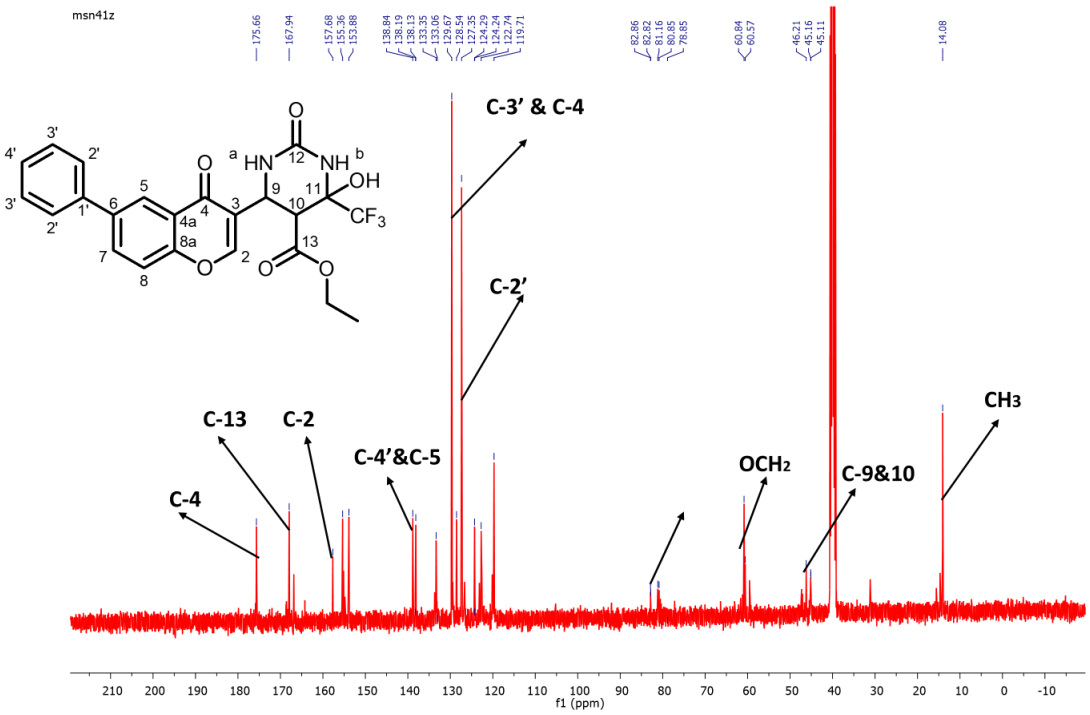


FIGURE 74: ^{13}C NMR spectrum of **51C** in $CDCl_3$ (at 100 MHz).

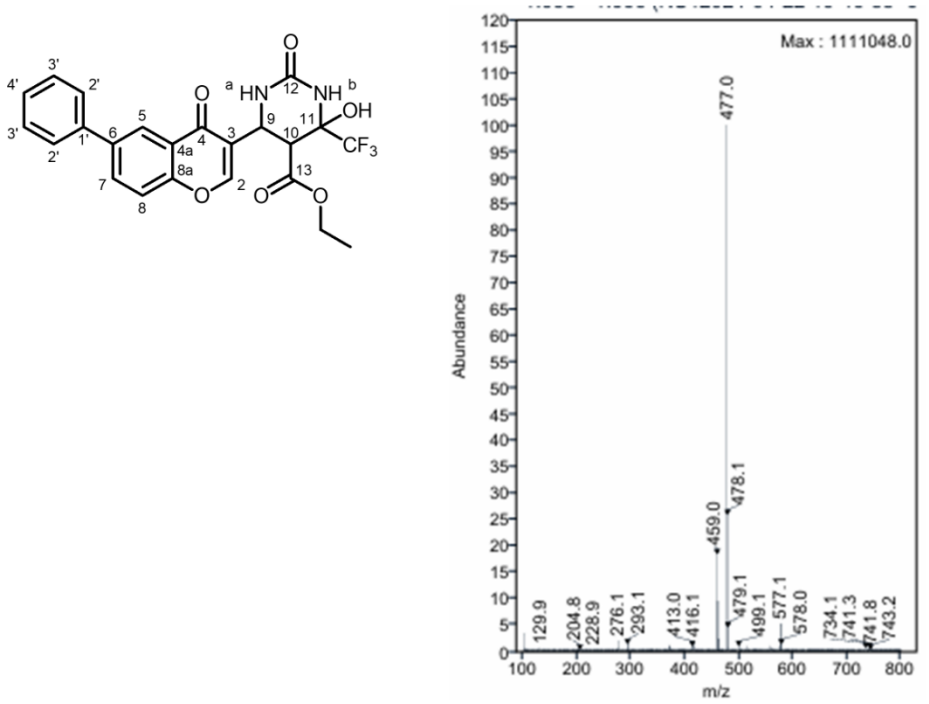


FIGURE 75: LC-MS spectrum of **51C.**

© University of Venda

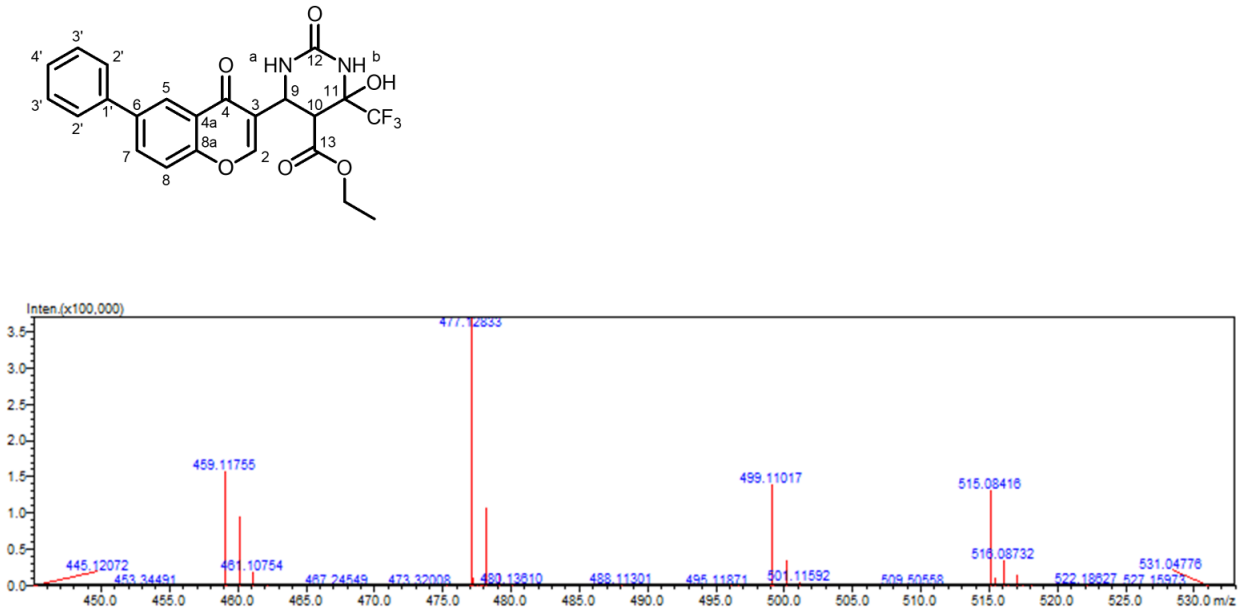


FIGURE 76: HR-MS spectrum of **51C.**

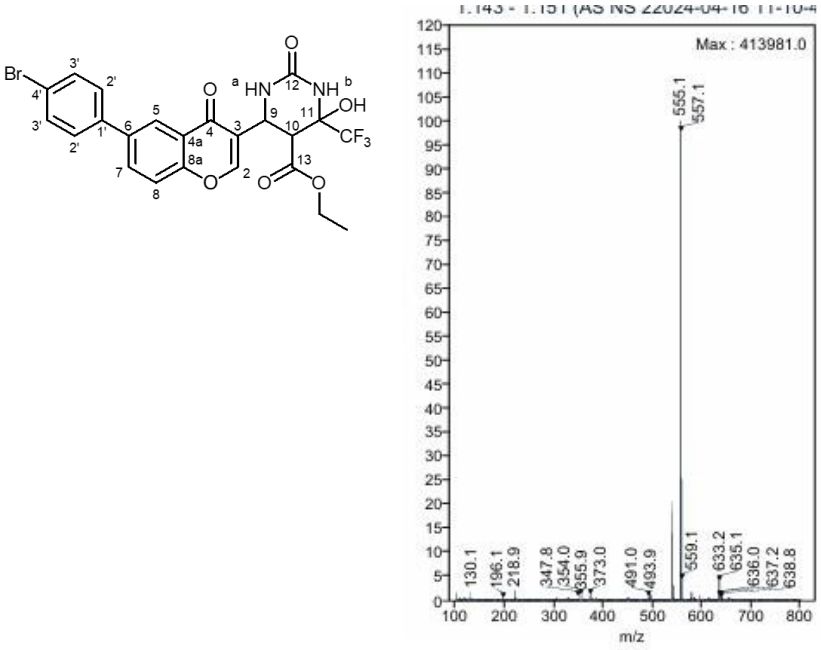
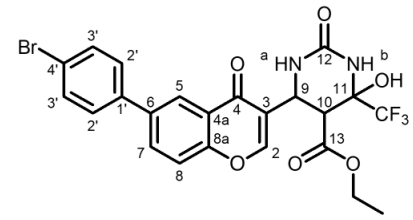


FIGURE 77: LC-MS spectrum of **51B.**

© University of Venda



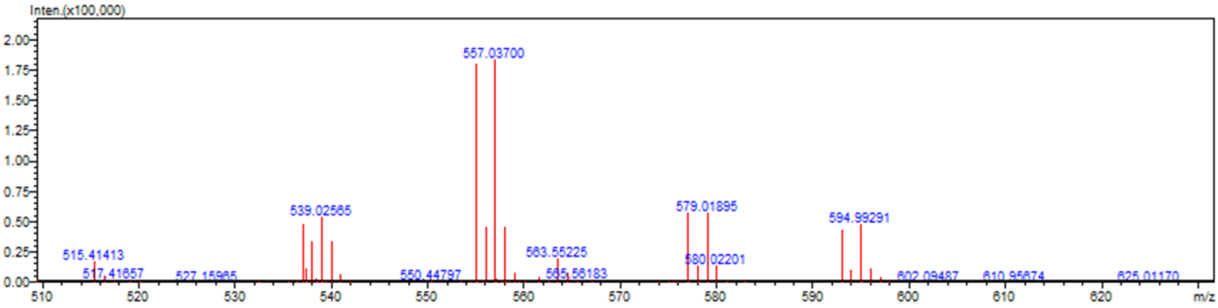


FIGURE 78: HR-MS spectrum of **51B.**

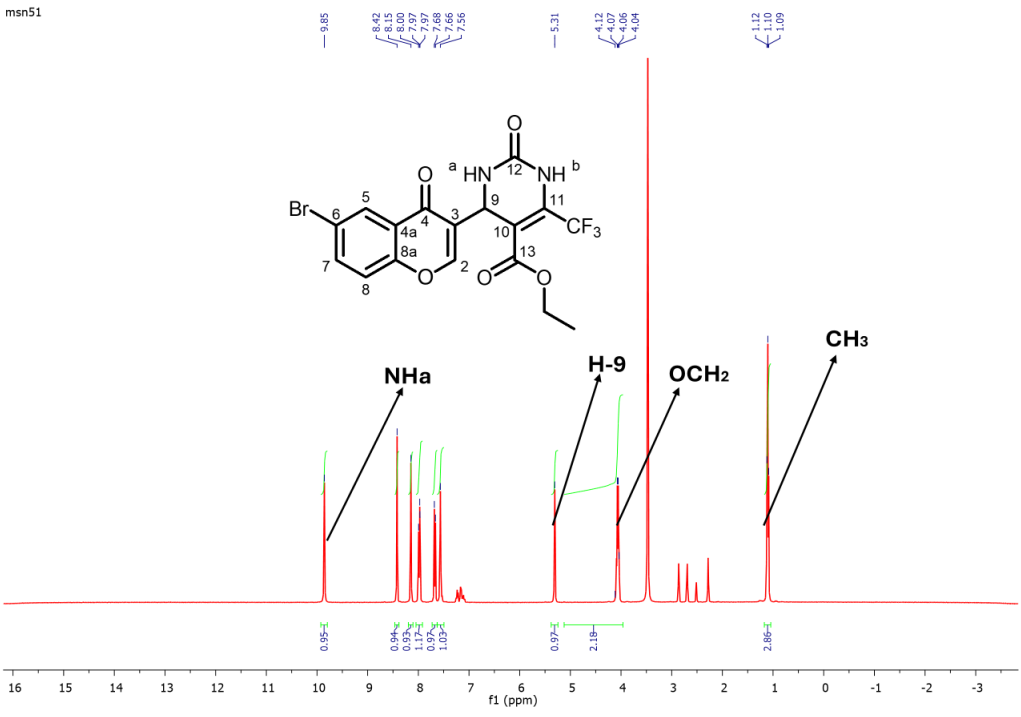


FIGURE 79: ^{1}H NMR spectrum of **52D** in $CDCl_3$ (at 100 MHz).

© University of Venda

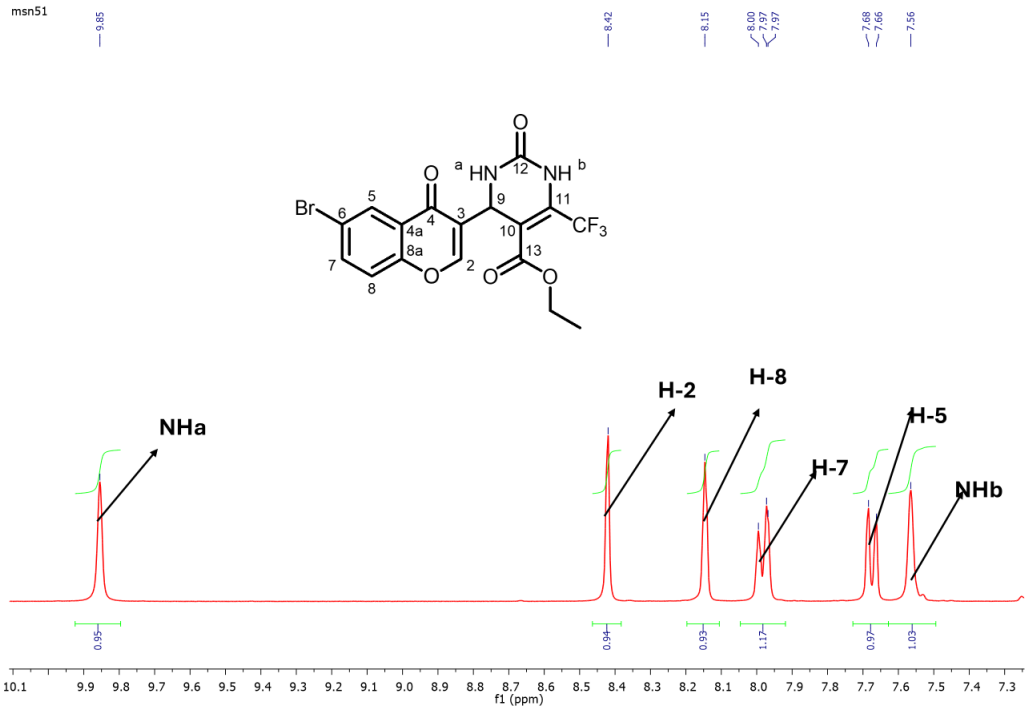


FIGURE 80: Expanded ^{1}H NMR spectrum of **52D** in $CDCl_3$ (at 100 MHz).

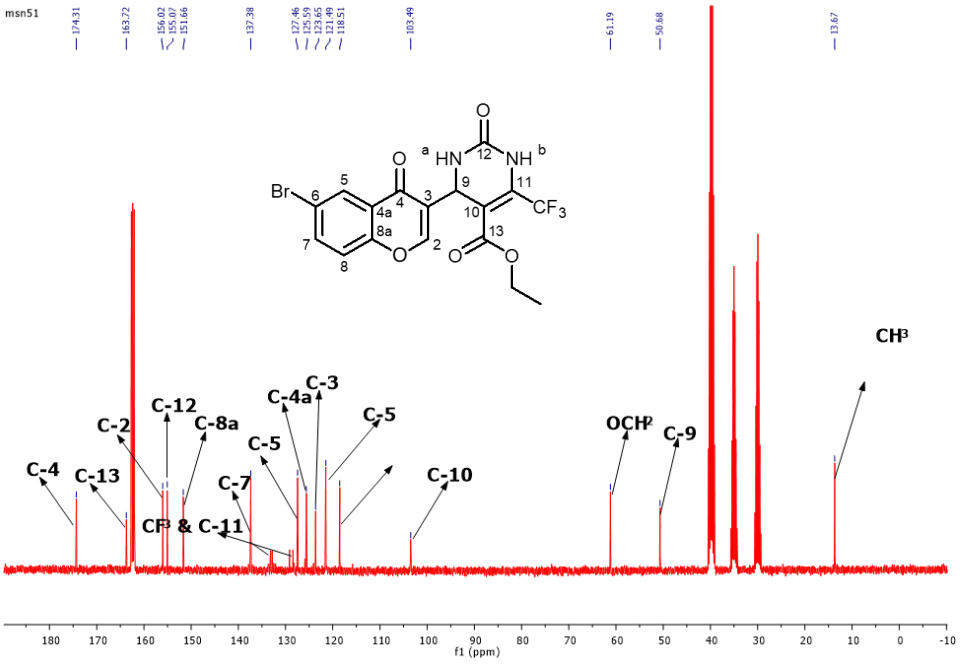


FIGURE 81: ^{13}C NMR spectrum of **52D** in $CDCl_3$ (at 100 MHz).

© University of Venda

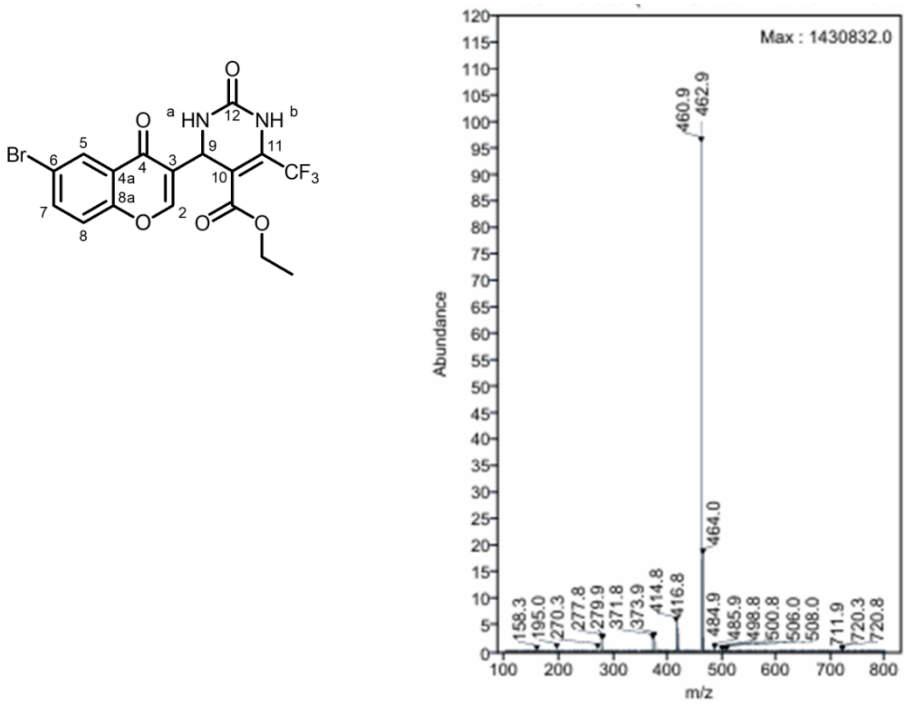


FIGURE 82: LC-MS spectrum of **52D.**

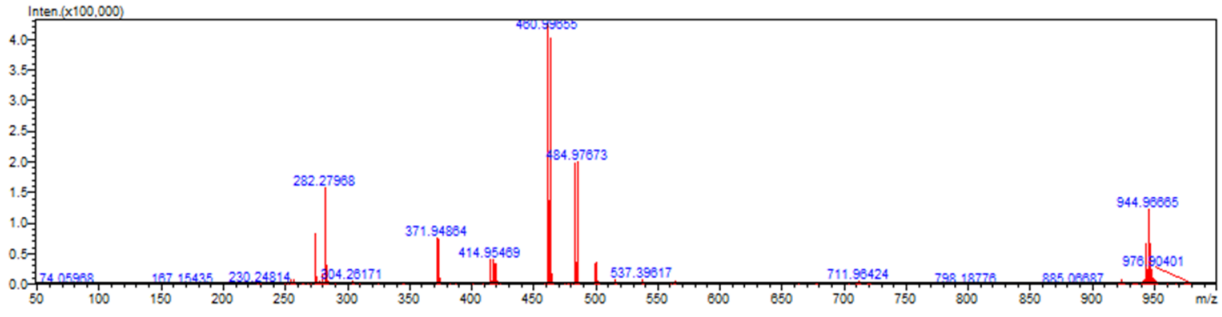


FIGURE 83: HR-MS spectrum of **52D.**

© University of Venda

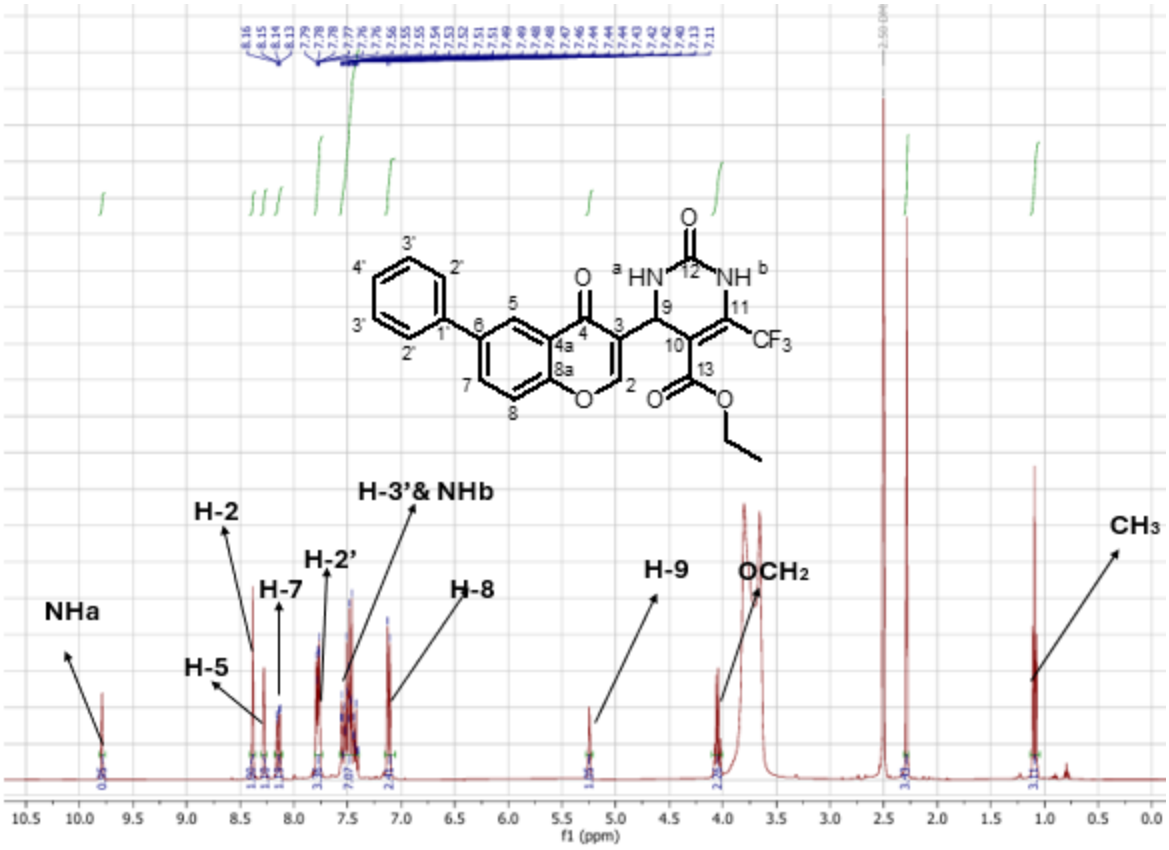


FIGURE 84: ^{1}H NMR spectrum of **52B** in $CDCl_3$ (at 100 MHz).

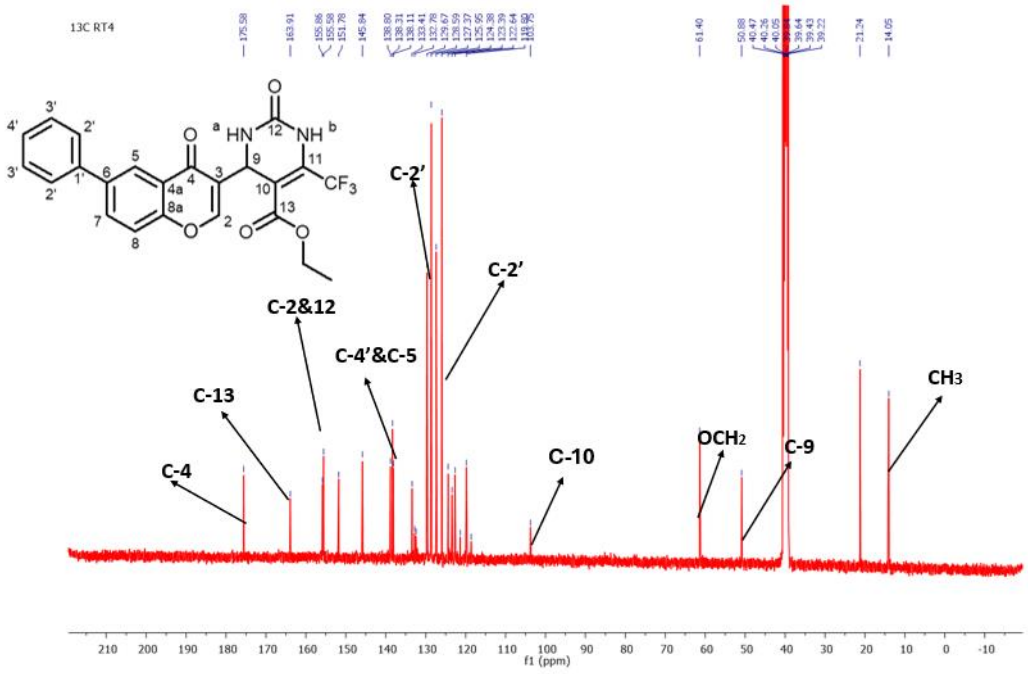


FIGURE 85: ^{13}C NMR spectrum of **52B** in $CDCl_3$ (at 100 MHz).

© University of Venda

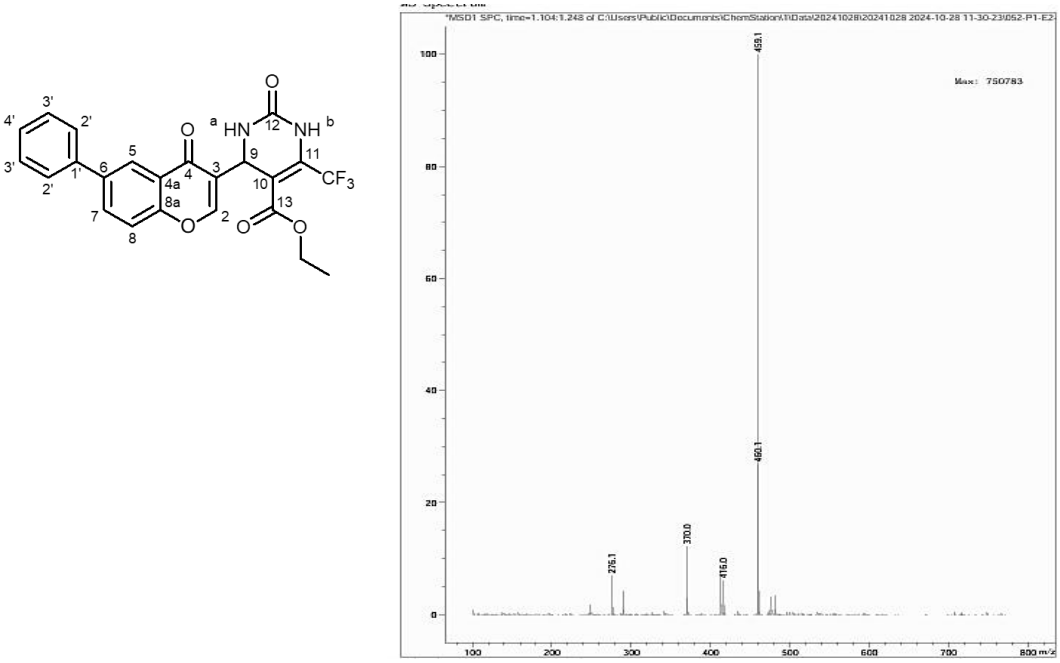


FIGURE 86: LC-MS spectrum of **52D.**

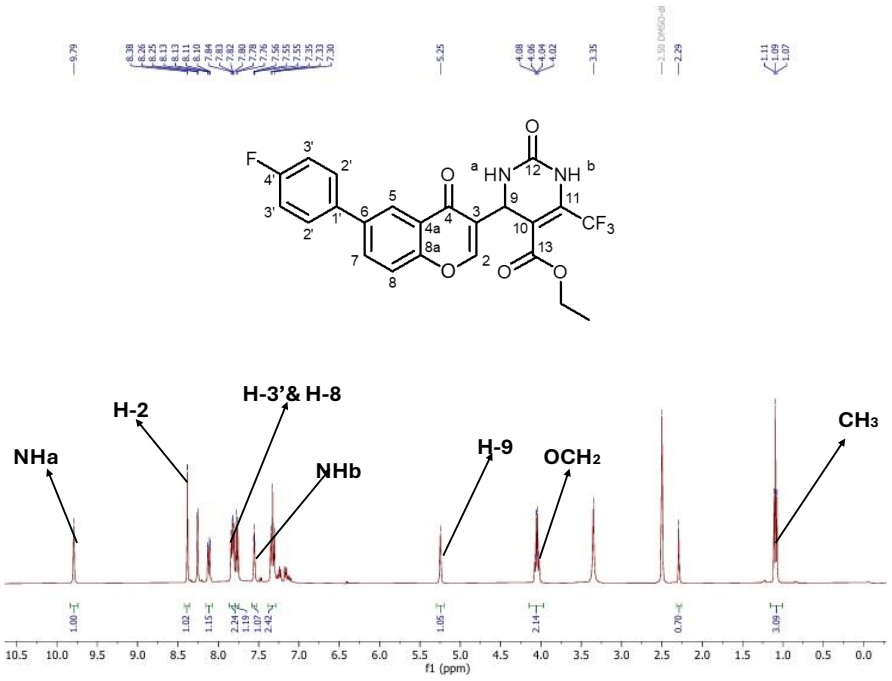


FIGURE 87: ^{1}H NMR spectrum of **52A** in $CDCl_3$ (at 100 MHz).

© University of Venda

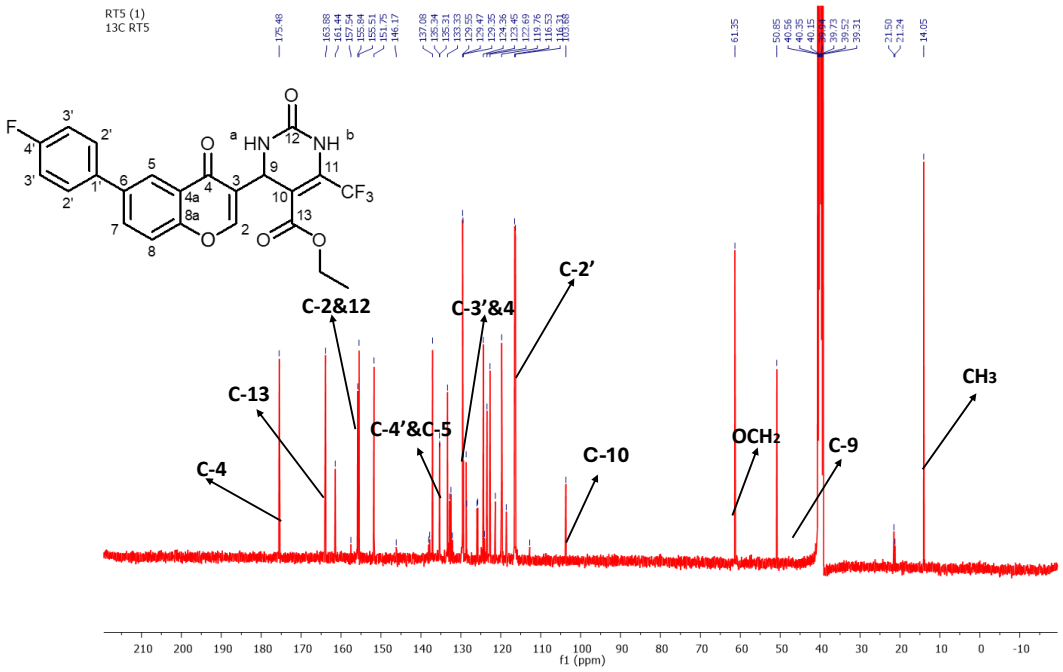


FIGURE 88: ^{13}C NMR spectrum of **52A** in $CDCl_3$ (at 100 MHz).

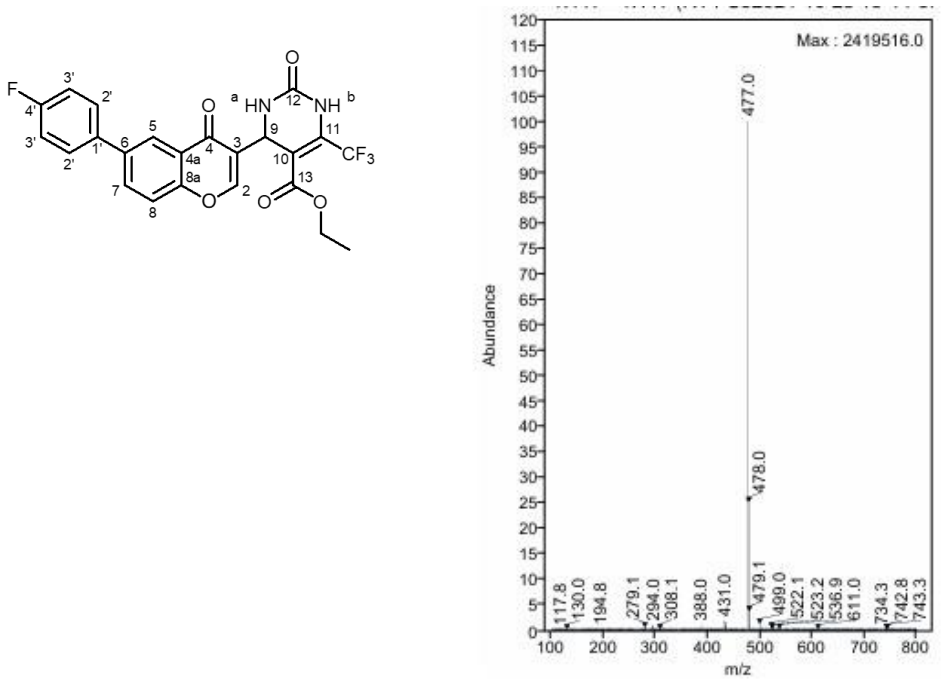


FIGURE 89: LC-MS spectrum of **52A.**

© University of Venda